

THEORY OF THE RADIO EMISSION OF PULSARS

V. S. BESKIN, A. V. GUREVICH, and YA. N. ISTOMIN

P.N. Lebedev Physical Institute, Academy of Sciences of the USSR, Moscow, U.S.S.R.

(Received 8 February, 1988)

Abstract. A consistent theory of excitation, stabilization, and propagation of electromagnetic oscillations in a relativistic one-dimensional electron-positron plasma flowing along curved magnetic field lines is presented. It is shown that in such a medium which is typical of the magnetosphere of a neutron star there exist unstable natural modes of oscillations. Nonlinear saturation of the instability leads to an effective energy conversion into transverse oscillations capable of leaving the magnetosphere of a pulsar. The polarization spectrum and the directivity pattern of generated radiation are determined. A comparison with observations has shown that the theory makes it possible to explain practically all the basic characteristics of observed pulsar radio emission.

1. Introduction

As is well known, almost immediately after the discovery of pulsating radio sources—pulsars in 1967 they were identified with rotating single neutron stars. Already by 1975 the character of the main processes proceeding in pulsar magnetosphere was outlined (Goldreich and Julian, 1969; Sturrock, 1971; Ruderman and Sutherland, 1975) and the parameters of the outflowing plasma which is evidently responsible for the observed emission were determined (Ruderman and Sutherland, 1975; Tademaru, 1973). By the present time a huge and continuously increasing body of information is stored (Manchester and Taylor, 1977; Taylor and Stinebring, 1986) (over 400 radio pulsars with periods from 1.56 ms to 4.30 s are known, the periods are found within an accuracy to 13 digits, time resolution goes down to fractions of microseconds). But the very mechanism of pulsar radio emission has remained unknown.

In fact, the studies had not gone farther than the qualitative considerations of the late sixties which had been formulated by Ginzburg *et al.* (1969) and Ginzburg (1971), when it became clear that the mechanism of radio emission must be coherent because only in this case can an exceedingly high brightness temperature of radio emission be explained which in some pulsars reaches 10^{30} K. This coherence may be due either to the existence in the radiating region of charged particle clusters with the dimension smaller than the radiation wavelength ('antenna' mechanism) (Radhakrishnan and Cocke, 1969; Smith, 1970; Goldreich and Keeley, 1971) or to the inverse distribution of particles over energy levels ('maser' mechanism) (Chiu and Canuto, 1971; Kaplan and Tsytovich, 1973; Zheleznyakov, 1973). But even the question of which of these two mechanisms is to be chosen has remained open up to recently. The numerous models constructed both on the basis of the antenna (Komesaroff, 1970; Benford and Buschauer, 1977; Cheng and Ruderman, 1977; Buschauer and Benford, 1978; Ochelkov and Usov, 1984; Usov, 1987) and maser (Blandford, 1975; Kawamura and Suzuki,

1977; Melrose, 1978; Shaposhnikov, 1981) mechanisms of coherence have failed to give quantitative predictions facilitating such a choice.

The main reason for this is that the main problem of electrodynamics of a relativistic plasma moving in a curvilinear magnetic field has been neither formulated nor solved: there existed, in fact, no theory describing an increase and stabilization of perturbations in such a plasma when its density is rather high. And as will be shown below, it is only under this condition that electromagnetic oscillations are rapidly generated. The solution of the general problem has been recently obtained by Beskin *et al.* (1987b) and Istomin (1988). Here we show that an application of the results of this theory to pulsar magnetosphere makes it possible to explain the origin and the main properties of observed radio emission.

In Section 2 we discuss in detail the properties of plasma in pulsar magnetosphere and make a brief review of the present state of the theory of radio emission. The dielectric permittivity tensor in a relativistic plasma moving along the lines of a curvilinear magnetic field is determined in Section 3 on the basis of the linear theory developed by Beskin *et al.* (1987a, b). This will make it possible to find the normal oscillation modes in this plasma. It is shown that at high enough plasma density a hydrodynamic instability is excited that leads to a rapid increase of two additional normal modes of electromagnetic oscillations which we will call curvature-plasma modes. The nonlinear processes leading to stabilization of unstable modes and to the formation of their spectrum are considered in Section 4. It is also shown that the curvature-plasma modes are effectively transformed into ordinary and extraordinary modes of transverse waves capable of leaving freely the pulsar magnetosphere and generating observed radio emission.

In Section 5, the theoretical conceptions developed in previous section are applied for a concrete calculation of propagation, amplification, and formation of the spectrum of electromagnetic radiation in pulsar magnetosphere.

Finally, Section 6 is devoted to comparison of the predictions of the theory with observational data. It is shown that the theory makes it possible to explain the characteristics of pulsar radio emission: the radiation intensity, the range of observed frequencies, the energy spectrum, the shape of the mean profile, the directivity pattern, and polarization. We should emphasize that the theory is based only on the general considerations concerning the properties of the flux of relativistic electron-positron plasma flowing in the magnetosphere of a neutron star, which at the present time may be regarded as sufficiently reliably established (Sturrock, 1971; Tademaru, 1973; Ruderman and Sutherland, 1975; Gurevich and Istomin, 1985). No other additional hypotheses or assumptions are used.

2. Magnetospheric Plasma and Pulsar Radio Emission

2.1. THE BASIC PROPERTIES OF MAGNETOSPHERIC PLASMA

As has already been said, radio pulsars are connected with rotating neutron stars ($M \sim M_{\odot}$, $R \simeq 10$ km) on the surface of which there exist strong magnetic fields

$B_0 \sim 10^{11} - 10^{13}$ G. The plasma that fills the pulsar magnetosphere is magnetized, i.e., can move only along magnetic field lines. Such a magnetization is violated in the neighbourhood of the 'light surface' $R_s \simeq R_L = c/\Omega$ (Ω is the angular velocity of neutron star rotation), where the velocity of drift motion of particles approaches the light velocity c . Charged particles can intersect the 'light surface', i.e., leave the pulsar magnetosphere only in the case if they are located on open magnetic field lines which overstep the limits of the light surface.

It is clear that a stationary plasma outflow along open field lines is possible only if plasma is constantly generated in the pulsar magnetosphere. It has turned out that such a generation ('vacuum breakdown') may actually take place near magnetic poles of a neutron star (Sturrock, 1971; Ruderman and Sutherland, 1975; Arons and Scharlemann, 1979; Jones, 1981; Gurevich and Istomin, 1985). According to this theory, near the pulsar surface there exists a region (a 'double layer' or a 'gap') in which a longitudinal (parallel to the magnetic field) electric field is nonzero. In other words, between the star surface and the pulsar magnetosphere there appears a certain potential difference $\Psi \neq 0$. The primary particles that have got into this region are accelerated up to energies $\mathcal{E} = e\Psi \sim (10^7 - 10^8)m_e c^2$. Moving further along curved field lines, the primary particles beam will effectively generate hard γ -quanta, which in their turn must be absorbed in a strong magnetic field forming electron-positron pairs (Sturrock, 1971; Tademaru, 1973; Ruderman and Sutherland, 1975).

If the magnetic field B_0 on the star surface is not too strong, so that $B_0 < 5 \times 10^{12}$ G, then the secondary electrons and positrons will be produced on nonzero Landau levels (Beskin, 1982a; Daugherty and Harding, 1983; Shabad and Usov, 1985, 1986; Herold *et al.*, 1985). Passing over to lower levels, these secondary particles will also emit γ -quanta which will lead to the production of new secondary particles. This cascade production must proceed until the pulsar magnetosphere becomes transparent for the softest γ -quanta. As a result, the density of the secondary electron-positron plasma proves to be substantially higher than the density of the primary particles beam. Since this secondary plasma is generated in the region of a zero longitudinal electric field, it can freely leave the magnetosphere moving along open magnetic field lines.

We should stress that the density of the secondary plasma will be substantially higher than the primary beam density in a strong magnetic field too ($B_0 \gtrsim 5 \times 10^{12}$ G), when a synchrotron emission of γ -quanta is absent (Beskin, 1982a; Daugherty and Harding, 1983). This is due to the fact that each primary particle accelerated in the 'gap' generates many secondary electron-positron pairs.

Thus, plasma generation in pulsar magnetosphere is determined by the processes of primary particle production in the 'gap'. Important quantities here are the potential difference Ψ between the star surface and magnetosphere and the electric current \mathbf{j} carried over by fast particles. As was shown by Beskin *et al.* (1984, 1986), their values are expressed in terms of the dimensionless parameter

$$Q = 2P^{11/10} \dot{P}^{-4/10}, \quad (2.1)$$

which is the function of the observed quantities: P , the period (in s) and

$\dot{P}_{-15} = 10^{15} \text{ dP/dt}$, the deceleration rate of pulsar rotation; the corresponding dependences are written down a bit later.

Let us present the main parameters of the electron-positron plasma which flows in pulsar magnetosphere. Its density is convenient to represent in the form

$$n_e = \lambda \frac{\Omega B}{2\pi c |e|} = \lambda n_c, \quad (2.2)$$

where n_c is the Goldreich–Julian corotation density (the primary beam has the same density in the order of magnitude), and λ is determined by multiplicity of secondary plasma generation. According to the calculations carried out by many authors (Sturrock, 1971; Tademaru, 1973; Daugherty and Harding, 1982; Arons, 1983; Jones, 1983; Gurevich and Istomin, 1985) λ depending on the physical parameters: the strength of the magnetic field B_0 , the star rotation frequency Ω , the character of particle ejection from the star surface. For instance, according to Gurevich and Istomin (1985) for pulsars with $Q < 1$ we can present the following estimate:

$$\lambda \sim 10^4 P^{3/7} (B_0/10^{12} \text{ G})^{-3/7}.$$

With moving away from the pulsar surface the plasma density decreases proportionally to B . At the star surface we have $n_c \sim (10^{11} - 10^{14}) \text{ cm}^{-3}$.

In the energy spectrum of particle we can distinguish between a fast (primary beam) and a slow (secondary plasma) components. A primary one-charge beam has an energy $\mathcal{E} \sim e\Psi \sim 10^7 m_e c^2$ the width of energy distribution being small: $\Delta\mathcal{E}/\mathcal{E} \sim 10^{-2}$ (Gurevich and Istomin, 1985), so in the first approximation the beam may be regarded as monoenergetic. The sign at the charge of the primary beam coincides with the sign at the corotation density (Goldreich and Julian, 1969)

$$\rho_c = - \frac{\mathbf{B}\Omega}{2\pi c} \quad (2.3)$$

in the polar region and, therefore, depends on the angle χ between the rotation axis and the magnetic dipole axis. According to Beskin (1982b) and Gurevich and Istomin (1985), for a sufficiently large particle outflow from the star surface, the cascade production is possible both for the ‘electron’ ($\rho_c < 0$, i.e., $\chi < \pi/2$) and ‘positron’ ($\rho_c > 0$, i.e., $\chi > \pi/2$) cases.

As regards a drop of the potential Ψ which determines, in fact, the primary beam energy, its value, as has already been said, is connected with the condition under which the ‘vacuum gap’ arises. This quantity is convenient to express in terms of the maximal possible decrease of the potential in the ‘gap’ region $\Psi_{\max} \simeq 4\pi\rho_c R_0^2$, where $R_0 \simeq R(\Omega R/c)^{1/2}$ is the polar cap radius (Goldreich and Julian, 1969; Ruderman and Sutherland, 1975). According to Beskin *et al.* (1984, 1986), for pulsars with $Q < 1$

$$\Psi \simeq Q^2 \Psi_{\max}.$$

In case $Q > 1$, we have $\Psi \simeq \Psi_{\max}$. Consequently, for pulsars with $Q \ll 1$ a cascade particle production starts already for the potentials $\Psi \ll \Psi_{\max}$, whereas for pulsars with

$Q > 1$ practically the whole value of potential drop possible near the polar regions of a neutron star should be used for this purpose. The absolute value of the quantity Ψ (and, therefore, the primary beam energy) depend weakly on real parameters of the pulsar (Ruderman and Sutherland, 1975; Gurevich and Istomin, 1985).

Possessing the charge density $\rho_e \simeq \rho_c$, a primary beam leads, naturally, also to the appearance of electric current running along open field lines. Its density is convenient to write in the form

$$j = i_0 c \rho_c,$$

where $i_0 \lesssim 1$ and ρ_c is given by Equation (2.3). As was shown by Beskin *et al.* (1984, 1986), $i_0 \simeq Q$ for pulsars $Q < 1$ and $i_0 \simeq 1$ for pulsars with $Q > 1$. We can see that the current is also determined by the parameter Q .

Finally, the total energy $W_{\text{part}} = \int \mathbf{j} \Psi \, ds$ transferred by particles in the region of open field lines can be written in the form

$$W_{\text{part}} = i_0 \frac{\Psi}{\Psi_{\text{max}}} W_{\text{max}},$$

where

$$W_{\text{max}} \simeq R_0^2 c \rho_c \Psi_{\text{max}} \simeq 4 \times 10^{31} P^{-4} (B/10^{12} \text{ G})^2 \text{ erg s}^{-1}$$

is the maximal possible energy transferred by particles*. We can see that $W_{\text{part}} \simeq W_{\text{max}}$ for pulsars with $Q > 1$ and $W_{\text{part}} \ll W_{\text{max}}$ for pulsars with $Q \ll 1$.

Note that according to the models of particle generation (Sturrock, 1971; Tademaru, 1973; Ruderman and Sutherland, 1975) the production of a secondary plasma is impossible near the magnetic axis, the outflowing plasma will fill a conic region (the so-called hollow cone). The internal radius of the cone r_{in} on the star surface is expressed through the quantity Q (2.1) (cf. Beskin *et al.*, 1984) as

$$r_{\text{in}} \simeq Q^{7/9} R_0, \quad (2.4)$$

where again R_0 is the polar cap radius. For pulsars with $Q < 1$, near the internal boundary of the hollow cone there flows an intensive jet of surface current I_{in} whose relative fraction turns out to increase with decreasing Q , so that

$$I_{\text{in}}/I_{\text{tot}} \simeq Q^{-4/9},$$

where $I_{\text{tot}} = i_0 c \rho_c R_0^2$ is the total electric current circulating in the pulsar magnetosphere. The profile of the current corresponding to pulsars with $Q < 1$ is shown in Figure 1(a). We can see that in this case the outflowing current occupies practically the whole polar cap surface. As concerns pulsars with $Q > 1$, as is seen from Figure 1(b), they generate particles only within a ring with $r_{\text{in}} \simeq R_0$ located near the external boundary of the polar region.

* The quantity W_{max} represents, in fact, complete losses of rotational energy of a neutron star $W_{\text{tot}} = J \Omega \, d\Omega/dt$ (for more details see Beskin *et al.*, 1983).

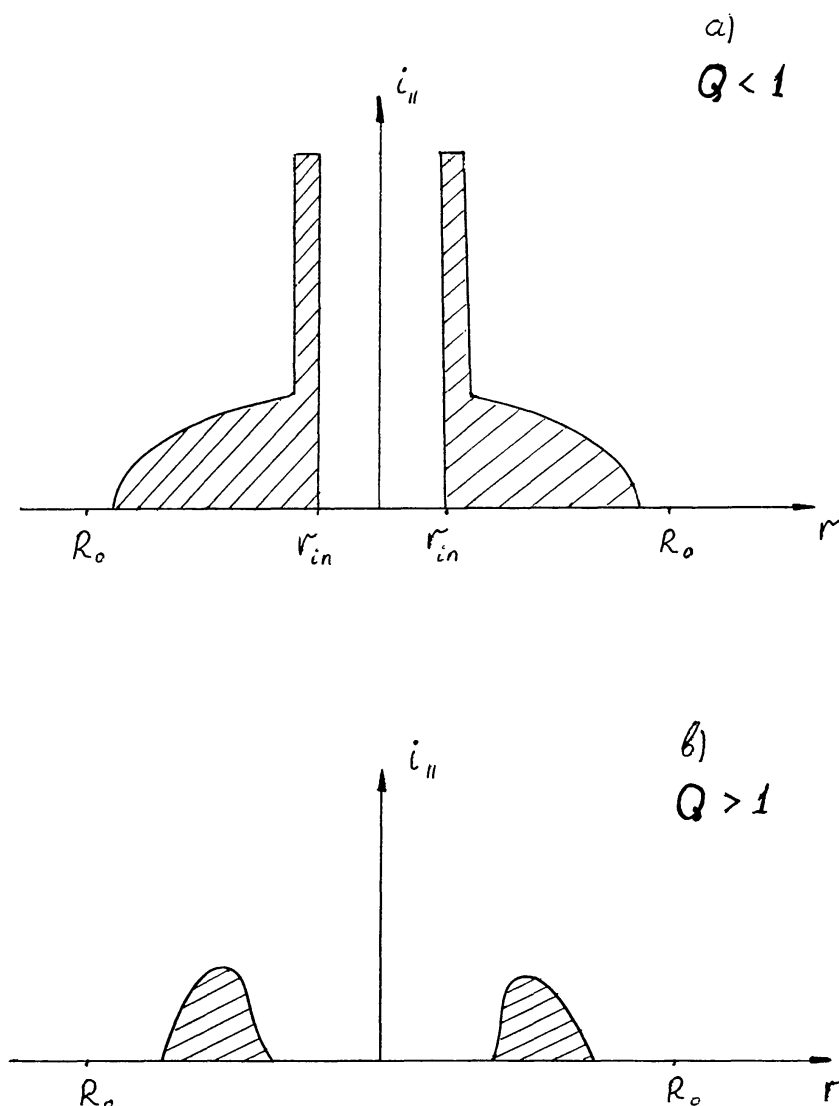


Fig. 1. Profile of current running in pulsar magnetosphere in the region of open field lines: (a) pulsars with $Q < 1$; (b) pulsars with $Q > 1$.

Now let us proceed to the discussion of the properties of secondary electron-positron plasma. According to Tadamaru (1973), Ruderman and Sutherland (1975), Daugherty and Harding (1982), Gurevich and Istomin (1985), the particle energy of secondary plasma stretches from $\mathcal{E}_{\min}^+ = \gamma_{\min}^+ m_e c^2$ to $\mathcal{E}_{\max} \sim 10^5 m_e c^2$. For energies $\mathcal{E}^\pm < \mathcal{E}_{\min}^\pm$ the particle spectrum sharply breaks. Such a break, as has already been said, is due to the character of plasma generation. Low-energy photons are not absorbed in the magnetosphere and, therefore, do not produce low-energy particles. According to Ruderman and Sutherland (1975)

$$\gamma_{\min}^{(0)} \simeq 200-400. \quad (2.5)$$

As to the region of energies $\mathcal{E}_{\min}^\pm < \mathcal{E}^\pm < \mathcal{E}_{\max}$, here for the fields $B_0 < 5 \times 10^{12}$ G the spectrum of secondary particles is close to the power-law one ($dN/d\gamma \propto \gamma^{-\bar{\nu}}$) with the

factor $\bar{\nu}$ close to two (Tademaru, 1973; Daugherty and Harding, 1982). As is well known, this case corresponds to energy equipartition about the spectrum. Figure 2 gives an example of such a spectrum borrowed from the paper by Daugherty and Harding (1982).

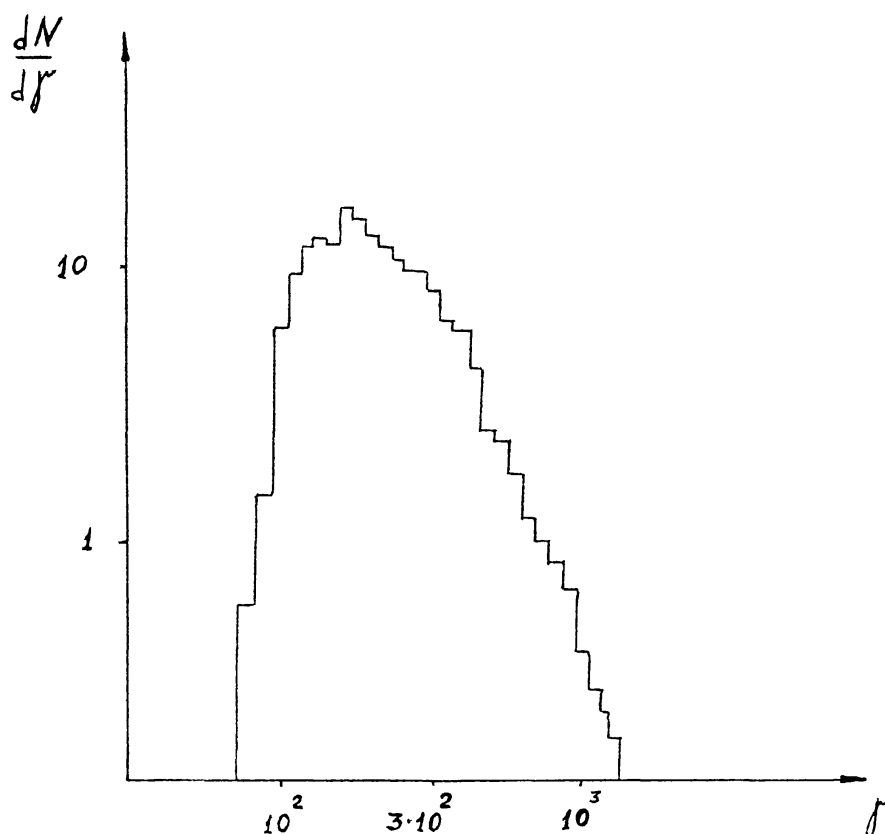


Fig. 2. An example of the spectrum of a secondary electron-positron plasma generated by a primary particle of energy 10^{13} eV (Daugherty and Harding, 1983).

We should stress, however, that the functions of electron and positron distribution in pulsar magnetosphere do not, generally speaking, coincide with each other, the lowest particle energy being smaller than (2.5). The point is that under quasi-neutral conditions an outflowing plasma is known to screen the longitudinal component of the electric field E_{\parallel} . For this it is necessary that the density of the electric charge contained in the plasma ρ_e should be close to the corotation charge density ρ_c (2.3) (Goldreich and Julian, 1969). The charge density in an accelerated particle beam is not, generally speaking, equal to ρ_c . Therefore, in the region of a quasi-neutral plasma, a relatively weak longitudinal electric field appears that decelerates one of the plasma components and accelerates the other due to which the density ρ_c is created and maintained in the magnetosphere. The jump of the potential $\Delta\Psi$ which creates this field is small

$$e |\Delta\Psi|/m_e c^2 \lesssim \gamma_{\min}^{(0)}.$$

It is much smaller than the jump of the potential Ψ in the region of acceleration and generation of particles.

The total electric current I running within a given tube of field lines must be conserved. As a result, we derive two equations that determine the quantities γ_{\min}^+ and γ_{\min}^- :

$$n^+ - n^- = (1 - i_0)\rho_c/|e|;$$

$$\frac{n^+}{\gamma_{\min}^{+2}} - \frac{n^-}{\gamma_{\min}^{-2}} = 2 \frac{\bar{v} + 1}{\bar{v} - 1} (1 - i_0)\rho_c/|e|,$$

which under the condition $\gamma_{\min}^{(0)2} \gg \lambda$ give

$$\gamma_{\min}^+ = \left[\frac{(\bar{v} - 1)}{2(\bar{v} + 1)(1 - i_0)} \lambda \right]^{1/2} \simeq \lambda^{1/2}; \quad \gamma_{\min}^- \simeq \gamma_{\min}^{(0)} \quad \text{at } \rho_c > 0;$$

$$\gamma_{\min}^+ \simeq \gamma_{\min}^{(0)}; \quad \gamma_{\min}^- = \left[\frac{(\bar{v} - 1)}{2(\bar{v} + 1)(1 - i_0)} \lambda \right]^{1/2} \simeq \lambda^{1/2} \quad \text{at } \rho_c < 0.$$
(2.6)

We see that the sign at the charge of the slow component coincides with the sign at the corotation charge (2.3), i.e., with the sign at the charge of the primary beam. Since $\lambda^{1/2} \simeq 10^2$, the characteristic energy of one of the components must be several times smaller than that of the other (Cheng and Ruderman, 1977). Since slow particles have a smaller mass, they play the role of electrons, whereas fast particles play the role of ions in an ordinary plasma.

Thus, in the region of open field lines a magnetospheric plasma represents relativistic fluxes of electrons and positrons whose mean energies are distinct. We, henceforth, assume for simplicity that the slow component corresponds to a certain type of particles, for instance, electrons and the fast component to positrons.

2.2. MODELS OF PULSAR RADIO EMISSION

The general picture presented above has made it possible, in spite of the absence of a quantitative theory to make several assertions concerning the properties of observed radio emission. First of all, a phenomenological model of an 'hollow cone' was formulated (Ruderman and Sutherland, 1975; Oster and Sieber, 1976) which explained qualitatively some characteristics of radio emission (Backer, 1976; Taylor and Stinebring, 1986). This model was constructed under the assumption that the radiation intensity is determined by a plasma flux along open field lines in pulsar magnetosphere. Since, as has already been mentioned, a secondary plasma cannot be generated near the magnetic axis, the directivity pattern of radio emission, as shown in Figure 3, must also have the form of an hollow cone. The external opening of the pattern is determined by the opening of the unclosed field lines whereas the internal by the condition (2.4). As a result, the hollow cone model, in which the form of the directivity pattern repeats the profile of the outflowing plasma density, made it possible to explain qualitatively not only the existence of 'two-hump' and 'one-hump' average profiles (Backer, 1976; Beskin *et al.*, 1984; Taylor and Stinebring, 1986), but also some polarization and frequency characteristics of observed radio emission (Rankin, 1983a, b).

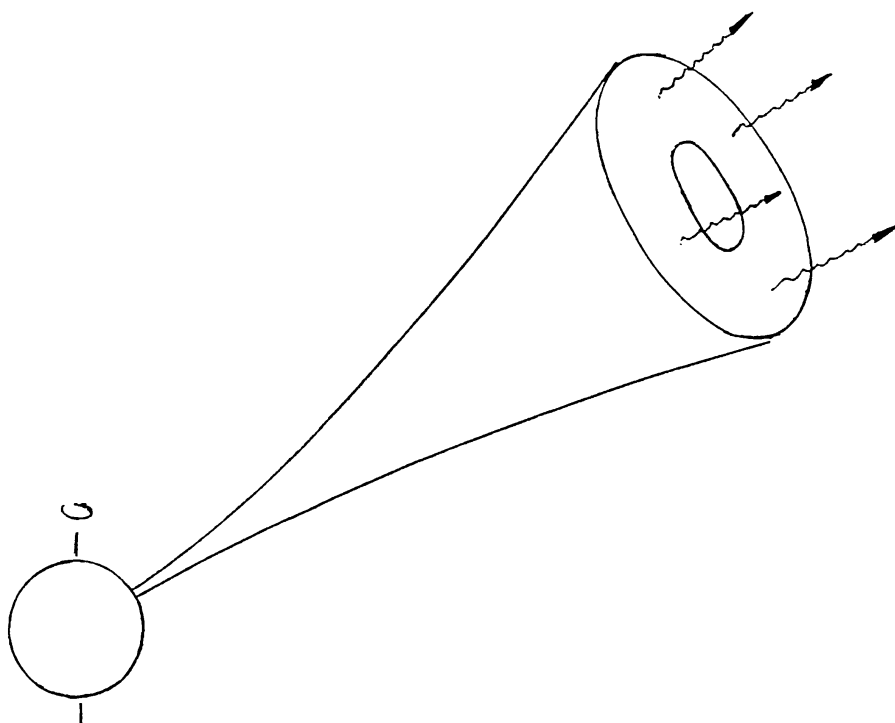


Fig. 3. The 'hollow cone' model.

Besides, some processes were investigated which could in principle lead to the explanation of the coherence mechanism. These are, firstly, several plasma instabilities and nonlinear phenomena possible in a relativistic electron-positron plasma of a pulsar (Hinata, 1976; Benford and Buschauer, 1977; Cheng and Ruderman, 1977; Lominadze *et al.*, 1979, 1983; Suvorov and Chugunov, 1980; Asseo *et al.*, 1980, 1983; Gedalin and Machabeli, 1983; Michailovski *et al.*, 1985a; Verga and Fontan, 1985; Usov, 1987). These instabilities could be responsible for particle bunching necessary in the antenna coherence mechanism. On the other hand, the plasma waves themselves could be transformed into transverse ones due to nonlinear processes and, therefore, lead to the observed radio emission (Michailovskii, 1980; Onischenko, 1981; ter Haar and Tsytovich, 1981). Indeed, making use of the relations (2.2) and (2.6) we obtain that at distances $r \sim (10-100)R$ from the star surface the characteristic frequency $\nu_p \sim \omega_p/\gamma_{\min}^{3/2}$, where

$$\omega_p = (4\pi e^2 n_e / m_e)^{1/2}$$

gets into the range 100 MHz–10 GHz, i.e., just coincides with the frequencies of the observed pulsar radio emission. It should also be noted that because the particle motion in a strong magnetic field is one-dimensional, the characteristic plasma frequency $\nu_p \sim \gamma^{-3/2}$ so far as

$$\delta v_{\parallel} = \delta p_{\parallel} / m_e \gamma^3.$$

Secondly, additional consideration were expressed in favour of the maser amplification mechanism (Ginzburg *et al.*, 1969). Indeed, we may regard a relativistic plasma

flowing out of the pulsar magnetosphere as a system with an inverse particle population with respect to energies. The energy losses (i.e., transition onto lower energy levels) are due to the so-called 'curvature' radiation connected with the particle motion along curved field lines (Radhakrishnan and Cocke, 1969; Ochelkov and Usov, 1980). Such losses play the principal role if particles are on lower Landau levels, i.e., when their synchrotron radiation is absent. That is why transverse waves in the pulsar magnetosphere could also be expected to be unstable.

Recall that the theory of curvature radiation of one particle can be easily obtained from the well-known formulae for synchrotron radiation (Landau and Lifshitz, 1975) by way of replacing the Larmor radius $r_B = v\mathcal{E}/eBc$ by the radius of magnetic field line curvature ρ . In particular, the expression for the spectral power of curvature radiation of one particle has the form

$$\mathcal{P}_\omega = \frac{\sqrt{3}}{2\pi} \frac{e^2}{\rho} \frac{\mathcal{E}}{m_e c^2} \frac{\omega}{\omega_c} \int_{\omega/\omega_c}^{\infty} K_{5/3}(y) dy, \quad (2.7)$$

where $K_{5/3}$ is the McDonald function and the frequency

$$\omega_c = \frac{3}{2} \frac{c}{\rho} \left(\frac{\mathcal{E}}{m_e c^2} \right)^3 \quad (2.8)$$

is close to the frequency of maximal radiation. If we substitute into the last formula the value $\rho \sim (10^8 - 10^9)$ cm (which corresponds to distances 10–100 km from the neutron star) and the characteristic energy (2.6) $\mathcal{E} \simeq 100 m_e c^2$ of the secondary electron-positron plasma, then the frequency of curvature radiation again gets in the range 100 MHz–10 GHz, i.e., also coincides with the frequencies of observed radio emission.

Thus, on the basis only of the theory of plasma production in pulsar magnetosphere we have come in a natural way to radio band frequencies. This fact was used in many radioemission theories both within the antenna (Komesaroff, 1970; Goldreich and Keeley, 1971; Buschauer and Benford, 1978; Cheng and Ruderman, 1977) and maser (Blandford, 1975; Kawamura and Suzuki, 1977; Melrose, 1978; Shaposhnikov, 1981) mechanisms. In particular, in the framework of the maser amplification mechanism numerous attempts were made to find natural modes of electromagnetic oscillations for which the reabsorption coefficient μ_j would appear to be negative because of closeness of the frequency ω_c to the observed frequency range (Kawamura and Suzuki, 1977; Melrose, 1978; Shaposhnikov, 1981; Chugunov and Shaposhnikov, 1988). This problem has not, however, been solved.

The point is that the main progress of the theory was connected mainly with the problem of natural modes of relativistic plasma oscillations in a homogeneous magnetic field (Godfrey *et al.*, 1975; Suvorov and Chugunov, 1975; Hardee and Rose, 1976; Hardee and Morrison, 1979; Lominadze *et al.*, 1979, 1983; Volokitin *et al.*, 1985; Arons

and Barnard, 1986), when the basic effect – the curvature radiation – is absent. An accurate account of the curvature of magnetic field lines, i.e., an account of the effects due to curvature radiation required solution of the problem concerning the dielectric properties of inhomogeneous relativistic plasma which, as been mentioned above, has been solved only recently (Beskin *et al.*, 1987b; Istomin, 1988).

Since this problem has not been solved, the influence of the curvature of magnetic field lines has been taken into account either in the framework of the Einstein's coefficients method (Shaposhnikov, 1981) or within some other approximations (Hinata, 1976; Asseo *et al.*, 1980, 1983) which did not provide the necessary characteristics of natural mode oscillations*. For example, in the paper by Chugunov and Shaposhnikov (1988) which is the most advanced in our opinion, in a dense plasma one can only establish the connection of the total optical depth $\tau_j = \int \mu_j dl$ of a normal mode j with its refractive index n_j and the polarization coefficient \mathcal{K}_j whose values remain unknown. In the case of not a dense plasma, where the Einstein's coefficients method is valid, no substantial wave amplification occurs (Chugunov and Shaposhnikov, 1988). What has been said above refers in full measure also to a nonlinear interaction of normal waves, which was considered in the majority of paper only for the case of a homogeneous magnetic field (Hinata, 1976; Lominadze *et al.*, 1979, 1983; Michailovskii, 1980; Onischenko, 1981; ter Haar and Tsytovich, 1981; Michailovskii *et al.*, 1985a).

Thus, to determine the dielectric properties of a relativistic inhomogeneous plasma, including the character of nonlinear interaction, is the key problem in the analysis of the possibility of maser amplification of electromagnetic waves in pulsar magnetosphere. Our paper is devoted just to this problem. But before proceeding to it, we will present the basic results of the linear theory for the case of a homogeneous magnetic field, which we will use henceforth.

2.3. DIELECTRIC PERMITTIVITY OF A HOMOGENEOUS PLASMA

Consider a relativistic electron-positron plasma placed in a strong homogeneous magnetic field \mathbf{B} . Since the external field \mathbf{B} is strong, all particles in a non-excited state are located on lower Landau levels. The unperturbed distribution function of electrons and positrons should, therefore, be written in the form (Suvorov and Chugunov, 1973)

$$F^\pm(\mathbf{p}) = F_\parallel^\pm(p_\parallel)\delta(\mathbf{p}_\perp), \quad (2.9)$$

where p_\parallel and \mathbf{p}_\perp are longitudinal and transverse components of the momentum. Choosing now the z -axis along the direction of the magnetic field and the wave vector \mathbf{k} in the xz -plane, we obtain the following expression for the dielectric tensor $\varepsilon_{\alpha\beta}(\omega, \mathbf{k})$

* In papers of Asseo *et al.* (1980, 1983) and recently published paper of Larroche and Pellat (1987) the cylindrical wave modes propagating in relativistic plasma along the curvilinear strong magnetic field were postulated. The waves are unstable only in the strongly inhomogeneous plasma. Such formulation of the problem is far from the real conditions in pulsar magnetosphere, where the cylindrical modes and sharp gradients are absent.

(Godfrey *et al.*, 1975; Suvorov and Chugunov, 1975; Hardee and Rose, 1975):

$$\varepsilon_{\alpha\beta} = \begin{pmatrix} 1 + \left\langle \frac{\omega_p^2 \gamma \tilde{\omega}^2}{\omega^2 (\omega_B^2 - \gamma^2 \tilde{\omega}^2)} \right\rangle; & i \left\langle \frac{\omega_p^2}{\omega^2} \frac{\omega_B \tilde{\omega}}{(\omega_B^2 - \gamma^2 \tilde{\omega}^2)} \right\rangle; & \left\langle \frac{\omega_p^2}{\omega^2} \frac{\gamma k_x v_{\parallel} \tilde{\omega}}{(\omega_B^2 - \gamma^2 \tilde{\omega}^2)} \right\rangle \\ -i \left\langle \frac{\omega_p^2}{\omega^2} \frac{\omega_B \tilde{\omega}}{(\omega_B^2 - \gamma^2 \tilde{\omega}^2)} \right\rangle; & 1 + \left\langle \frac{\omega_p^2 \gamma \tilde{\omega}^2}{\omega^2 (\omega_B^2 - \gamma^2 \tilde{\omega}^2)} \right\rangle; & -i \left\langle \frac{\omega_p^2}{\omega^2} \frac{\omega_B k_x v_{\parallel}}{(\omega_B^2 - \gamma^2 \tilde{\omega}^2)} \right\rangle \\ \left\langle \frac{\omega_p^2 \gamma k_x v_{\parallel} \tilde{\omega}}{\omega^2 (\omega_B^2 - \gamma^2 \tilde{\omega}^2)} \right\rangle; & i \left\langle \frac{\omega_p^2}{\omega^2} \frac{\omega_B k_x v_{\parallel}}{(\omega_B^2 - \gamma^2 \tilde{\omega}^2)} \right\rangle; & 1 - \left\langle \frac{\omega_p^2}{\gamma^2 \tilde{\omega}^2} \right\rangle + \\ & & + \left\langle \frac{\omega_p^2}{\omega^2} \frac{\gamma k_x^2 v_{\parallel}^2}{\omega^2 (\omega_B^2 - \gamma^2 \tilde{\omega}^2)} \right\rangle \end{pmatrix}; \quad (2.10)$$

where

$$\omega_p^2 = \frac{4\pi n_e^{\pm} e^2}{m_e}, \quad \omega_B = \frac{eB}{m_e c}; \quad \tilde{\omega} = \omega - k_z v_{\parallel}; \quad \gamma = \left(1 - \frac{v_{\parallel}^2}{c^2}\right)^{-1/2}.$$

In what follows, brackets $\langle \rangle$ stand for averaging over the longitudinal distribution function $F_{\parallel}^{\pm}(p_{\parallel})$ and summation over the types of particles

$$\langle \cdots \rangle = \sum_{e^+, e^-} \int_{-\infty}^{\infty} dp_{\parallel} \cdots F_{\parallel}^{\pm}(p_{\parallel}),$$

where $\int_{-\infty}^{\infty} dp_{\parallel} F^{\pm}(p_{\parallel}) = 1$. It is interesting that Equation (2.10) can also be derived as a result of quantum calculus (Canuto and Ventura, 1972) which takes into account a discrete character of the transverse energy of particles.

First of all note one fact which will, henceforth, be of use. It concerns the cyclotron resonance the condition for which can be written in the form

$$\omega_B/\gamma = \omega - k_z v_{\parallel}.$$

For a secondary electron-positron plasma this relation is fulfilled only at distances $r \sim R_c$, where

$$R_c \simeq 2 \times 10^3 R \left(\frac{B_0}{10^{12} \text{ G}} \right)^{1/3} \left(\frac{v}{1 \text{ GHz}} \right)^{-1/3} \left(\frac{\gamma}{100} \right)^{-1/3} \left(\frac{\tilde{\omega}}{\omega} \right)_{0.01}^{-1/3} \quad (2.11)$$

and for fast-rotating pulsars R_c is outside the light cylinder (Michailovskii *et al.*, 1982; Gedalin and Machabeli, 1983). At small distances $r \ll R_c$ from the star surface, the characteristic frequencies satisfy the inequalities

$$\tilde{\omega} \ll \omega \ll \omega_B/\gamma \ll \omega_B. \quad (2.12)$$

Consequently, here one can disregard the terms $\tilde{\omega}^2 \gamma^2$ as compared with ω_B^2 . As a result, at small distances from the star (2.12), ‘cyclotron’ corrections to unity in the expression (2.10) for the dielectric permittivity tensor prove to be small (Elitzur, 1974):

$$\delta\epsilon_{xx} = \delta\epsilon_{yy} \simeq \left\langle \frac{\omega_p^2 \gamma \tilde{\omega}^2}{\omega^2 \omega_B^2} \right\rangle \sim 10^{-14} - 10^{-20}. \quad (2.13)$$

The main role in the dielectric properties of plasma must be played by the ‘Cherenkov’ correction,

$$\delta\epsilon_{zz} = - \left\langle \frac{\omega_p^2}{\gamma^3 \tilde{\omega}^2} \right\rangle. \quad (2.14)$$

A smallness of the cyclotron correction as compared with the Cherenkov one is due both to a large magnitude of the magnetic field and to a small quantity $\tilde{\omega} = \omega - k_z v_{\parallel}$ in the numerator of (2.13) and in the denominator of the cyclotron correction (2.14).

Consequently, we can draw an important conclusion that the main dispersion characteristics of normal modes propagating in pulsar magnetosphere can be obtained in the approximation of an infinitely strong magnetic field. The effects due to cyclotron resonance are in this approximation, of course, disregarded. As was shown by Michailovskii *et al.* (1982, 1985b), the cyclotron absorption possible at large distances from the star surface does not, however, have a decisive effect upon propagation of transverse waves and can be taken into account separately. As regards the dielectric permittivity tensor (2.10), in the infinite magnetic field approximation it takes an especially simple form

$$\epsilon_{\alpha\beta} = \begin{pmatrix} 1 & 0 & 0 \\ 0 & 1 & 0 \\ 0 & 0 & 1 - \left\langle \frac{\omega_p^2}{\gamma^3 \tilde{\omega}^2} \right\rangle \end{pmatrix}. \quad (2.15)$$

2.4. NORMAL MODES OF ELECTROMAGNETIC OSCILLATIONS

First of all we are now interested in the normal modes of oscillations whose frequencies are close to radio-frequency range. As distinct from the majority of previous papers in which the analysis was carried out in the rest system of plasma (Lominadze *et al.*, 1979, 1983; Gedalin and Machabeli, 1983), we will write the expressions for the refractive indices $n_j = ck_j/\omega$ in the laboratory coordinate system. Such a choice is explained by the fact that only in this case does a correct (without involving non-inertial coordinate systems) transition to the case of a curved magnetic field become possible. Besides, no questions concerning the Lorentz-frequency transformation in a transition from one frame of reference into another arise.

Owing to the simple form of the dielectric permittivity tensor (2.15) the solutions of

the dispersion equation

$$\det(n^2 \delta_{\alpha\beta} - n_\alpha n_\beta - \varepsilon_{\alpha\beta}) = 0$$

can be written in an explicit form

$$n_1^2 = 1; \quad (2.16)$$

$$n^2 = 1 - \theta^2 \left\langle \frac{\omega_p^2}{\gamma^3 \tilde{\omega}^2} \right\rangle. \quad (2.17)$$

In what follows, we consider only the most interesting for us case of small angles θ between the vectors \mathbf{k} and \mathbf{B} . As is seen from the analysis of the relations (2.16) and (2.17), in the electron-positron plasma there exist four normal oscillation modes whose frequencies lie in the radio range. The dependence of their refractive indices n_j on the angle θ is shown in Figure 4. Figure 4(a) corresponds to the condition

$$A \equiv \frac{\omega_p^2 \gamma_c}{\omega^2} \ll 1,$$

where $\gamma_c = \langle \gamma^{-3} \rangle^{-1/3}$, which is fulfilled at distances

$$r > R_A = 100R \left(\frac{\lambda}{10^4} \right)^{1/3} \left(\frac{\gamma}{100} \right)^{1/3} \left(\frac{B}{10^{12} \text{ G}} \right)^{1/3} \left(\frac{P}{1 \text{ s}} \right)^{-1/3} \left(\frac{v}{1 \text{ GHz}} \right)^{-2/3}$$

from the surface of a neutron star, and Figure 4(b) corresponds to the condition $A \gg 1$ valid at small distances.

We can see that both for angles $\theta \ll \theta_*$ and $\theta \gg \theta_*$, where

$$\theta_* = \left(\frac{\omega_p^2}{\omega^2} \left\langle \frac{1}{\gamma^3} \right\rangle \right)^{1/4}, \quad (2.18)$$

two plasma (l -modes) and two transverse (t -modes) normal waves of radio range can propagate in magnetospheric plasma. Note also the possibility of mutual transformation of t - and l -modes for $A \gg 1$ in the range of angles $\theta \sim \theta_*$.

The solutions of Equations (2.16) and (2.17) determining the dispersion properties of normal waves can be written in an explicit form. We shall do this for the case $A \gg 1$, which is the most interesting one as will be shown below.

First of all, the equality (2.16) corresponds to a linearly polarized transverse wave t_1 whose electric vector is perpendicular to the plane containing the vectors \mathbf{k} and \mathbf{B} . As we see, the refractive index n_1 of this wave is identical unity. This is not surprising because in an infinite magnetic field a free motion of particles across magnetic field lines is impossible. For this reason the response of such a medium to any wave whose electric vector is perpendicular to the external magnetic field is equal to zero. We shall call it an 'extraordinary' wave.

The properties of the other three normal waves are determined by the relation (2.17).

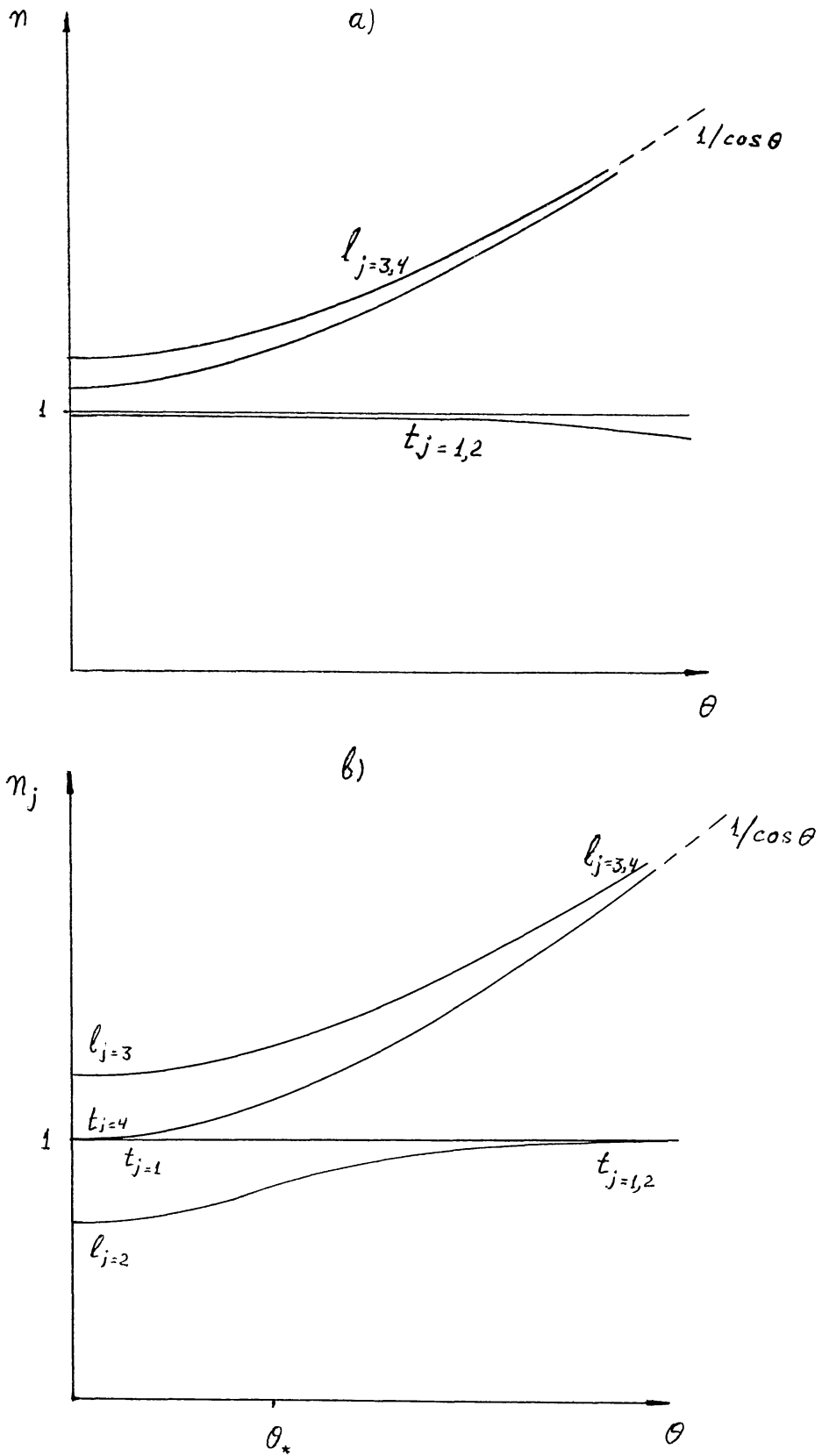


Fig. 4. Normal oscillation modes of a relativistic electron-positron plasma in a strong magnetic field: (a) $A \ll 1$; (b) $A \gg 1$.

When $A \gg 1$, it can be written in the form

$$n^2 = 1 - \theta^2 \frac{1}{\tilde{\omega}^2} \left\langle \frac{\omega_p^2}{\gamma^3} \right\rangle. \quad (2.19)$$

The possibility to take the quantity $\tilde{\omega} = \omega(1 - n(v_{\parallel}/c) \cos \theta)$ outside the sign of averaging over the distribution function of particles is connected just with fulfillment of the condition $A \gg 1$. This means that for $A \gg 1$ we may put $v_{\parallel} = c$ in the expression for $\tilde{\omega}$. Consequently, in the region $A \gg 1$ normal waves in the radio-frequency range are, in fact, hydrodynamic modes.

As a result, the relation (2.19) give the following expressions for the refractive indices of the normal modes

$$n_2 = 1 + \theta^2/4 - \left(\left\langle \frac{\omega_p^2}{\omega^2 \gamma^3} \right\rangle + \frac{\theta^4}{16} \right)^{1/2}; \quad (2.20a)$$

$$n_3 = 1 + \theta^2/4 + \left(\left\langle \frac{\omega_p^2}{\omega^2 \gamma^3} \right\rangle + \frac{\theta^4}{16} \right)^{1/2}; \quad (2.20b)$$

$$n_4 = 1 + \theta^2/2 = 1/\cos \theta. \quad (2.20c)$$

Polarization of the normal waves is determined by the relations

$$(E_x/E_z)_2 = -\frac{\theta}{2} \left[\left(\left\langle \frac{\omega_p^2}{\omega^2 \gamma^3} \right\rangle + \frac{\theta^4}{16} \right)^{1/2} + \frac{\theta^2}{4} \right]^{-1/2}; \quad (2.21a)$$

$$(E_x/E_z)_3 = -\frac{\theta}{2} \left[\left(\left\langle \frac{\omega_p^2}{\omega^2 \gamma^3} \right\rangle + \frac{\theta^4}{16} \right)^{1/2} - \frac{\theta^2}{4} \right]^{-1/2}; \quad (2.21b)$$

$$(E_x/E_z)_4 \simeq \frac{1}{4} \frac{\theta}{A} \frac{1}{\gamma_c^4} \ll 1. \quad (2.21c)$$

The corrections to the relations (2.20) and (2.21) are presented, for example, by Lominadze and Pataraya (1982).

It is readily seen that for angles $\theta \ll \theta_*$ the normal modes $j = 2, 3$ are purely longitudinal, and (Lominadze *et al.*, 1979)

$$n_{2,3} = 1 \pm \left(\left\langle \frac{\omega_p^2}{\gamma^3} \right\rangle \frac{1}{\omega^2} \right)^{1/2}. \quad (2.22)$$

But as is seen from Figure 4(b), they behave differently with increasing θ . For angles $\theta \gg \theta_*$ the normal wave $j = 2$ becomes a transverse electromagnetic wave with $n_2 \approx 1$ whose electric vector lies in a plane containing vectors \mathbf{k} and \mathbf{B} . We shall call it an 'ordinary' mode*. As to the normal wave $j = 3$, for large angles θ its refractive index

* The chosen terminology corresponds to the determination of ordinary and extraordinary waves in magnetoactive plasma when the magnetic field approaches to infinity ($\omega_B \gg \omega$). We must notice that in the paper of Beskin *et al.* (1987a) the designations were *vice versa*.

tends to the value (2.20b), which corresponds to dispersion of the 'drift' or Alfvén type $\omega = \mathbf{k}\mathbf{v}$. Note that the energy of this wave is negative because in a coordinate system moving with a particle flux it has a negative frequency $\omega' = \gamma\tilde{\omega} < 0$.

Finally, the fourth normal mode $j = 4$ is a purely drift or Alfvén wave (2.20c) in the entire range of angles.

2.5. THE CYCLOTRON-RESONANCE REGION

In conclusion we make some remarks concerning the cyclotron resonance region $r \simeq R_c$. The point is that up to now an analysis of cyclotron absorption has been carried out in the assumption that the distribution functions of electrons and positrons practically coincide (Hardee and Rose, 1976; Hardee and Morrison, 1979; Michailovskii *et al.*, 1982; Gedalin and Machabeli, 1983; Beskin *et al.*, 1987a). As a result, the nondiagonal components ε_{xy} , ε_{yx} , ε_{yz} , ε_{zy} of the dielectric permittivity tensor (2.10) which are odd in the electric charge e turned out to be identical zeros, and this made the problem much simpler.

When the distribution functions of electrons and positrons do not coincide, this is generally speaking not the case. Indeed, making use of the fact that at large distances from the star

$$|1 - n| \ll 1/\gamma_{\min}^2 \ll \theta^2, \quad (2.23)$$

so that $\tilde{\omega} = \frac{1}{2}\omega(\gamma^{-2} + \theta^2)$, we obtain, for instance, that

$$\varepsilon_{xy} = -\varepsilon_{yx} = i \left\langle \frac{\omega_p^2 \omega_B}{\omega^2} \frac{\tilde{\omega}}{(\omega_B^2 - \gamma^2 \tilde{\omega}^2)} \right\rangle \simeq \frac{i}{2} \frac{\omega_p^2}{\omega \omega_B} \left\langle \frac{1}{\gamma^2} \right\rangle_{\pm},$$

where

$$\left\langle \frac{1}{\gamma^2} \right\rangle_{\pm} = \left\langle \frac{\text{sign } e}{\gamma^2} \right\rangle \equiv \left\langle \frac{1}{\gamma^2} \right\rangle_{+} - \left\langle \frac{1}{\gamma^2} \right\rangle_{-} \sim \left\langle \frac{1}{\gamma^2} \right\rangle \neq 0$$

and, therefore, $\varepsilon_{xy} \neq 0$, $\varepsilon_{xz} \neq 0$. The quantity ε_{xy} turns out generally speaking not small as compared with $\delta\varepsilon_{xx} = \varepsilon_{xx} - 1$.

First of all, we shall be interested here in transverse modes for which $n^2 \simeq 1$. Employing the explicit form of the tensor $\varepsilon_{\alpha\beta}$ (2.10), we obtain

$$n_{1,2}^2 = 1 + \varepsilon_{\perp\perp} - \frac{\theta}{2} S + \frac{\theta^2}{2} \delta\varepsilon_{zz} \pm \frac{1}{2} [(\theta^2 \delta\varepsilon_{zz} - \theta S)^2 - 4(\varepsilon_{xy} + \theta\varepsilon_{yz})^2]^{1/2}, \quad (2.24)$$

where the quantities $\varepsilon_{\perp\perp} = \varepsilon_{xx} - 1 = 1 - \varepsilon_{yy}$, $S = \varepsilon_{xz} + \varepsilon_{zx}$, $\delta\varepsilon_{zz} = \varepsilon_{zz} - 1$ are small as compared with unity, and we are dealing only with the region of small angles $\theta \ll 1$. Polarization of the normal modes is determined by the relation

$$\left(\frac{E_x}{E_y} \right)_{1,2} = - \frac{\theta^2 \delta\varepsilon_{zz} - \theta S \pm [(\theta^2 \delta\varepsilon_{zz} - \theta S)^2 - 4(\varepsilon_{xy} + \theta\varepsilon_{yz})^2]^{1/2}}{2i |\varepsilon_{xy}|}. \quad (2.25)$$

The leading terms in (2.24) and (2.25) are, infact, $\varepsilon_{\perp\perp}$, ε_{xy} , and $\theta^2 \delta\varepsilon_{zz}$. The plus sign in Equations (2.24) and (2.25) corresponds to an extraordinary and the minus sign to an ordinary wave.

As has already been mentioned, at small distances from the star $z \ll R_c$, the main contribution in the expressions (2.24) and (2.25) is made by the 'Cherenkov' correction (2.14). The condition of smallness of the quantity ε_{xy} as compared with $\theta^2 \delta\varepsilon_{zz}$ can be written in the form $\mu_c \ll 1$, where

$$\mu_c = \frac{\varepsilon_{xy}}{\theta^2 \delta\varepsilon_{zz}} \simeq \frac{\tilde{\omega}}{\omega_B} \frac{\left\langle \frac{1}{\gamma^2} \right\rangle_{\pm}}{\left\langle \frac{1}{\gamma^3} \right\rangle}.$$

But, as can be easily verified, in the cyclotron-resonance region $r \simeq R_c$, where $\omega_B \simeq \gamma_c \tilde{\omega} = \frac{1}{2} \gamma \omega \theta^2$, the condition $\mu_c \ll 1$ is violated. Since according to (2.25)

$$\left(\frac{E_x}{E_y} \right)_{1,2} = \frac{1 \pm (1 + 4\mu_{\text{res}})^{1/2}}{2i\mu_{\text{res}}},$$

so that

$$(E_x/E_y)_1 \simeq i\mu_{\text{res}}; \quad (E_x/E_y)_2 \simeq -i/\mu_{\text{res}}, \quad (2.26)$$

where now $\mu_{\text{res}} = \langle 1/\gamma^2 \rangle_{\pm} \langle 1/\gamma^3 \rangle^{-1} \gamma_{\text{res}}^{-1} \lesssim 1$, we arrive at the conclusion that in the cyclotron resonance region the normal wave polarization contains a noticeable circular component. At the same time, the ratio

$$\frac{\varepsilon_{xy}}{\varepsilon_{\perp\perp}} \simeq \frac{1}{\theta_{\text{res}}^2} \left\langle \frac{1}{\gamma^2} \right\rangle_{\pm}$$

remains less than unity in the region $r \simeq R_c$ because, according to (2.23), $\theta_{\text{res}}^2 \gg \langle 1/\gamma^2 \rangle_{\pm}$.

Thus, the above analysis demonstrates that the main contribution in the cyclotron absorption (as in the case of identical distribution functions of electrons and positrons, Michailovskii *et al.*, 1982, 1985a, b; Beskin *et al.*, 1986, 1987a) is made by the quantity $\varepsilon_{\perp\perp}$; and, therefore,

$$\text{Im } n_{1,2} = \frac{1}{2} \text{Im} \left\langle \frac{\omega_p^2 \gamma}{\omega^2} \frac{\tilde{\omega}^2}{(\omega_B^2 - \gamma^2 \tilde{\omega}^2)} \right\rangle. \quad (2.27)$$

As regards polarization of normal waves, it substantially differs from the linear one near the cyclotron resonance. We make use of this fact in Section 6 in the analysis of observations.

3. Linear Electrodynamics of Relativistic Electron-Positron Plasma in a Curvilinear Magnetic Field

We have considered the electrodynamic properties of relativistic plasma in a homogeneous magnetic field. But, the most important for the curvature mechanism of electromagnetic wave excitation is the fact that plasma particles move along a curvilinear magnetic field because it is only in this case that there occurs curvature radiation. The curvature radius of a magnetic field line ρ exceeds greatly the radiated wavelength $\lambda_w \sim \rho/\gamma^3$ (2.8). But the radiation processes are characterized not by the wavelength but by the formation length $\sim \rho/\gamma$ which is much larger. The directivity pattern of radiation is so narrow ($\sim 1/\gamma$) that on the length equal to the formation length the radiation oversteps the boundaries of amplification cone. Hence, inhomogeneity plays a decisive role in generation of curvature radiation. Besides, since all plasma particles move at velocities close to the velocity of light, also possible is Cherenkov interaction of particles with oscillation modes whose refractive index is slightly more than unity. A simultaneous existence and interaction of curvature and Cherenkov radiations does not only completely determine the increments of wave amplification but also leads to the appearance of new important oscillation modes which do not exist in a homogeneous plasma.

3.1. DIELECTRIC PERMITTIVITY OF INHOMOGENEOUS PLASMA

Now let us proceed to the discussion of dielectric properties of a relativistic electron-positron plasma placed in a curved magnetic field. At each point introduce three vectors: \mathbf{b} in the direction of the magnetic field, \mathbf{n} along the normal, and \mathbf{l} along the binormal. As shown in Figure 5, these vectors correspond to an orthogonal coordinate system z, x, y .

As has been shown by Beskin *et al.* (1987a), the dielectric permittivity tensor

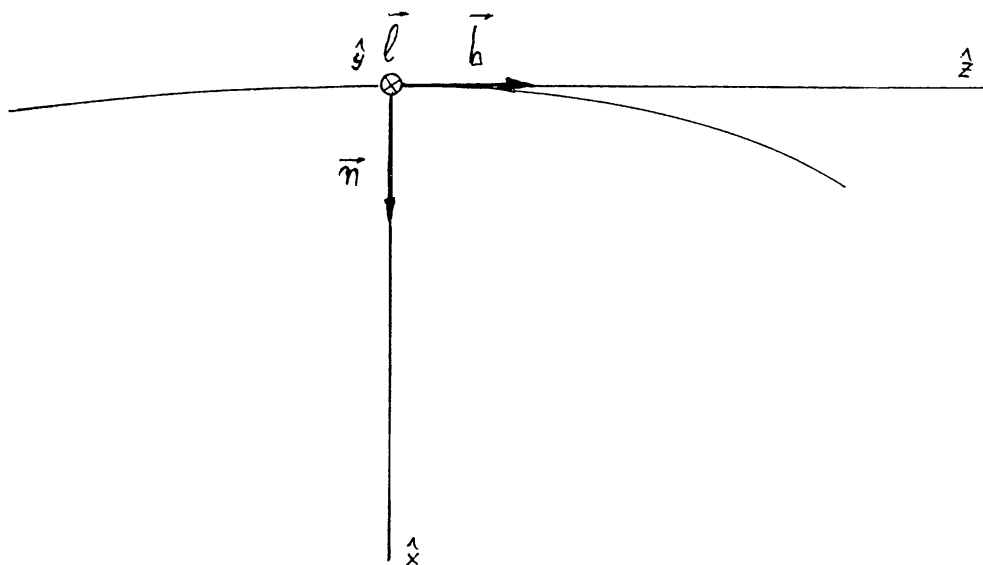


Fig. 5. A local coordinate system connected with a magnetic field line (z, x, y). $\mathbf{b}, \mathbf{n}, \mathbf{l}$ is a triplet of unit vectors.

$\varepsilon_{\alpha\beta}(\omega, \mathbf{k}, \mathbf{r})$ can be found in the following way. First it is necessary to establish the response of the medium to a plane wave

$$\mathbf{E} = \mathbf{E}^A \exp(-i\omega_0 t + i\mathbf{k}_0 \mathbf{r}), \quad (3.1)$$

$$\mathbf{B} = \frac{1}{\omega_0} [\mathbf{k}_0 \mathbf{E}^A] \exp(-i\omega_0 t + i\mathbf{k}_0 \mathbf{r}),$$

i.e., to calculate the conductivity tensor $\sigma_{\alpha\beta}^0(\omega, \mathbf{k}, \mathbf{r})$ which enters in the expression for the current

$$j_\alpha(\omega_0, \mathbf{k}_0, \mathbf{r}) = \sigma_{\alpha\beta}^0(\omega_0, \mathbf{k}_0, \mathbf{r}) E_\beta^A \exp(-i\omega_0 t + i\mathbf{k}_0 \mathbf{r}). \quad (3.2)$$

Since the medium is inhomogeneous, its response (3.2) is not already a plane wave, so that the tensor $\sigma_{\alpha\beta}^0$ depends besides ω and \mathbf{k} , also on the coordinate \mathbf{r} . This means, in particular, that normal waves in an inhomogeneous medium are not plane either. The effective dielectric permittivity tensor is determined in terms of the tensor $\sigma_{\alpha\beta}^0$ by the relations

$$\varepsilon_{\alpha\beta}(\omega, \mathbf{k}, \mathbf{r}) = \delta_{\alpha\beta} + \frac{4\pi i}{\omega} \sigma_{\alpha\beta}(\omega, \mathbf{k}, \mathbf{r}), \quad (3.3)$$

$$\sigma_{\alpha\beta}(\omega, \mathbf{k}, \mathbf{r}) = \int \int \frac{d\mathbf{k}' d\mathbf{R}}{(2\pi)^3} \sigma_{\alpha\beta}^0\left(\omega, \mathbf{k}', \mathbf{r} + \frac{\mathbf{R}}{2}\right) \exp[i(\mathbf{k}' - \mathbf{k})\mathbf{R}].$$

Let us recall that the expression (3.3) refers to a stationary medium when an unperturbed distribution function of particles does not depend on the time.

To find the response $\sigma_{\alpha\beta}^0(\omega, \mathbf{k}, \mathbf{r})$ we shall use the method of integration over trajectories (Shafranov, 1963) according to which the expression for the electric current induced by a plane wave (3.1) can be written as

$$j_\alpha(\omega_0, \mathbf{k}_0, \mathbf{r}, t) = -e^2 \sum_{e^+, e^-} n_e^\pm \int d\mathbf{p} v_\alpha \int_{-\infty}^t dt' \exp(-i\omega_0 t + i\mathbf{k}_0 \mathbf{r}') \times \\ \times \left\{ \mathbf{E}^A + \frac{1}{\omega_0} [\mathbf{v}' [\mathbf{k}_0 \mathbf{E}^A]] \right\} \frac{\partial F^\pm}{\partial \mathbf{p}(t')}; \quad (3.4)$$

where F^\pm is an unperturbed distribution function of particles whose trajectories are given by the functions $\mathbf{r}' = \mathbf{r}(t')$, $\mathbf{v}' = \mathbf{v}(t')$. Consequently,

$$\sigma_{\alpha\beta}^0(\omega, \mathbf{k}, \mathbf{r}) = -e^2 \sum_{e^+, e^-} n_e^\pm \int d\mathbf{p} v_\alpha \int_{-\infty}^t dt' \exp[i\omega(t - t') - i\mathbf{k}(\mathbf{r} - \mathbf{r}')] \times \\ \times \left\{ \delta_{\beta\gamma} \left(1 - \frac{\mathbf{k}\mathbf{v}'}{\omega} \right) + \frac{k_\gamma v'_\beta}{\omega} \right\} \frac{\partial F^\pm}{\partial p'_\gamma}. \quad (3.5)$$

When we substitute the conductivity tensor $\sigma_{\alpha\beta}^0(\omega, \mathbf{k}, \mathbf{r})$ (3.5) into the expression (3.3), we can integrate over \mathbf{k}' and \mathbf{R} . Taking into account that the quantity $\mathbf{r} - \mathbf{r}'$ in (3.5) is a function of the coordinate \mathbf{r} , momentum \mathbf{p} , and the time difference $t - t'$

$$\mathbf{r} - \mathbf{r}' = \mathbf{L}(\mathbf{r}, \mathbf{p}, t - t'),$$

we obtain

$$\begin{aligned} \sigma_{\alpha\beta} = & -e^2 \sum_{e^+, e^-} n_e^\pm \int d\mathbf{p} v_\alpha \int_{-\infty}^t dt' \exp[i\omega(t - t') - i\mathbf{k}\mathbf{R}^*] \det^{-1} \left(\delta_{\mu\nu} - \frac{1}{2} \frac{\partial L_\mu}{\partial r_\nu} \right) \times \\ & \times \left[\left(1 - \frac{\mathbf{k}\mathbf{v}'}{\omega} \right) \delta_{\beta\sigma} + \frac{k_\sigma v'_\beta}{\omega} + \frac{i}{2\omega} \frac{\partial}{\partial r_\sigma} v'_\beta - \frac{i}{2\omega} \delta_{\beta\sigma} \frac{\partial}{\partial r_\chi} v'_\chi \right] \frac{\partial F^\pm}{\partial p'_\sigma} \Big|_{\mathbf{r}=\mathbf{r}+\mathbf{R}^*/2}, \quad (3.6) \end{aligned}$$

where the vector $\mathbf{R}^*(\mathbf{r}, \mathbf{p}, t - t')$ is the solution of the expression

$$\mathbf{R}^* = \mathbf{L}(\mathbf{r} + \mathbf{R}^*/2, \mathbf{p}, t - t'). \quad (3.7)$$

We should emphasize that the operators $\partial/\partial\mathbf{r}$ acts also on the derivative $\partial F/\partial\mathbf{p}'$.

The expression (3.6) is also valid for any inhomogeneous medium as soon as the following conditions are satisfied

$$kL_c \gg 1, \quad \frac{\text{Im } k}{|\mathbf{k}|} \ll 1, \quad (3.8)$$

where L_c is the characteristic dimension of inhomogeneity, which in our case is equal to the curvature radius ρ of a magnetic field line; $\text{Im } k$ is the imaginary part of the wave vector, which is the space increment of wave amplification (or damping). As regards the distribution function of particles $F^\pm(\mathbf{p}, \mathbf{r})$ it will be anisotropic in a strong magnetic field of a neutron star (cf. Equation (2.9))

$$\begin{aligned} F^\pm(\mathbf{p}, \mathbf{r}) = & F_\parallel^\pm(p_\parallel) \delta(\mathbf{p}_\perp - \mathbf{p}_{dr}^\pm) = \\ = & \int dp_\parallel F_\parallel^\pm(p_\parallel) \delta[\mathbf{p} - p_\parallel \mathbf{b}(\mathbf{r}) - \mathbf{p}_{dr}^\pm], \quad (3.9) \end{aligned}$$

where $\int F_\parallel^\pm(p_\parallel) dp_\parallel = 1$, p_\parallel is the component of the momentum parallel to a magnetic field line, and the momentum \mathbf{p}_{dr}^\pm is the drift of charged particles moving in a curved magnetic field: i.e.,

$$\mathbf{p}_{dr}^\pm = \pm \frac{v_\parallel}{\omega_B \rho} p_\parallel \mathbf{l}.$$

As in Section 2, the expression (3.6) can be substantially simplified if we take into account two important facts: in the internal region of the magnetosphere ($r < (10^2 - 10^3)R$) $\omega_B \gg \omega$ and $p_{dr}/m_e c \ll \gamma_c^{-1}$. When these conditions are satisfied, the quantity ω_B can be made to tend to infinity, which implies that the transverse motion

is completely 'frozen' – i.e.,

$$\frac{\partial F^\pm}{\partial p'_\sigma} = \int \frac{\partial F^\pm}{\partial p_\parallel} \frac{p'_\sigma}{p_\parallel} \delta(\mathbf{p} - p_\parallel \mathbf{b}) dp_\parallel. \quad (3.10)$$

For further calculations it is necessary to know the trajectory of particle motion

$$\mathbf{r} - \mathbf{r}' = \mathbf{v}(t - t') - \frac{1}{2}\mathbf{a}(t - t')^2 + \frac{1}{6}\dot{\mathbf{a}}(t - t')^3 + \dots;$$

$$\mathbf{a} = \frac{v_\parallel^2}{\rho} \mathbf{n};$$

$$\dot{\mathbf{a}} = -\frac{v_\parallel^3}{\rho^2} \left[\mathbf{b} + \mathbf{n} \left(\mathbf{b} \frac{d\rho}{d\mathbf{r}} \right) + \frac{\rho}{\rho_\tau} \mathbf{l} \right];$$

ρ_τ being the radius of magnetic field line torsion. Since in the region of radiation generation $\rho_\tau \gg \rho$, we, henceforth, put $\rho_\tau \rightarrow \infty$. The expression (3.6) for the conductivity tensor contains the value of the distribution function at the point $\mathbf{r} + \mathbf{R}^*/2$. Therefore, we have to find the particle velocities \mathbf{v} , \mathbf{v}' , and \mathbf{R}^* also at the point $\mathbf{r} + \mathbf{R}^*/2$. We have

$$\begin{aligned} \mathbf{w} &= v_\parallel \mathbf{b} \left(\mathbf{r} + \frac{\mathbf{R}^*}{2} \right) = v_\parallel \mathbf{b} + \frac{v_\parallel^2}{2\rho} (t - t') \mathbf{n} - \frac{1}{8} \frac{v_\parallel^3}{\rho^2} (t - t')^2 \left[\mathbf{b} + \mathbf{n} \left(\mathbf{b} \frac{d\rho}{d\mathbf{r}} \right) \right] + \dots, \\ \mathbf{v}(t', \mathbf{w}) &= v_\parallel \mathbf{b} - \frac{v_\parallel^2}{2\rho} (t - t') \mathbf{n} - \frac{1}{8} \frac{v_\parallel^3}{\rho^2} (t - t')^2 \left[\mathbf{b} + \mathbf{n} \left(\mathbf{b} \frac{d\rho}{d\mathbf{r}} \right) \right] + \dots, \\ \mathbf{R}^* &= v_\parallel (t - t') \mathbf{b} - \frac{1}{24} \frac{v_\parallel^3}{\rho^2} (t - t')^3 \left[\mathbf{b} + \mathbf{n} \left(\mathbf{b} \frac{d\rho}{d\mathbf{r}} \right) \right] + \dots. \end{aligned} \quad (3.11)$$

It is of importance to note that the quantity \mathbf{R}^* in (3.11) is an odd function of the difference $t - t'$. Generally, it can be shown that the quantity $\omega(t - t') - \mathbf{k}\mathbf{R}^*$ entering in (3.6) is an odd function of the argument $t - t'$. This corresponds to the fact that in time reversal $t \rightarrow -t$ the conductivity remains the same as for a reversed wave $\omega \rightarrow -\omega$, $\mathbf{k} \rightarrow -\mathbf{k}$ (with an accuracy to permutation of indices). To this important property there must satisfy the value of dielectric permittivity (as well as conductivity) in a weakly inhomogeneous medium when the conditions (3.8) are satisfied.

Substituting the expressions (3.10), (3.11) into (3.6), we derive the following expression for the required dielectric permittivity tensor $\varepsilon_{\alpha\beta} = \delta_{\alpha\beta} + (4\pi i/\omega)\sigma_{\alpha\beta}$:

$$\begin{aligned} \varepsilon_{\alpha\beta} &= \delta_{\alpha\beta} - i \sum_{e^+, e^-} \frac{\omega_p^2}{\omega} \int dp_\parallel m_e v_\parallel \frac{\partial F^\pm}{\partial p_\parallel} \int_0^\infty d\tau E(\omega, \mathbf{k}, p_\parallel, \tau) \left[b_\alpha b_\beta \left(1 - \frac{v_\parallel^2 \tau^2}{4\rho^2} \right) + \right. \\ &\quad \left. + (n_\alpha b_\beta - n_\beta b_\alpha) \frac{v_\parallel}{2\rho} \tau - (n_\alpha b_\beta + n_\beta b_\alpha) \frac{v_\parallel^2}{8\rho^2} \left(\mathbf{b} \frac{d\rho}{d\mathbf{r}} \right) \tau^2 - n_\alpha n_\beta \frac{v_\parallel^2}{4\rho^2} \tau^2 \right]; \\ E(\omega, \mathbf{k}, p_\parallel, \tau) &= \exp \left[i(\omega - k_z v_\parallel) \tau + \frac{i}{24} \frac{v_\parallel^3 \tau^3}{\rho^2} \left[k_z + k_x \left(\mathbf{b} \frac{d\rho}{d\mathbf{r}} \right) \right] \right]. \end{aligned}$$

We are considering modes which propagate at a sufficiently small angle to the direction of the magnetic field $\theta \lesssim 1/\gamma_c$ (i.e., these modes alone turn out to be unstable), the terms containing the derivative of the curvature radius $d\rho/d\mathbf{r}$ may be neglected. Finally, integrating over $d\tau$, we have

$$\varepsilon_{\alpha\beta}(\omega, \mathbf{k}, \mathbf{r}) = \delta_{\alpha\beta} - 2\pi i \frac{\rho^{2/3}}{k_z^{1/3}} \sum_{e^+, e^-} \frac{\omega_p^2}{\omega} \int dp_{\parallel} \frac{\partial F_{\parallel}^{\pm}}{\partial p_{\parallel}} \begin{pmatrix} \frac{\mathcal{F}''(\xi)}{(k_z \rho)^{2/3}} & 0 & -i \frac{\mathcal{F}'(\xi)}{(k_z \rho)^{1/3}} \\ 0 & 0 & 0 \\ i \frac{\mathcal{F}'(\xi)}{(k_z \rho)^{1/3}} & 0 & \mathcal{F}(\xi) \end{pmatrix}_{\alpha\beta}, \quad (3.12)$$

where

$$\mathcal{F}(\xi) = \text{Ai}(\xi) + i \text{Gi}(\xi) = \frac{1}{\pi} \int_0^{\infty} d\tau \exp(i\tau\xi + i\tau^3/3);$$

and primes denote derivatives with respect to the variable

$$\xi = 2(\omega - k_z v_{\parallel}) \frac{\rho^{2/3}}{k_z^{1/3} v_{\parallel}}. \quad (3.13)$$

Integrating in Equation (3.12) by parts, one can write the tensor $\varepsilon_{\alpha\beta}(\omega, \mathbf{k}, \mathbf{r})$ in an equivalent form

$$\varepsilon_{\alpha\beta} = \begin{pmatrix} 1 + 4\pi \frac{\rho^{2/3}}{k_z^{4/3}} \left\langle \omega_p^2 \frac{\text{Gi}'''(\xi) - i \text{Ai}'''(\xi)}{\gamma^3 v_{\parallel}^2} \right\rangle & 0 & -4\pi \frac{\rho}{k_z} \left\langle \omega_p^2 \frac{\text{Ai}''(\xi) + i \text{Gi}''(\xi)}{\gamma^3 v_{\parallel}^2} \right\rangle \\ 0 & 1 & 0 \\ 4\pi \frac{\rho}{k_z} \left\langle \omega_p^2 \frac{\text{Ai}''(\xi) + i \text{Gi}''(\xi)}{\gamma^3 v_{\parallel}^2} \right\rangle & 0 & 1 + 4\pi \frac{\rho^{4/3}}{k_z^{2/3}} \left\langle \omega_p^2 \frac{\text{Gi}'(\xi) - i \text{Ai}'(\xi)}{\gamma^3 v_{\parallel}^2} \right\rangle \end{pmatrix}_{\alpha\beta}. \quad (3.14)$$

The expression (3.14) is an extension of the dielectric permittivity tensor (2.15) to the case of a curves infinitely strong magnetic field.

We should note here that for a real argument ξ the Hermitian part of the tensor $\varepsilon_{\alpha\beta}$ is connected with the function $\text{Gi}(\xi)$ and the anti-Hermitian with the Airy function $\text{Ai}(\xi)$. In particular, for $\xi \gg 1$ the anti-Hermitian part of the tensor $\varepsilon_{\alpha\beta}$ will be exponentially small. It can be easily verified that for $n \simeq 1$ the condition $\xi \gg 1$ just corresponds

to the frequencies $\omega \gg \omega_c \simeq (c/\rho)\gamma^3$ for which, according to Equation (2.7), the intensity of curvature radiation will also be exponentially small.

We should stress that the argument ξ is actually a complex quantity. As has already been said, we are first of all interested in natural modes propagating at small angles to the direction of relativistic particle motion, i.e., $\text{Re} k_z > 0$, the damping corresponding to the condition $\text{Im} k_z > 0$ and the amplification to $\text{Im} k_z < 0$. Everywhere below we consider only the case $\text{Re} k \gg \text{Im} k$, so the imaginary part of \mathbf{k} should be taken into account only in the numerator of (3.13). As to the frequency ω , in our formulation of the problem it should be regarded as a real quantity. In the end, wave amplification corresponds to the inequality $\text{Im} \xi > 0$.

Show finally how the limiting transition of the dielectric permittivity tensor (3.14) to the case of a direct magnetic field is realized. As is seen from (3.13), for large ρ the condition $|\xi| \gg 1$ will be satisfied. Making use of the asymptotics (Nikishov and Ritus, 1986)

$$\mathcal{F}(\xi) = \frac{i}{\pi\xi} + \frac{2i}{\pi\xi^4} + \dots, \quad (3.15)$$

which is valid as $|\xi| \rightarrow \infty$ in the sector

$$-\pi/3 < \arg \xi < \pi/2,$$

we come to

$$\varepsilon_{\alpha\beta} = \begin{pmatrix} 1 - \frac{3}{2} \left\langle \frac{\omega_p^2 v_{\parallel}^2}{\gamma^3 \rho^2 \tilde{\omega}^4} \right\rangle & 0 & -i \left\langle \frac{\omega_p^2 v_{\parallel}}{\gamma^3 \rho \tilde{\omega}^3} \right\rangle \\ 0 & 1 & 0 \\ i \left\langle \frac{\omega_p^2 v_{\parallel}}{\gamma^3 \rho \tilde{\omega}^3} \right\rangle & 0 & 1 - \left\langle \frac{\omega_p^2}{\gamma^3 \tilde{\omega}^2} \right\rangle \end{pmatrix}. \quad (3.16)$$

In the limit $\rho \rightarrow \infty$ this tensor, as expected, tends to the dielectric permittivity tensor of a homogeneous plasma (2.15).

3.2. NORMAL MODES OF ELECTROMAGNETIC OSCILLATIONS

Let us now discuss normal modes of electromagnetic oscillations. The dispersion equation for the tensor (3.14) has the form

$$(1 - n^2)^2 + (1 - n^2)(1 - n^2 \cos^2 \theta) \delta \varepsilon_{zz} + (1 - n^2)(1 - n^2 \sin^2 \theta \cos^2 \varphi) \delta \varepsilon_{xx} + \\ + (1 - n^2 + n^2 \sin^2 \theta \sin^2 \varphi) (\delta \varepsilon_{zz} \delta \varepsilon_{xx} - \varepsilon_{xz} \varepsilon_{zx}) = 0, \quad (3.17)$$

where

$$\delta \varepsilon_{xx} = \varepsilon_{xx} - 1, \quad \delta \varepsilon_{zz} = \varepsilon_{zz} - 1, \quad k_z = k \cos \theta, \quad k_x = k \sin \theta \cos \varphi.$$

The properties of the solutions of Equation (3.17) depend essentially on the quantity $\delta\epsilon_{zz}$. In particular, for $\delta\epsilon_{zz} \ll 1$ the refractive indices n_j will be equal to

$$n_{t_1}^2 = 1, \quad (3.18)$$

$$n_{t_2}^2 = 1 + \delta\epsilon_{xx} + \delta\epsilon_{zz} \sin^2 \theta, \quad (3.19)$$

both these waves corresponding to transverse oscillations. As concerns the case $\delta\epsilon_{zz} \gg 1$, we shall first write down the expressions for n_j^2 only for the vector \mathbf{k} which lies in the plane of a curved magnetic field, i.e., when $k_y = k \sin \theta \sin \varphi = 0$. With an account of the fact that $\delta\epsilon_{xx} \ll \delta\epsilon_{zz}$ we have

$$n_{t_1}^2 = 1, \quad (3.20)$$

$$n^2 = 1 + \frac{\delta\epsilon_{zz} \sin^2 \theta + \delta\epsilon_{xx} + \delta\epsilon_{zz} \delta\epsilon_{xx} - \epsilon_{xz} \epsilon_{zx}}{1 + \delta\epsilon_{zz} \cos^2 \theta}. \quad (3.21)$$

We should emphasize that Equation (3.21), like the relation (2.17), determines the refractive coefficient implicitly, so that its solution describes both transverse and plasma waves. On the other hand, the same as for a homogeneous magnetic field, the normal waves (3.18) and (3.20) correspond to polarization for which the electric vector of the wave is perpendicular for the plane in which the magnetic field line lies. For $k_y = 0$ this wave (which will also be called extraordinary) does not interact with the plasma contained in an infinitely strong magnetic field, and therefore cannot amplify.

Let us now classify the solutions (3.18)–(3.21) depending on the physical parameters—plasma density n_e (and, therefore, Langmuir frequency ω_p), curvature radius of magnetic field lines ρ , and oscillation frequency ω . Figure 6 illustrates three regions on the plane $\omega - \rho$ in which the properties of normal waves differ substantially. The coordinates of the ‘particular’ point

$$\omega_* \simeq \omega_p \gamma_c^{1/2};$$

$$\rho_* \simeq \frac{c}{\omega_p} \gamma_c^{5/2},$$

depend here only on the quantity $\gamma_c = \langle \gamma^{-3} \rangle^{-1/3}$ and the electron-positron plasma density.

(1) Region I ($\delta\epsilon_{zz} \gg 1$)

Region I corresponds to the case $|1 - n| \gg 1/\gamma_c^2$, when in the expression for

$$\tilde{\omega} = \omega - k_z v_{\parallel} = \frac{1}{2} \omega \left[\frac{1}{\gamma^2} + \theta^2 + 2(1 - n) \right],$$

the quantity $1/\gamma^2$ can be disregarded. In view of this, the condition $\delta\epsilon_{zz} \gg 1$ can be written in the form $a \gg 1$, where

$$a = 4\pi \left\langle \frac{\omega_p^2}{\gamma^3} \right\rangle \frac{\rho^{4/3}}{k_z^{2/3} c^2}; \quad (3.22)$$

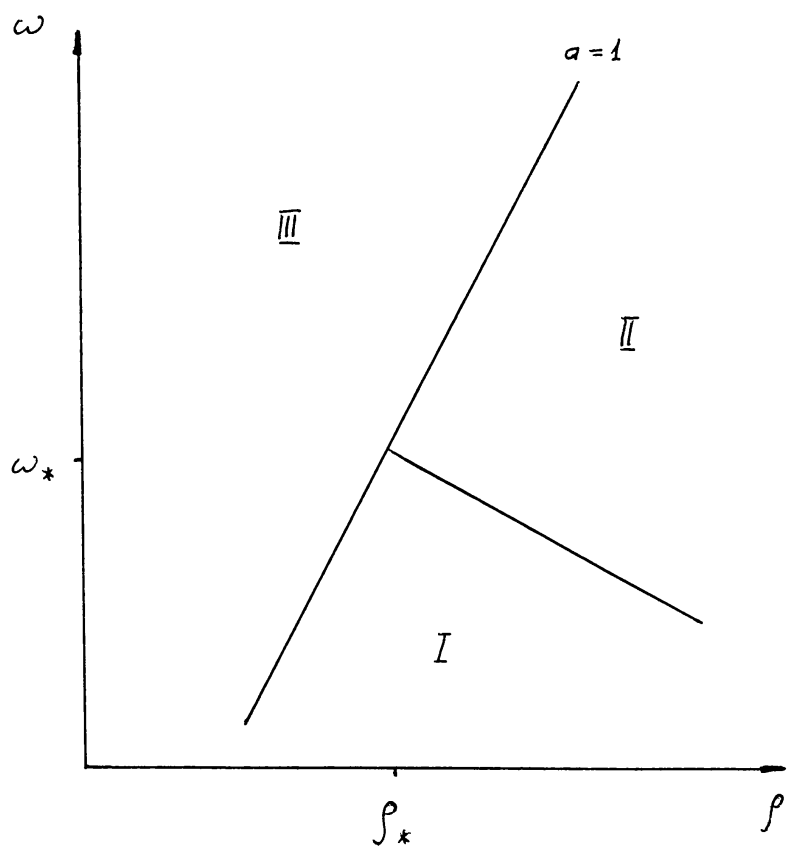


Fig. 6. Three regions of parameters on $\omega - \rho$ -plane. Unstable curvature-plasma modes take place in region I. In region III only two transverse waves can propagate.

and the dispersion equation (3.17) can be written as

$$\xi - b = ia\xi \mathcal{F}'(\xi) + ia \mathcal{F}'''(\xi) + a^2[\mathcal{F}'''(\xi)\mathcal{F}'(\xi) - \mathcal{F}''^2(\xi)], \tag{3.23}$$

where

$$b = (k_z \rho)^{2/3} \theta^2. \tag{3.24}$$

According to Equation (3.13), the refractive index n_j is connected with the root ξ_j of the dispersion equation (3.17) by simple relation

$$n_j^2 = 1 + \theta^2 - \frac{\xi_j}{(k_z \rho)^{2/3}}. \tag{3.25}$$

The straight line $a = 1$ separates regions I and III. As to the boundary separating regions I and II, the corresponding condition is formulated below.

First of all we are interested in normal oscillations for which $\text{Im } \xi > 0$. Making use of the asymptotic properties of (3.15) which contains all unstable modes, we obtain that the dispersion equation (3.23) has five branches of nondamping oscillations: for $\theta < \theta_{\parallel}$, where

$$\theta_{\parallel} = a^{3/20} \theta_*; \tag{3.26}$$

and θ_* is given by Equation (2.18), the roots of Equation (3.23) are equal to

$$\xi_{2,3} = \pm \left(\frac{a}{\pi} \right)^{1/2}; \quad (3.27)$$

$$\xi_{4,5,6} = \exp \left(\frac{2\pi}{5} im \right) \left(\frac{2a}{\pi} \right)^{1/5}, \quad m = 0, 1, 2. \quad (3.28)$$

If $\theta \gg \theta_*$ (which is, of course, possible only in the case $a^{3/20} \theta_* \ll 1$), we have here

$$\xi_2 = b = (k_z \rho)^{2/3} \theta^2; \quad (3.29)$$

$$\xi_{3,4,5,6} = \exp \left(\frac{\pi i}{3} m \right) \frac{2^{1/6}}{\pi^{1/3}} \frac{a^{1/3}}{(k_z \rho)^{1/9} \theta^{1/3}}, \quad m = 3, 0, 1, 2. \quad (3.30)$$

We have left number 1 for the extraordinary mode $n_1^2 \equiv 1$ (see Equations (3.18) and (3.20)). The asymptotic expressions (3.27)–(3.30) are valid only for $|\xi| \gg 1$.

One can easily check that the roots 2 and 3 in Equations (3.27), (3.29), and (3.30) exactly corresponds to the normal modes $j = 2, 3$ for a homogeneous magnetic field. Therefore, the relations (2.20a) and (2.20b) remain valid for the refractive indices n_j and (2.21a) and (2.21b) for their polarizations. And this is not surprising because, according to (3.22), $a \rightarrow \infty$ corresponds to the limit $\rho \rightarrow \infty$. On the other hand, for a finite curvature radius ρ the mode $t - l$ which existed in the direct magnetic field splits up into three branches of oscillations (3.28) and (3.30), as is demonstrated in Figure 7. Two of them, as is seen from the relations (3.28) and (3.30) will be unstable. For these modes

$$\text{Im } n_{5,6} = \begin{cases} -2^{2/5} \sin \left(\frac{2\pi}{5} l \right) \left\langle \frac{\omega_p^2}{\gamma^3} \right\rangle^{1/5} \frac{1}{k_z^{4/5} \rho^{2/5} c^{2/5}}, & l = 1, 2, \quad \theta \ll a^{3/20} \theta_*, \\ -\frac{3^{1/2}}{2^{7/6}} \left\langle \frac{\omega_p^2}{\gamma^3} \right\rangle^{1/3} \frac{1}{k_z \rho^{1/3} c^{2/3} \theta^{1/3}}, & \theta \gg a^{3/20} \theta_*, \end{cases} \quad (3.31)$$

i.e., $\text{Im } n$ depends in a power-law manner on the curvature radius ρ . The polarization of such waves is close to transverse polarization: i.e.,

$$\left(\frac{E_z}{E_x} \right)_{4,5,6} \simeq i \frac{c}{\rho \tilde{\omega}_{4,5,6}}; \quad \left| \frac{E_z}{E_x} \right| \ll 1. \quad (3.32)$$

Note that as distinct from the case of a homogeneous magnetic field, the longitudinal component of the electric field E_z of normal modes $j = 4, 5, 6$ is nonzero even in the case $\theta = 0$. As we shall see below, the existence of modes which we call curvature-plasma waves just leads to the appearance of a powerful pulsar radioemission.

For $a \gg 1$, with an increase of the angle θ four of the five roots ξ_j pass over to the lower half plane, so that the normal waves corresponding to them become damping. The motion of the roots is shown in Figure 8 (see also Equation (3.30)). For example, the

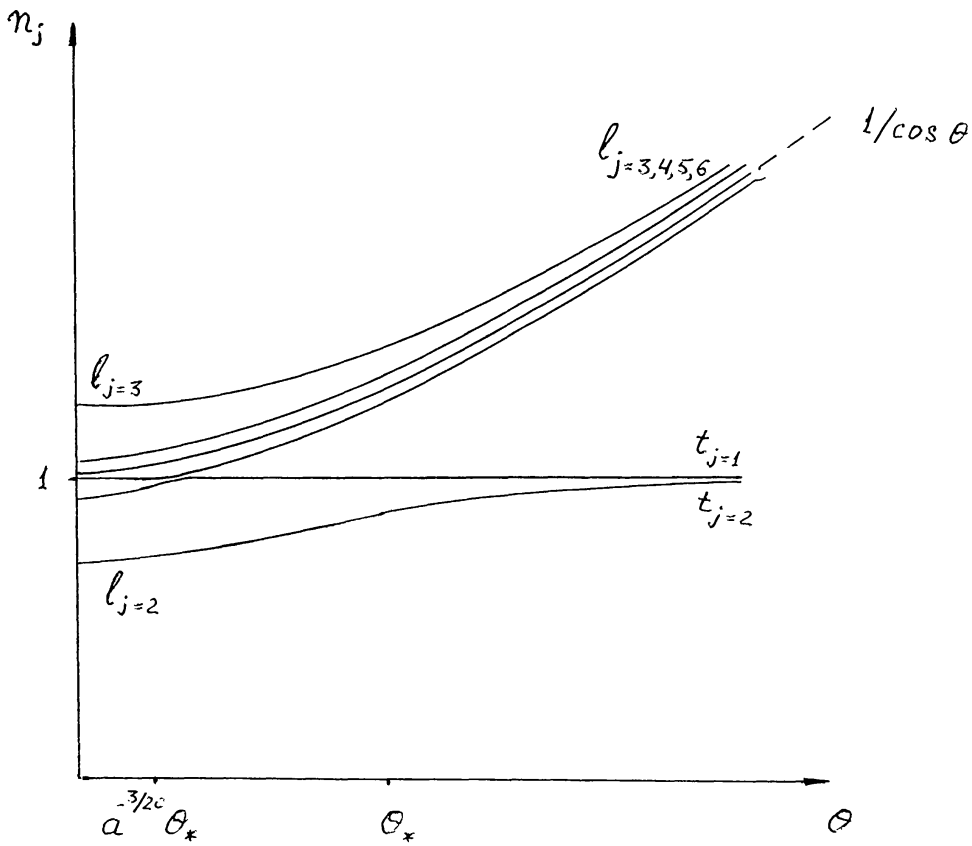


Fig. 7. Normal oscillation modes of a relativistic electron-positron plasma in a strong curved magnetic field (region I). Unstable curvature-plasma waves correspond to drift oscillations with $n \simeq 1/\cos \theta$.

roots corresponding to amplified waves with $m = 1$ ($j = 5$) and $m = 2$ ($j = 6$) in Equations (3.28) and (3.30) pass over to the lower half plane for $\theta = \theta_{\parallel 5,6}^{\text{out}}$, where

$$\theta_{\parallel 5,6}^{\text{out}} = u_{5,6} a^{3/4} \theta_*; \quad u_5 = 0.28; \quad u_6 = 0.77. \quad (3.33)$$

The only nondamping normal wave here is the mode ξ_2 (3.29).

Note also that for $a \approx 1$ an unstable wave with $m = 1$ ($j = 5$) and a transverse mode ξ_2 (3.29) mutually transform. This is shown in detail in Figure 9. We can see that for $a > 1.15$ the root ξ_5 of the unstable mode $m = 1$ passes over onto the lower half plane with increasing θ (i.e., such a wave damps for large θ), while for $a < 1.15$ this mode passes over to the asymptotics $\xi = b = (k_z \rho)^{2/3} \theta^2$ and, therefore, propagates freely for $(k_z \rho)^{2/3} \theta^2 \gg 1$ as a transverse mode.

We should emphasize that the amplified modes found above correspond in fact to hydrodynamic instability. It should be so because the limit $a \gg 1$ corresponds to a large particle density. In particular, the solutions (3.27)–(3.30) can be obtained directly from the asymptotic expression (3.16) for the dielectric permittivity tensor by way of the substitution $\tilde{\omega} \rightarrow \omega - k_z c$, $v_{\parallel} \rightarrow c$. The hydrodynamic character of the instability is also confirmed by the fact that the imaginary parts of the refractive index (3.31) depend on the particle density n_e in a power-law manner.

Finally, we shall present exact expressions for the case when the vector \mathbf{k} has a

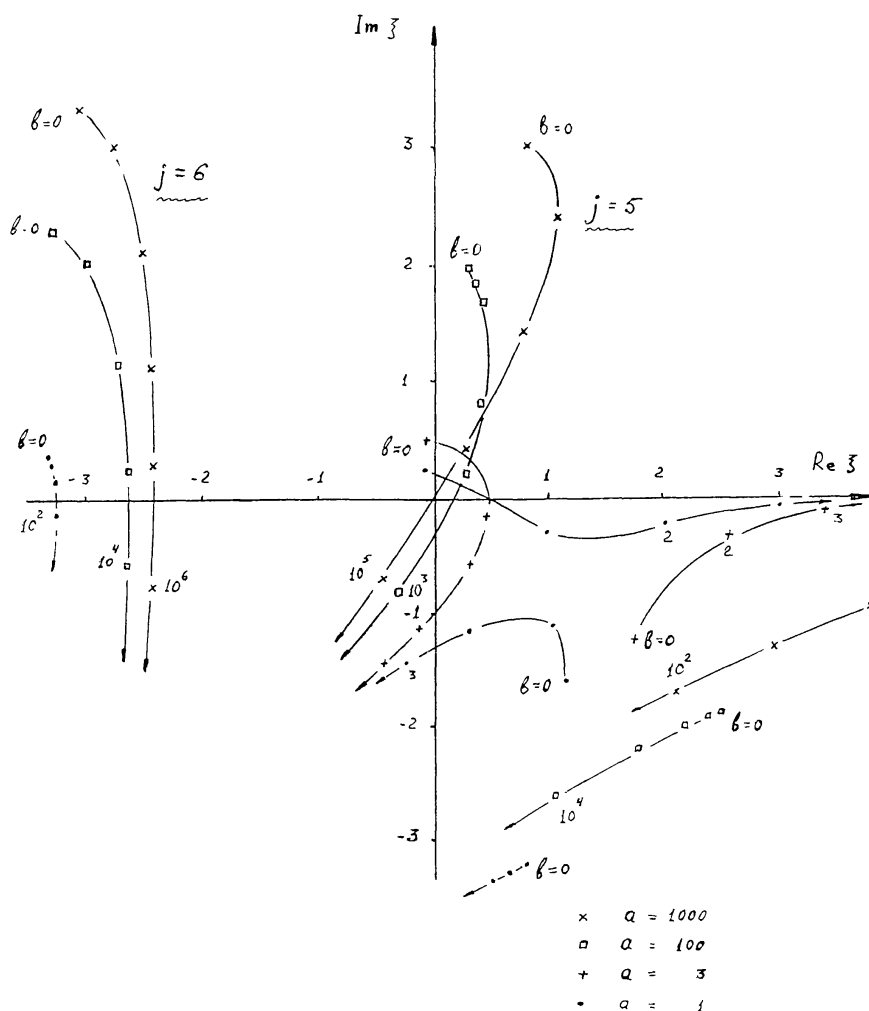


Fig. 8. Motion of the roots ξ_j of the dispersion equation (3.23) subject to the parameter $b = (k_z \rho)^{2/3} \theta^2$.

component perpendicular to the plane in which the magnetic field line lies, i.e., when $k_y = k \sin \theta \sin \varphi \neq 0$. In this case the solution of the dispersion equation (3.17) has the form

$$n^2 = 1 + \frac{\delta \varepsilon_{zz} \theta^2 + \delta \varepsilon_{xx} + \mathcal{D} \pm [(\delta \varepsilon_{zz} \theta^2 + \delta \varepsilon_{xx} + \mathcal{D})^2 - 4 \theta^2 \cos^2 \varphi \mathcal{D} (1 + \delta \varepsilon_{zz})]^{1/2}}{2(1 + \delta \varepsilon_{zz})},$$

where $\mathcal{D} = \delta \varepsilon_{zz} \delta \varepsilon_{xx} - \varepsilon_{xz} \varepsilon_{zx}$. Rewriting this equation with an account of the quantities a, b, ξ introduces above (see Equations (3.13), (3.22), (3.24)), we obtain

$$\xi - b = \frac{1}{2} \left\{ \frac{2a}{\pi \xi^4} - b \pm \left[\left(\frac{2a}{\pi \xi^4} - b \right)^2 + \frac{8ab \cos^2 \varphi}{\pi \xi^4} \right]^{1/2} \right\}. \quad (3.34)$$

In the derivation of (3.34) we have also made use of the asymptotical dielectric permittivity tensor (3.16). Note also that Equation (3.34) includes now the 'extraordinary' mode $j = 1$ too.

An analysis of Equation (3.34) shows that its solutions coincides with the solutions

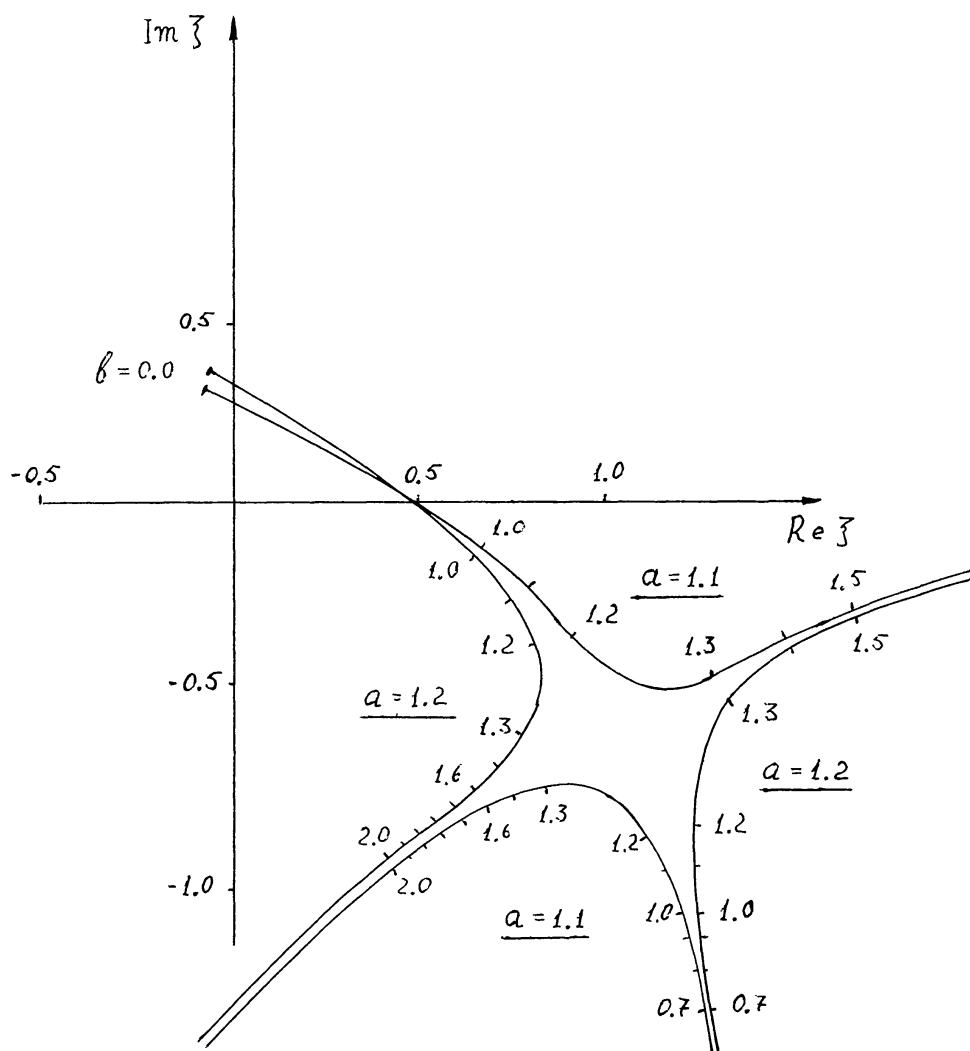


Fig. 9. The region of transformation of two normal waves. Digits again indicate the values of the quantity b .

(3.27)–(3.30) only for angles θ and φ which satisfy the condition $\theta < \theta_{\perp}/\cos \varphi$, where

$$\theta_{\perp} = a^{-3/20} \theta_{*} . \quad (3.35)$$

If the inverse inequality $\theta > \theta_{\perp}/\cos \varphi$ is fulfilled, then the solutions of Equation (3.34) are

$$\xi_4 = b , \quad (3.36)$$

$$\xi_{1,5,6} = \exp \left(\frac{\pi i l}{2} \right) \left(\frac{2a}{\pi b} \right)^{1/4} \cos^{1/2} \varphi , \quad l = 0, 1, 2 .$$

The dispersion properties of the normal waves $j = 2, 3$ are determined as before by the relations (2.20a) and (2.20b).

Thus, we see that the ‘amplification cone’ strongly extended along the x -axis as is shown in Figure 10. So, the ratio of the angles θ_{\parallel} and θ_{\perp} (Equations (3.26) and (3.35)),

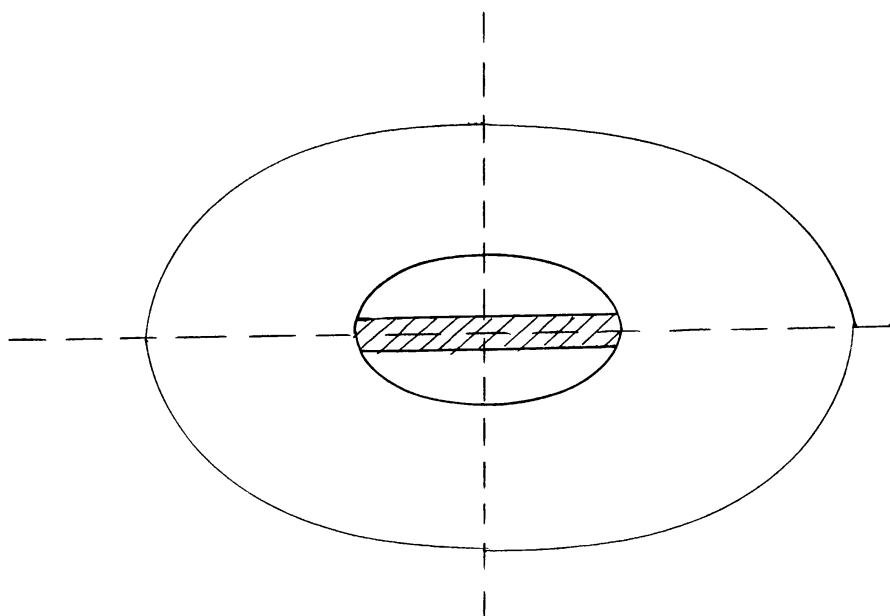


Fig. 10. The structure of amplification cone. The internal region corresponds to the largest increments (3.28). In the dashed region the linear transformation of normal waves $j = 1$ and $j = 4$ is not effective.

in the limits of which the amplification of curvature-plasma waves is the most effective, will be equal to

$$\theta_{\parallel}/\theta_{\perp} \simeq a^{3/10} \gg 1.$$

The same refers also to the entire amplification cone. Indeed, according to (3.33) and (3.36), the external dimensions of the amplification cone are given by

$$\theta_{\perp}^{\text{out}} \simeq a^{1/4} \theta_*, \quad \theta_{\parallel}^{\text{out}} \approx a^{3/4} \theta_*,$$

so that

$$\theta_{\perp}^{\text{out}} \ll \theta_{\parallel}^{\text{out}}.$$

Let us pay attention to another fact connected with the possibility of mode transformation in the range of angles $\theta \simeq \theta_{\perp}$, which is shown in Figure 11. We see that for $k_y \neq 0$, as the angle θ increases, the curvature-plasma mode $j = 4$ is transformed into the transverse wave $j = 1$ with $n_j \simeq 1$ and the transverse wave $j = 1$ into the curvature-plasma mode. The parameter

$$\frac{1}{k_z} \frac{d\mathcal{K}_j}{dl |n_1 - n_2|} \simeq a^{-3/10} \cos^{-3} \varphi,$$

which (as is known), allows us to judge of the validity of the geometrical optics approximation (Ginzburg, 1970), appears to be more than unity only for the angles

$$\cos \varphi < a^{-1/10} \ll 1,$$

(2) *Region II* ($a \gg 1$, $|1 - n| \ll \gamma_c^{-2}$)

Region II occupies a sector $a > 1$, $|1 - n| < \gamma_c^{-2}$. In this sector the dispersion equation (3.17) has four roots which practically coincide with the corresponding solutions for a homogeneous magnetic field. This is exactly how it should be because, as is seen from Figure 6, region II corresponds to the limit $\rho \rightarrow \infty$. Consequently, in this region there exist two longitudinal and two transverse normal waves shown in Figure 4. There are no unstable modes here, so an effective amplification is impossible in region II. We shall not therefore consider this case in detail.

(3) *Region III* ($a \ll 1$)

In this region, as is clear from the above analysis, along with an extraordinary there exists only one more transverse mode t_2 . Indeed, as is seen from the dispersion equation (3.23), for $a \ll 1$ we can neglect in a first approximation the terms in the right-hand side, owing to which

$$\xi_2 = (k_z \rho)^{2/3} [\theta^2 + \gamma^{-2}],$$

which just corresponds to a transverse mode with $n_2^2 \simeq 1$. The right-hand side of Equation (3.23) determines the imaginary part of the refractive index. As a result we come to

$$n_{t_2}^2 = 1 + \frac{a}{(k_z \rho)^{2/3}} \langle \mathcal{F}'''(\xi) + (k_z \rho)^{2/3} \theta^2 \mathcal{F}'(\xi) \rangle.$$

For $a \ll 1$ all the rest of the roots of the dispersion equation (3.23) lie in the region $-\pi < \arg \xi < -\pi/3$, where for $|\xi| \gg 1$,

$$\mathcal{F}(\xi) = \frac{1}{\pi^{1/2} \xi^{1/4}} \exp(-\frac{2}{3} \xi^{3/2}),$$

i.e., in the lower half-plane. Consequently, the normal waves which correspond to such roots will damp fastly.

Thus, in region III there may propagate only two transverse modes (3.18) and (3.19) with the refractive index n_j close to unity. Note that this conclusion remains valid also in the case $\omega \gg \omega_c$. The point is that in the upper half-plane, owing to the asymptotics (3.15), the function $\mathcal{F}(\xi)$ along with its derivatives tends moduli to zero as $|\xi| \rightarrow \infty$, so that the corrections to unity in Equation (3.19) will be small irrespective of the form of the argument ξ .

3.3. LOW-DENSITY LIMIT

Since for a given curvature radius ρ the limit $a \rightarrow 0$ corresponds to a small particle density, one can expect that just in this limit the anti-Hermitian part of the dielectric permittivity tensor (3.14) must be connected with the intensity of curvature radiation of individual particles in a vacuum (2.7). To demonstrate this, write the expression for the reabsorption coefficient for the normal mode t_2 . Using the expressions (3.12) and

(3.19), we have

$$\mu_{t_2} = -\frac{8\pi^2}{c} e^2 \frac{1}{k_z} \int dp_{\parallel} \frac{\partial F_{\parallel}}{\partial p_{\parallel}} [\text{Ai}''(\xi) + (k_z \rho)^{2/3} \theta^2 \text{Ai}(\xi)], \quad (3.38)$$

where for a small particle density one can put $\xi = (k_z \rho)^{2/3} (\theta^2 + \gamma^{-2})$. The extraordinary mode in the approximation $a \ll 1$ gives $\mu_{t_1} = 0$, so all the radiation must be connected with the normal wave t_2 . On the other hand, the reabsorption coefficient can be determined by means of the Einstein coefficients method (Ginzburg, 1970). For the distribution function of particles (3.9), in the low-density limit we obtain

$$\mu_{t_2} = -\frac{(2\pi)^3 c^2}{\omega^3} \int dp_{\parallel} \frac{\partial F_{\parallel}}{\partial p_{\parallel}} \mathcal{P}_{\omega}(\Omega) k_z, \quad (3.39)$$

where $\mathcal{P}_{\omega}(\Omega) d\omega d\Omega$ is the radiation intensity of one particle per unit interval of frequencies $d\omega$ and in a unit solid angle $d\Omega$. Comparing Equations (3.38) and (3.39) and taking into account that $\text{Ai}''(\xi) = \xi \text{Ai}(\xi)$ and that for angles $\theta \ll 1$ we can put $k_z = \omega/c$, we have

$$\mathcal{P}_{\omega}(\Omega) = \frac{1}{\pi} \frac{e^2}{\rho} \gamma^3 \left(\frac{\omega \rho}{c \gamma^3} \right)^{5/3} (1 + 2\gamma^2 \theta^2) \text{Ai} \left[\left(\frac{\omega \rho}{c \gamma^3} \right)^{2/3} (1 + \gamma^2 \theta^2) \right].$$

Integrating this expression over the solid angle $d\Omega = \pi d\theta^2$ we obtain

$$\begin{aligned} \mathcal{P}_{\omega} &= \int d\Omega \mathcal{P}_{\omega}(\Omega) = \frac{e^2}{\rho} \gamma \left(\frac{\omega \rho}{c \gamma^3} \right)^{1/3} \int_{x_0}^{\infty} dx (2x - x_0) \text{Ai}(x) = \\ &= \frac{\sqrt{3}}{2\pi} \frac{e^2}{\rho} \gamma \int_{\eta}^{\infty} [2y^{2/3} \eta^{1/3} - \eta] K_{1/3}(y) dy, \end{aligned} \quad (3.40)$$

where $x_0 = (\omega \rho / c \gamma^3)^{2/3}$, $\eta = \omega / \omega_c$, and $\omega_c = \frac{3}{2}(c/\rho) \gamma^3$. It can be readily verified that

$$\int_{\eta}^{\infty} (2y^{2/3} \eta^{1/3} - \eta) K_{1/3}(y) dy \equiv \eta \int_{\eta}^{\infty} dy K_{5/3}(y);$$

and, therefore, the intensity (3.40) exactly coincides with the expression (2.7). Thus, the results of calculations by the method of kinetic equation for $n_e \rightarrow 0$ fully correspond to the results of the Einstein coefficients method.

Finally, in the limit $a \ll 1$ it is easy to determine also the optical depth $\tau_{t_2} = \int \mu_{t_2} dl$. Indeed, in this limit one can neglect the effects of geometrical optics and assume that the normal wave t_2 propagates along a straight line. Using the expression (3.14), we obtain

$$\tau_{t_2} = - \left\langle 4\pi \frac{\omega}{c} \frac{\omega_p^2}{\gamma^3} \frac{\rho^{2/3}}{k_z^{4/3} c^2} \int_{-\infty}^{\infty} [\text{Ai}'''(x) + x_0 \gamma^2 \theta^2 \text{Ai}'(x)] dl \right\rangle,$$

where

$$x = \left(\frac{\omega \rho}{c \gamma^3} \right)^{2/3} (1 + \gamma^2 \theta^2) \equiv x_0 (1 + \gamma^2 \theta^2), \quad dl = \rho d\theta.$$

As a result, after integration

$$\begin{aligned} \tau_{t_2} &= - \left\langle 4\pi \left(\frac{\rho \omega}{c \gamma^3} \right)^2 \frac{\omega_p^2 \gamma}{\omega^2} \int_{x_0}^{\infty} \frac{\text{Ai}'(x) dx}{(x - x_0)^{1/2}} \right\rangle = \\ &= - \left\langle 4\pi^2 \frac{\omega_p^2 \gamma}{\omega^2} \left(\frac{\omega \rho}{c \gamma^3} \right)^2 \text{Ai}^2(u) \right\rangle, \end{aligned} \quad (3.41)$$

where $u = x_0/2^{2/3}$, and we have employed the relation (Nikishov and Ritus, 1986)

$$\frac{1}{\pi} \int_{x_0}^{\infty} \frac{\text{Ai}'(x) dx}{(x - x_0)^{1/2}} = \text{Ai} \left(\frac{x_0}{2^{2/3}} \right) \text{Ai}' \left(\frac{x_0}{2^{2/3}} \right).$$

Since $\text{Ai}(u) \text{Ai}'(u) < 0$ for $u > 0$, the total optical depth appears to be positive (3.41). We would like to emphasize, however, that in the region of parameters where the expression (3.41) holds, the quantity $\tau_{t_2} \ll 1$, so that the absorption of the mode t_2 in region III can be neglected. As was to be expected, for $\omega \gg \omega_c$, i.e., when $u \gg 1$, the quantity τ_{t_2} turns out to be exponentially small. The expression (3.41) coincides with the value of τ obtained by Chugunov and Shaposhnikov (1988).

3.4. THE REGION OF CYCLOTRON RESONANCE

Concluding this section we present, without derivation, the expression for the component ε_{yy} of the dielectric permittivity tensor $\varepsilon_{\alpha\beta}$ in the case of a finite magnetic field. As has already been said, the main attention should be given to the region near the cyclotron resonance. As shown by the calculation,

$$\begin{aligned} \varepsilon_{yy} &= 1 + \left\langle \pi \frac{\omega_p^2}{\omega^2} \frac{\tilde{\omega}}{\gamma} \frac{\rho^{2/3}}{k_z^{1/3} v_{\parallel}} \times \right. \\ &\quad \left. \times [-\text{Gi}(x^+) - \text{Gi}(x^-) + i \text{Ai}(x^+) + i \text{Ai}(x^-)] \right\rangle, \end{aligned} \quad (3.42)$$

where

$$x^{\pm} = 2 \left(\tilde{\omega} \pm \frac{\omega_B}{\gamma} \right) \frac{\rho^{2/3}}{k_z^{1/3} v_{\parallel}}.$$

Equation (3.42) makes it possible to extend the expressions (2.14) and (2.15) for 'cyclotron' corrections to the case of a curved magnetic field.

As one would expect, an account of a finite curvature of magnetic field lines leads

to widening of cyclotron resonances $((2\pi\rho^{2/3}/k_z^{1/3}v_{\parallel})\text{Ai}(x^{\pm}))$ instead of $\pi\delta(\tilde{\omega} \pm \omega_B/\gamma)$. However, as can be easily verified, in the range of parameters of interest ($\rho \sim 10^9$ cm, $\omega \sim 10^9$ s $^{-1}$, and in the cyclotron-resonance region one can put $\omega_B/\gamma = \tilde{\omega}$) the quantity

$$\frac{\omega_B}{\gamma} \frac{\rho^{2/3}}{k_z^{1/3}v_{\parallel}} \gg 1, \quad (3.43)$$

due to which the energy range of particles within which they are in resonance with the wave remains rather narrow. In particular, if the width of the distribution function

$$\frac{\Delta\mathcal{E}}{\mathcal{E}} \gg \frac{\omega^{1/3}c^{2/3}\gamma_c}{\omega_B\rho^{2/3}} = 10^{-6} \left(\frac{v}{1\text{ GHz}}\right)^{-2/3} \left(\frac{\rho}{10^9\text{ cm}}\right)^{2/3} \left(\frac{\tilde{\omega}}{\omega}\right)^{-1},$$

then Equation (3.42) will essentially coincide with the corresponding expression (2.10) for a homogeneous magnetic field.

Indeed, in this case practically for all particle energies the arguments x^+ and x^- will be modulo much greater than unity. Consequently, we can use asymptotic expressions (cf. Abramowitz and Stegun, 1964) of the form

$$\text{Ai}(x) = \frac{1}{2\pi^{1/2}x^{1/4}} \exp(-\frac{2}{3}x^{3/2}) + \dots, \quad (3.44)$$

$$\text{Gi}(x) = 1/\pi x + 2/\pi x^4 + \dots,$$

$$\text{Ai}(-x) = \frac{1}{\pi^{1/2}x^{1/4}} \sin(\frac{2}{3}x^{3/2} + \pi/4) + \dots, \quad (3.45)$$

$$\text{Gi}(-x) = \frac{1}{\pi x} + \frac{1}{\pi^{1/2}x^{1/4}} \cos(\frac{2}{3}x^{3/2} + \pi/4) + \dots.$$

For a sufficiently wide distribution function, the oscillating factors in Equations (3.44) and (3.45) became neglectable and the asymptotics $1/\pi x$ will give the result exactly coinciding with the limit of the homogeneous magnetic field. Only in the case if the inverse inequality in Equation (3.43) is fulfilled, the influence of the curvature of magnetic field lines appears to be substantial. In particular, in the range of energies for which $x^- < 0$, $x^+ < 0$ the imaginary part will oscillate (Shaposhnikov, 1981; Beskin *et al.*, 1987a).

It is, however, clear that the condition (3.43) is enough rigorous, at least for the main electron-positron plasma. Only a primary beam may be an exception, for which resonance appears at small distances from the star surface, where $\tilde{\omega}/\omega \ll 1$ and the condition (3.43) becomes less rigorous. But even in this case the natural beam width $\Delta\mathcal{E}/\mathcal{E} \sim 10^{-2}$ turns out to be rather large (Gurevich and Istomin, 1985). Consequently, one can draw a conclusion that the influence of the magnetic field line curvature on the cyclotron resonance in pulsar magnetosphere is not very strong and can be neglected in a first approximation.

4. Nonlinear Processes in an Inhomogeneous Relativistic Electron-Positron Plasma

4.1. SPECIFIC FEATURES OF NONLINEAR INTERACTION IN A CURVED MAGNETIC FIELD

In the previous section we investigated the linear properties of a plasma flowing in pulsar magnetosphere along open magnetic field lines. It was shown that in a curved magnetic field there appear unstable curvature-plasma modes with substantial increments. In real conditions, as shown in Section 5, in the magnetosphere of a neutron star an amplification of these waves is so strong that it is necessary to take into account nonlinear effects. Besides, the effects of plasma inhomogeneity are of importance. As we have seen, a curved magnetic field changes the character of resonance interaction between particles and waves. Beside the Cherenkov mechanism of radiation which works in a homogeneous field, in an inhomogeneous field it becomes also possible for particles to radiate the curved oscillations. This changes substantially the electromagnetic properties of a relativistic electron-positron plasma – not only its linear but also nonlinear characteristics. Besides, the curvature of a field leads to the interaction not only of waves having electric field components along a strong magnetic field, as in the homogeneous case, but also of waves whose electric vector is perpendicular to the magnetic field line, as is the case with curvature-plasma waves (3.32).

Here we will consider nonlinear processes that restrict the growth of unstable modes as well as nonlinear interactions between different modes. As shown below, the energy of excited waves is much lower than the energy of outflowing plasma and, therefore, we consider nonlinear processes within the weak turbulence theory. But the plasma inhomogeneity effects are substantial and one should use equations that take into account the influence of these effects upon nonlinear processes. These equations were derived by Istomin (1988).

4.2. QUASI-LINEAR APPROXIMATION

First of all consider a quasi-linear approximation which takes into account a reaction of electromagnetic oscillations to the evolution of distribution functions of charged particles. According to Istomin (1988), the quasi-linear equation for the case of a weakly inhomogeneous plasma (the condition (3.8)) has the form

$$\begin{aligned} \frac{dF^\pm}{dt} = & \frac{e^2}{4} \sum_{\mathbf{k}} E_\mu^{0*}(\mathbf{k}) E_\lambda^0(\mathbf{k}) \left\{ \delta_{\mu\sigma} \left(1 - \frac{\mathbf{k}\mathbf{v}}{\omega} \right) + \frac{k_\sigma v_\mu}{\omega} - \right. \\ & \left. - \frac{i}{2\omega} \delta_{\mu\sigma} v_\alpha \frac{\partial}{\partial r_\alpha} + \frac{i}{2\omega} v_\mu \frac{\partial}{\partial r_\sigma} \right\} \frac{\partial}{\partial p_\sigma} \int_{-\infty}^t dt' \exp[i\omega(t-t') - i\mathbf{k}\mathbf{R}^*], \quad (4.1) \\ \det^{-1} \left| \delta_{\alpha\beta} - \frac{1}{2} \frac{\partial L_\alpha(\mathbf{r} + \mathbf{R}^*/2)}{\partial r_\beta} \right| & \left[\delta_{\lambda\nu} \left(1 - \frac{\mathbf{k}\mathbf{v}'}{\omega} \right) + \frac{k_\nu v'_\lambda}{\omega} + \right. \\ & \left. + \frac{i}{2\omega} \frac{\partial}{\partial r_\nu} v'_\lambda - \frac{i}{2\omega} \delta_{\lambda\nu} \frac{\partial}{\partial r_\chi} v'_\chi \right] \frac{\partial F^\pm}{\partial p'_\nu} + \text{c.c.} \end{aligned}$$

The notation here is the same as in Section 3 (Equations (3.4)–(3.7)). The quantity $\mathbf{E}^0(\mathbf{k})$ is the amplitude of an electromagnetic wave which has the local wave number $\mathbf{k}(\mathbf{r})$ determined by the wave phase $\Phi(\mathbf{r})$: i.e.,

$$\mathbf{E}(\mathbf{r}) = \sum_{\mathbf{k}} \mathbf{E}^0(\mathbf{k}) \exp[i\Phi(\mathbf{r})] ; \quad \mathbf{k} = \nabla \Phi .$$

The distribution function evolution described by Equation (4.1) is due to excitation of curvature-plasma oscillations. Since waves are emitted in the direction of particle motion with a small angle spread $\Delta\theta \sim 1/\gamma$, the distribution function $F^\pm(\mathbf{r}, \mathbf{p}, t)$ also acquires a spread over transverse momenta p_x . The value $p_x/p_\parallel \sim \gamma^{-1}$ is, however, not large; so that Equation (4.1) can be integrated over p_x . As a result, with an account of the relation (3.10) we obtain the equation for the evolution of the longitudinal distribution function $F_\parallel^\pm(p_\parallel)$, of the form

$$\begin{aligned} \frac{dF_\parallel^\pm}{dt} = & \frac{e^2}{4} \sum_{\mathbf{k}} E_\mu^0{}^*(\mathbf{k}) E_\lambda^0(\mathbf{k}) \int_0^\infty d\tau \left(b_\mu + n_\mu \frac{v_\parallel}{2\rho} \tau \right) \frac{\partial}{\partial p_\parallel} \times \\ & \times \left\{ \exp \left[i(\omega - \mathbf{k}b v_\parallel) \tau + i\mathbf{k}b \frac{v_\parallel^3}{24\rho^2} \tau^3 \right] \left(b_\lambda - n_\lambda \frac{v_\parallel}{2\rho} \tau \right) \frac{\partial F_\parallel^\pm}{\partial p_\parallel} \right\} . \end{aligned} \quad (4.2)$$

The relaxation of the longitudinal distribution function is seen to be due not only to longitudinal components of the wave field (as in a homogeneous magnetic field), but also to transverse ones, and by virtue of (3.32) the contribution of transverse components is of the same order of magnitude as the contribution of longitudinal ones. This results from the nonlocal character of interaction between resonance particles and waves, when the effect at a given point is affected by its closest neighbourhood, where the transverse component of the electric field has a nonzero projection to the direction of the magnetic field because of its curvature. The right-hand side of Equation (4.2) contains the same Airy function (and its derivatives)

$$\text{Ai} \left[2(\omega - k_z v_\parallel) \frac{\rho^{2/3}}{k_z^{1/3} v_\parallel} \right]$$

as the dielectric permittivity tensor $\varepsilon_{\alpha\beta}$ (3.14) which determines the increment of unstable curvature-plasma waves. The instability exists only in the hydrodynamic limit, when the characteristic spread of the distribution function over the longitudinal velocities is not large and

$$\frac{1}{2\gamma^2} < \frac{\tilde{\omega}}{\omega} = |1 - n| .$$

This means that after the stationary state is established and the right-hand side of Equation (4.2) vanishes, the distribution function of particles must be cut off for energies

$\gamma > \gamma_{cr}$, where

$$\gamma_{cr} \simeq \left(\frac{\gamma_{\min}^{3/2} \omega^2 \rho}{\omega_p c} \right)^{1/5} \simeq \gamma_{\min} \left(\frac{\omega}{\omega_c} \right)^{1/5} A^{-1/5}.$$

For the characteristic frequencies of curvature radiation $\omega \sim \omega_c$ (2.8) the quantity γ_{cr} in the order of magnitude is γ_{\min} . Thus, the quasi-linear relaxation leads to a considerable deceleration of a relativistic plasma flux. For the distribution functions of electrons and positrons of the form $F_{\parallel}^{\pm}(p_{\parallel}) \sim p_{\parallel}^{-\bar{\nu}} (\bar{\nu} \simeq 2)$ the fraction of energy lost on the average per particle is given by

$$m_e c^2 \gamma_{\min} \left(\ln \frac{\gamma_{\max}}{\gamma_{\min}} - 1 \right),$$

where γ_{\max} is the maximum value of the Lorentz-factor of particles due to the mechanism of particle generation in the polar region of pulsar magnetosphere, $\gamma_{\max} \simeq 10^4$ – 10^5 .

We can see that if the quasi-linear approximation had been valid, a considerable part of the plasma flux energy would have converted into electromagnetic radiation. But as shown below, the nonlinear interaction of a higher order leads to saturation of instability on a lower level. Therefore, quasi-linear effects turn out to be inessential.

4.3. THREE-WAVE INTERACTION

Let there exist three waves with frequencies $\omega_1, \omega_2, \omega_3$; their electric fields have, respectively, the form

$$\mathbf{E}_j^0(\mathbf{r}) \exp\{i\Phi_j(\mathbf{r}) - i\omega_j t\}; \quad j = 1, 2, 3.$$

The local wave numbers are equal to

$$\mathbf{k}_j = \nabla \Phi_j = \mathbf{k}_j(\omega_j, \mathbf{r}).$$

Consider the case where $\omega_1 \simeq \omega_2 + \omega_3$. On a frequency $\omega_2 + \omega_3$ a nonlinear current \mathbf{j} describing a nonlinear wave interaction is given (cf. Istomin, 1988) by

$$j_{\alpha} = \sigma_{\alpha\sigma\lambda}^N E_{2\sigma}^0 E_{3\lambda}^0 \exp[i(\Phi_2 + \Phi_3) - i(\omega_2 + \omega_3)t],$$

where $\sigma_{\alpha\sigma\lambda}^N$ is a nonlinear plasma conductivity

$$\begin{aligned} \sigma_{\alpha\sigma\lambda}^N = & \sum_{e^+, e^-} e \int d\mathbf{p} v_{\alpha} [\hat{M}_{\sigma}(\omega_2 + \omega_3, \mathbf{k}_2 + \mathbf{k}_3) \hat{M}_{\lambda}(\omega_3, \mathbf{k}_3) + \\ & + \hat{M}_{\lambda}(\omega_2 + \omega_3, \mathbf{k}_2 + \mathbf{k}_3) \hat{M}_{\sigma}(\omega_2, \mathbf{k}_2)] F^{\pm}(\mathbf{p}, \mathbf{r}), \end{aligned} \quad (4.3)$$

and the operators $\hat{M}_{\chi}(\omega, \mathbf{k})$ are defined as

$$\begin{aligned} \hat{M}_{\chi}(\omega, \mathbf{k}) = & -\frac{e}{2} \int_{-\infty}^t dt' \exp[i\omega(t-t') - i\mathbf{k}\mathbf{R}^*] \det^{-1} \left| \delta_{\alpha\beta} - \frac{1}{2} \frac{\partial L_{\alpha}(\mathbf{r} + \mathbf{R}^*/2)}{\partial r_{\beta}} \right| \times \\ & \times \left[\delta_{\nu\chi} \left(1 - \frac{\mathbf{k}\mathbf{v}'}{\omega} \right) + \frac{k_{\nu} v'_{\chi}}{\omega} + \frac{i}{2\omega} \frac{\partial}{\partial r_{\nu}} v'_{\chi} - \frac{i}{2\omega} \delta_{\nu\chi} \frac{\partial}{\partial r_{\mu}} v'_{\mu} \right] \frac{\partial}{\partial p'_{\nu}} \Big|_{\mathbf{r} + \mathbf{R}^*/2}. \end{aligned}$$

A nonlinear response on frequencies $\omega_1 - \omega_2$ and $\omega_1 - \omega_3$ can be written in a similar way. The quantity $\sigma_{\alpha\sigma\lambda}^N$ (4.3) is proportional to the cube of the particle charge, and for quasi-neutral electron-positron plasma with identical distribution functions there would occur a complete mutual compensation of contributions from individual components. However, as mentioned in Section 2.1, the distribution functions of electrons and positrons in pulsar magnetosphere differ substantially from one another so that there is no compensation and the nonlinear conductivity which describes the three-wave interaction does not vanish.

For a distribution function of the form (3.9) ($\mathbf{p}_{dr} \rightarrow 0$) $\hat{M}_\chi(\omega, \mathbf{k})$ is equal to

$$\begin{aligned} \hat{M}_\chi(\omega, \mathbf{k}) = & -\frac{e}{2} \int_0^\infty d\tau \int_{-\infty}^\infty dp_\parallel \exp \left[i(\omega - \mathbf{k}\mathbf{b}v_\parallel)\tau + \frac{i}{24} \mathbf{k}\mathbf{b} \frac{v_\parallel^3}{\rho^2} \tau^3 \right] \times \\ & \times \left(b_\chi - n_\chi \frac{v_\parallel}{2\rho} \tau \right) \delta \left(\mathbf{p} - p_\parallel \mathbf{b} - \mathbf{n} p_\parallel \frac{v_\parallel}{2\rho} \tau \right) \frac{\partial}{\partial p_\parallel}. \end{aligned} \quad (4.4)$$

Substituting Equation (4.4) into (4.3) we find that

$$\begin{aligned} \sigma_{\alpha\sigma\lambda}^N = & \sum_{e^+, e^-} \frac{e^3}{4} \int_{-\infty}^\infty dp_\parallel v_\parallel \int_0^\infty d\tau \int_0^\infty d\tau' \left[b_\alpha + n_\alpha \frac{v_\parallel}{2\rho} (\tau + \tau') \right] \left[b_\sigma - n_\sigma \frac{v_\parallel}{2\rho} (\tau' - \tau) \right] \times \\ & \exp[i(\omega_2 - \omega_3)\tau' - i(\mathbf{k}_2 - \mathbf{k}_3)\mathbf{R}_1^*] \frac{\partial}{\partial p_\parallel} \left\{ \left[b_\lambda - n_\lambda \frac{v_\parallel}{2\rho} (\tau - \tau') \right] \times \right. \\ & \times \left. [\exp(i\omega_3 \tau - i\mathbf{k}_3 \mathbf{R}^*) + \exp(i\omega_2 \tau - i\mathbf{k}_2 \mathbf{R}^*)] \right\} \frac{\partial F_\parallel}{\partial p_\parallel}; \end{aligned} \quad (4.5)$$

$$\mathbf{R}_1^* = \mathbf{b} \left(v_\parallel \tau' - \frac{1}{24} \frac{v_\parallel^3}{\rho^2} \tau'^3 \right);$$

$$\mathbf{R}^* = \left(\mathbf{b} + \mathbf{n} \frac{v_\parallel}{2\rho} \tau' - \mathbf{b} \frac{v_\parallel^2}{8\rho^2} \tau'^2 \right) v_\parallel \tau - \mathbf{b} \frac{v_\parallel^3}{24\rho^2} \tau^3.$$

4.4. THE STATIONARY SPECTRUM OF UNSTABLE MODES

Consider a three-wave interaction of unstable curvature-plasma waves ($j = 5, 6$, Equation (3.28)) among themselves and with plasma modes ($j = 2, 3$ (3.27)). The laws of conservation of momentum $\mathbf{k}_{5,6} = \mathbf{k}_2 + \mathbf{k}_3^*$ and energy $\omega_{5,6} = \omega_2 + \omega_3$ are obeyed in the latter case only in a narrow-angle cone $\theta < \theta_* a^{-3/20} = \theta_\perp$ (3.35), $\theta_\perp \ll \theta_* \ll \theta_\parallel$

* In a nonhomogeneous medium the momentum is not conserved, but its non-conservation in the interaction act $\Delta k \simeq (jk/\rho)^{1/2}$ is very small as compared with the characteristic widths of the spectra of the excited waves and, therefore, it can be disregarded.

(3.26). Therefore, in the entire angle cone $(\theta_{\parallel}, \theta_{\perp})$ (see Figure 10), where the excitation of oscillations is most effective, essential is only the interaction among unstable curvature-plasma waves.

Unstable modes obeying the dispersion law

$$\omega = k_z c + \tilde{\omega},$$

where the quantity $\tilde{\omega}$ is determined by the expressions (3.25) and (3.28), can be described as single-drift mode, but with a complex amplitude rather rapidly changing in time: i.e.,

$$\mathbf{E}_l(\mathbf{r}, t) \exp[-i\omega_l t + i\Phi_l(\mathbf{r})];$$

$$\mathbf{k}_l = \nabla \Phi_l, \quad \omega_l = k_{zl} c.$$

Since the instability is of hydrodynamic character, when $\text{Re } \tilde{\omega} \simeq \text{Im } \tilde{\omega}$, the excited waves are in fact monochromatic and their electric field can be represented in the form of the integral

$$\mathbf{E}_l = \int \mathbf{E}_l(\mathbf{k}_l, \mathbf{r}, t) \exp[-i\omega_l t + i\Phi_l(\mathbf{r})] d\mathbf{k}_l. \quad (4.6)$$

Some harmonics can interact with one another in any order of nonlinearly because the dispersion $\omega \simeq k_z c$ implies a strong coupling between them. But due to the fact that they exist only in a narrow angle cone in the direction of the magnetic field, the most effective is three-wave interaction because the phase volume these harmonics occupy is small. A stationary solution is possible in this case because the decay of the wave into two leads to the fact that the wave vector leaves the amplification cone beyond which the waves damp strongly.

The calculation of the nonlinear conductivity is substantially simplified because for unstable modes $\tilde{\omega}/\omega \gg (c/\rho\omega)^{2/3} (a \gg 1)$ and the quantities \mathbf{R}_1^* and \mathbf{R}^* from the expression (4.5) can be put, respectively, equal to $\mathbf{R}_1^* = \mathbf{b}v_{\parallel} \tau'$, $\mathbf{R}^* = \mathbf{b}v_{\parallel} \tau$ (as in a homogeneous medium). As a result we have

$$\begin{aligned} \sigma_{\alpha\sigma\lambda}^N = & \frac{1}{2} \frac{|e^3| n_e}{m_e^2} \omega_1 \left\langle \frac{1}{v_{\parallel} \gamma^4} \left(3 + \frac{\omega}{\gamma^3} \frac{\partial}{\partial \tilde{\omega}} \right) \frac{1}{\tilde{\omega}_1^2} \left[b_{\alpha} b_{\sigma} b_{\lambda} I_1 + \right. \right. \\ & + i b_{\alpha} (b_{\sigma} n_{\lambda} - n_{\sigma} b_{\lambda}) \frac{v_{\parallel}}{\rho} I_2 + i n_{\alpha} b_{\sigma} b_{\lambda} \frac{v_{\parallel}}{\rho} I_3 + \\ & + b_{\alpha} n_{\sigma} n_{\lambda} \frac{v_{\parallel}^2}{\rho^2} I_4 + n_{\alpha} (b_{\sigma} n_{\lambda} - b_{\lambda} n_{\sigma}) \frac{v_{\parallel}^2}{\rho^2} I_5 + \\ & \left. \left. + i n_{\alpha} n_{\sigma} n_{\lambda} \frac{v_{\parallel}^3}{\rho^3} I_6 \right] \right\rangle, \quad (4.7) \end{aligned}$$

where

$$\begin{aligned}
 I_1 &= \frac{1}{\tilde{\omega}_2} + \frac{1}{\tilde{\omega}_3} ; \\
 I_2 &= \frac{1}{\tilde{\omega}_1 \tilde{\omega}_2} + \frac{1}{\tilde{\omega}_1 \tilde{\omega}_3} - \frac{1}{2\tilde{\omega}_2^2} - \frac{1}{2\tilde{\omega}_3^2} ; \\
 I_3 &= \frac{1}{\tilde{\omega}_1 \tilde{\omega}_2} + \frac{1}{\tilde{\omega}_1 \tilde{\omega}_3} + \frac{1}{2\tilde{\omega}_2^2} + \frac{1}{2\tilde{\omega}_3^2} ; \\
 I_4 &= \frac{3}{2} \frac{1}{\tilde{\omega}_1^2 \tilde{\omega}_2} + \frac{3}{2} \frac{1}{\tilde{\omega}_1^2 \tilde{\omega}_3} - \frac{1}{\tilde{\omega}_1 \tilde{\omega}_2^2} - \frac{1}{\tilde{\omega}_1 \tilde{\omega}_3^2} + \frac{1}{2\tilde{\omega}_2^3} + \frac{1}{2\tilde{\omega}_3^3} ; \\
 I_5 &= \frac{1}{2\tilde{\omega}_2^3} + \frac{1}{2\tilde{\omega}_3^3} - \frac{3}{2} \frac{1}{\tilde{\omega}_1^2 \tilde{\omega}_2} - \frac{3}{2} \frac{1}{\tilde{\omega}_1^2 \tilde{\omega}_3} ; \\
 I_6 &= \frac{3}{4} \frac{1}{\tilde{\omega}_2^4} + \frac{3}{4} \frac{1}{\tilde{\omega}_3^4} - \frac{3}{4} \frac{1}{\tilde{\omega}_1^2 \tilde{\omega}_2^2} - \frac{3}{4} \frac{1}{\tilde{\omega}_1^2 \tilde{\omega}_3^2} - \\
 &\quad - \frac{1}{2\tilde{\omega}_1 \tilde{\omega}_2^3} - \frac{1}{2\tilde{\omega}_1 \tilde{\omega}_3^3} + \frac{3}{\tilde{\omega}_1^3 \tilde{\omega}_2} + \frac{3}{\tilde{\omega}_1^3 \tilde{\omega}_3} .
 \end{aligned}$$

In a homogeneous field in a nonrelativistic limit ($\gamma \rightarrow 1$) the expression under the integral sign in Equation (4.7) transforms into the well-known result (Tsytovich, 1971)

$$\left(3 + \frac{\omega}{\gamma^3} \frac{\partial}{\partial \tilde{\omega}} \right) \frac{1}{\tilde{\omega}_1^2} I_1 = - \frac{v_{\parallel}}{\omega_1 \omega_2 \omega_3} \left(\frac{k_{z1}}{\omega_1} + \frac{k_{z2}}{\omega_2} + \frac{k_{z3}}{\omega_3} \right) .$$

In the curved field in Equation (4.7) we make in fact an expansion with respect to $c/\rho\tilde{\omega} \ll 1$. But since the transverse component of the electric field of unstable modes is $\rho\tilde{\omega}/c$ times larger than the longitudinal one (see Equation (3.32)), all the terms in the expression (4.7) are of the same order of magnitude. Substituting Equation (4.7) into the dispersion equation that takes into account the nonlinear conductivity

$$(n_1^2 \delta_{\alpha\beta} - n_{1\alpha} n_{1\beta} - \varepsilon_{\alpha\beta}) E_{1\beta} = \frac{4\pi i}{\omega_1} \sigma_{\alpha\beta\lambda}^N E_{2\beta} E_{3\lambda} ,$$

we obtain

$$\begin{aligned}
 &\left(\frac{4\tilde{\omega}_1^5 \rho^2}{c^2 \omega_p^2 \omega_1} \langle \gamma^{-3} \rangle^{-1} - 1 \right) E_{1z} = \frac{3}{2} i \frac{e}{m_e c} \langle \gamma^{-3} \rangle^{-1} \langle \gamma^{-4} \rangle E_{2z} E_{3z} \times \\
 &\times \left\{ \frac{\tilde{\omega}_1}{2} \left(\frac{\tilde{\omega}_3}{\tilde{\omega}_2^3} + \frac{\tilde{\omega}_2}{\tilde{\omega}_3^3} \right) + 2 \left(\frac{1}{\tilde{\omega}_2} + \frac{1}{\tilde{\omega}_3} + \frac{\tilde{\omega}_3}{2\tilde{\omega}_2^2} + \frac{\tilde{\omega}_2}{2\tilde{\omega}_3^2} \right) - \frac{3}{2} \frac{1}{\tilde{\omega}_1} \times \right. \\
 &\times \left. \left(\frac{\tilde{\omega}_3}{\tilde{\omega}_2} + \frac{\tilde{\omega}_2}{\tilde{\omega}_3} \right) + \left(\frac{4\tilde{\omega}_1^5 \rho^2}{c^2 \omega_p^2 \omega_1} \langle \gamma^{-3} \rangle^{-1} - 3 \right) \left[\frac{2}{\tilde{\omega}_1} + \frac{1}{2} \left(\frac{1}{\tilde{\omega}_2} + \frac{1}{\tilde{\omega}_3} \right) \right] \right\} \times \\
 &\times \exp[i(\omega_1 - \omega_2 - \omega_3)t - i(\Phi_1 - \Phi_2 - \Phi_3)] .
 \end{aligned} \tag{4.8}$$

The quantity $\tilde{\omega}$ is proportional here to the time derivative which acts on the wave packet amplitudes: i.e., $\tilde{\omega} = i \partial/\partial t$.

In the left-hand side of Equation (4.8) the turning of the wave vector due to inhomogeneity ($d\theta/dt \simeq c/p$) is disregarded, because in the region $a \gg 1$ we have

$$\frac{\rho}{c} |\tilde{\omega}| \gg \theta_{\parallel}^{-1}.$$

Now proceeding to the spectral expansion (4.6) and solving Equation (4.8), we obtain

$$E_{z_l}(\omega, \theta) \simeq \frac{m_e c}{e} \langle \gamma^{-4} \rangle^{-1} \langle \gamma^{-3} \rangle \left\langle \frac{\omega_p^2}{\gamma^3} \right\rangle^{-1/5} \left(\frac{c}{\rho} \right)^{3/5} \frac{\omega^{4/5}}{\omega_{\max}}, \quad (4.9)$$

where ω_{\max} is the maximal frequency of the excited curvature-plasma mode, i.e., the value of the frequency when the hydrodynamic instability vanishes

$$\tilde{\omega}/\omega = \frac{1}{2} \gamma_{\min}^{-2}.$$

According to (3.28)

$$\omega_{\max} \simeq \gamma_{\min}^{7/4} (\omega_p c / \rho)^{1/2}. \quad (4.10)$$

The condition (4.10) coincides, naturally, with the boundary (3.37) between regions I and II. The wave amplitude $E_l(\omega, \theta)$ is constant inside the amplification cone and is equal to zero outside the cone.

According to Equation (3.32), the total spectral amplitude is equal to

$$\begin{aligned} E_l(\omega) &= E_{l_x}(\omega) = \frac{\rho}{c} |\tilde{\omega}| E_{l_x}(\omega, \theta) \theta_{\parallel} = \\ &= \frac{m_e c}{e} \langle \gamma^{-3} \rangle^{7/5} \langle \gamma^{-4} \rangle^{-1} \omega_p^{4/5} \left(\frac{c}{\rho} \right)^{-1/5} \omega^{2/5} \omega_{\max}^{-1}. \end{aligned} \quad (4.11)$$

Saturation of the instability up to the level determined by the state (4.11) proceeds within a short time of the order of $|\tilde{\omega}|^{-1}$. The corresponding length $c/|\tilde{\omega}|$ is small as compared with the curvature radius, and therefore the stationary state can be regarded to be realized in fact at each space point where there exists instability. The spectral energy density U_{ω} can be determined from the considerations that the instability increment $|\tilde{\omega}|$ is responsible also for the wave coherence time. Since $|\tilde{\omega}| \ll \omega_{\max}$, then

$$U_{\omega} = \frac{1}{8\pi} E_l^2(\omega) |\tilde{\omega}| \simeq \frac{1}{8\pi} \left(\frac{m_e c}{e} \right)^2 \langle \gamma^{-3} \rangle^3 \langle \gamma^{-4} \rangle^{-2} \omega_p^2 \omega \omega_{\max}^{-2}. \quad (4.12)$$

The total energy density in the entire frequency range is equal to

$$U = \int U_{\omega} d\omega \simeq n_e m_e c^2 \langle \gamma \rangle \gamma_{\min}^{-2} \simeq \lambda^{-1} m_e c^2 \langle \gamma \rangle. \quad (4.13)$$

Thus we can see that the multiplicity parameter $\lambda \sim 10^3\text{--}10^5$ determines the coefficient of relativistic plasma energy transformation into the energy of unstable curvature-plasma oscillations and that it is a universal quantity depending only on specificities of plasma generation in each individual pulsar. The transformation coefficient $\eta = U/m_e c^2 n_e \langle \gamma \rangle$ is small and is equal to about $10^{-3}\text{--}10^{-5}$, which proves validity of the weak turbulence approximation.

4.5. MODE TRANSFORMATIONS

Now consider energy transformation of unstable curvature-plasma modes into normal waves $j = 1, 2$. Investigation of such a transformation is of essential interest because, as will be seen below, it is only these waves that can leave pulsar magnetosphere. First of all we will show that in a curved magnetic field a linear transformation of the energy of unstable modes into an extraordinary wave $j = 1$ is possible. The point is that as a result of nonlinear interaction of unstable waves $j = 5, 6$ the shift of their frequency $\tilde{\omega}$ must tend to zero because the saturation is characterized just by the condition $\partial/\partial t = 0$. This means that in a stationary state normal modes $j = 5, 6$ are not, in fact, distinct from the mode $j = 4$, and, therefore, the energy density $U_{\omega}^{(4)}(\theta) \simeq U_{\omega}^{(4)}/\theta_{\parallel}$ of the normal wave $j = 4$ also reaches the values determined by the relation (4.12).

On the other hand, as shown in Section 3, for angles $\theta \sim \theta_{\perp}$ the mode $j = 4$ is linearly transformed into the extraordinary wave $j = 1$. Since in a curved magnetic field the angle θ between the vectors \mathbf{k} and \mathbf{B} increases with a characteristic velocity $d\theta/dt = c/\rho$ then, as is seen from Figure 11, the energy of the normal wave $j = 4$ from the region $\theta < \theta_{\perp}$ will be permanently pumped over into the normal wave $j = 1$ for angles $\theta > \theta_{\perp}$. The energy outflow from the region $\theta < \theta_{\perp}$ in no way affects the magnitude of the stationary spectrum (4.12) because the characteristic time $\tau_{\theta} \simeq \rho\theta_{\perp}/c$ within which the angle θ varies exceeds greatly the saturation time $\Gamma = |\tilde{\omega}|^{-1}$. Indeed, as can be readily verified, according to Equations (3.28) and (3.25), the condition $\tau_{\theta} \gg \Gamma$ coincides with the condition $a \gg 1$ which is always satisfied in region I. Thus, we see that due to a permanent transformation of the mode $j = 4$ in a curved magnetic field, a transverse electromagnetic wave is effectively generated.

Next, the transformation of energy into an ordinary wave $j = 2$ ($\theta > \theta_{*}$) could proceed at the expense of decay of unstable modes $j = 5, 6$ into two plasma waves $j = 2$ and $j = 3$ ($\theta < \theta_{*}$). As has already been mentioned, this decay takes place for small angles $\theta \lesssim \theta_{\perp}$. However, this decay does not take place because the low-frequency mode $j = 3$, as has already been said, has a negative energy (Wilhelmson *et al.*, 1970). If this decay did take place, this would lead to an increase of the energy of a normal wave with a negative energy, which means the fall of its amplitude down to zero and, therefore, a complete cessation of three-wave interaction.

Nevertheless, an effective energy transformation into an ordinary wave $j = 2$ is possible. The point is that the three-wave interaction leading to the formation of a stationary spectrum of unstable modes has been considered above, in fact, in the framework of hydrodynamics, when the shift of the frequency $\tilde{\omega}$ exceeds greatly the kinetic velocity spread of particles: $|\tilde{\omega}/\omega| \gg \frac{1}{2}\gamma^{-2}$. This condition is well fulfilled in

the linear case. But an account of wave interaction leads to a decreasing frequency shift, and in particular for a curvature-plasma wave the three-wave interaction results in $\tilde{\omega} \rightarrow 0$. The stationary spectrum thus formed is a plasma density modulation moving with plasma along magnetic field lines. Now we have to take into account the kinetic spread of charged particles over velocities: scattering on density inhomogeneities they will radiate electromagnetic waves. Polarization of inhomogeneities is such that the radiated waves have an electric field component that lies in the plane of the magnetic field line. This is precisely the ordinary mode $j = 2$. A plasma wave is in fact scattered on an inhomogeneity created by a curvature-plasma oscillation: $\omega_2 = \omega_{5,6} + \omega'_2$. This process is most effective for waves propagating almost in the direction of the magnetic field $\theta_2 \lesssim \theta_*$ (2.18). Making use of the expression (4.5) for nonlinear conductivity under the condition $\tilde{\omega}_2 = \omega_p \langle \gamma^{-3} \rangle^{1/2} \gg \omega_2/2\gamma^2$ and $\tilde{\omega}_{5,6} = 0$ we obtain

$$\frac{\partial E_{2z}}{\partial t} = \pi \frac{e}{m_e} \omega_p \langle \gamma^{-3} \rangle^{-1/2} |E_{z1}| E_{2z} \frac{\rho^{2/3}}{\omega_l^{1/3} c^{5/3}} \times \\ \times \left\langle \frac{1}{\gamma^4} [3 \text{Ai}(\xi) + 2\xi \text{Ai}'(\xi)] \right\rangle; \quad \xi = \left(\frac{\omega_l \rho}{c \gamma^3} \right)^{2/3}. \quad (4.14)$$

For a given wave $E_{5,6}$ Equation (4.14) describes the plasma wave excitation. Knowing the spectrum of the curvature-plasma mode (4.9), we find the characteristic excitation increment of an ordinary wave is given by

$$\Gamma_2 \simeq \omega_p \left(\frac{c}{\omega_p \rho} \right)^{2/5} \gamma_{\min}^{-1/2}.$$

The increment Γ_2 is of the order of $\tilde{\omega}$ for unstable waves $j = 5, 6$ with the characteristic frequency $\omega = \omega_p \gamma_{\min}^{-3/2}$. This means that excitation of an ordinary wave is as rapid as an increase of unstable modes $j = 5, 6$.

Determine the energy density of an ordinary wave $j = 2$ within the range of angles $\theta \lesssim \theta_*$. This can be easily done by assuming that the increase of the amplitude of this wave will be stopped as soon as its reaction to the curvature-plasma wave becomes essential. The calculation quite analogous to Equation (4.14) leads to the following relation for 'monochromatic' amplitudes

$$(n^2 \delta_{\alpha\beta} - n_\alpha n_\beta - \varepsilon_{\alpha\beta}) E_{l\beta} = -2\pi \omega_p \langle \gamma^{-3} \rangle^{-1/2} \frac{|e|}{m_e c} \left(\frac{\rho^2}{\omega c^2} \right)^{2/3} E_{z2} E_{z2}^* \times \\ \times \left\langle \frac{\text{sign } e}{\gamma^4} (3 \text{Ai}' + 2\xi \text{Ai}'') \right\rangle.$$

Here also $\xi = (\omega \rho / c \gamma^3)^{2/3}$ and averaging is made over the distribution function of plasma particles. Now passing over to the spectral amplitudes $E_\omega(\Omega) = E_\omega(\theta)/\theta_\perp$ and making use of the relations (3.35) and (4.9) we obtain

$$JJ_1 = \langle \gamma^{-3} \rangle^{11/5} \langle \gamma^{-4} \rangle^{-1} \left(\frac{\tilde{\omega}}{\omega} \right)^{-2} \left(\frac{m_e c}{e} \right)^2 \left(\frac{c}{\rho} \right)^{26/15} \omega_p^{2/5} \frac{\omega^{-2/15}}{\omega_{\max}}, \quad (4.15)$$

where

$$J = \int d\omega' d\theta'^2 \frac{\omega^2}{(\omega - \omega')^2} E_{\omega'_2}(\Omega') E_{\omega - \omega'_2}^*(\Omega - \Omega') \quad (4.16)$$

and

$$J_1(\omega) = \left\langle \frac{\text{sign } e}{\gamma^4} [3 \text{Ai}'(\xi) + 2\xi \text{Ai}''(\xi)] \right\rangle.$$

First of all consider the expression for J_1 in square brackets. It is clear that the contribution of electrons and positrons will have opposite signs because the current quadratic in the amplitude E is known to be proportional to the charge cubed e^3 . Remembering that within the range $\mathcal{E}_{\min}^{\pm} < \mathcal{E}^{\pm} < \mathcal{E}_{\max}^{\pm}$ both the components have a power-law spectra with the index $\nu = 2$, we obtain for each of the components

$$\langle \rangle_{\pm} = \begin{cases} 3 \text{sign } e \text{Ai}'(0) \langle \gamma^{-4} \rangle; & \omega \ll \frac{c}{\rho} \gamma_{\min}^{\pm 3}, \\ c_1 \gamma_{\min}^{\pm} \text{sign } e \left(\frac{\omega \rho}{c} \right)^{-5/3}; & \frac{c}{\rho} \gamma_{\min}^{\pm 3} \ll \omega \ll \frac{c}{\rho} \gamma_{\max}^{\pm 3}, \\ \sim 0; & \omega \gg \frac{c}{\rho} \gamma_{\max}^{\pm 3}, \end{cases} \quad (4.17)$$

where

$$c_1 = \frac{1}{2} \int_0^{\infty} dx x^{3/2} (3 \text{Ai}' + 2x \text{Ai}'') = \frac{1}{4\pi^{1/2}} 3^{5/6} \Gamma(5/6) \simeq 0.40 > 0.$$

Since $\text{Ai}'(0) < 0$, then as we can see the expression (4.17) has opposite signs at $\omega > (c/\rho) \gamma_{\min}^{\pm 3}$ and $\omega < (c/\rho) \gamma_{\min}^{\pm 3}$. Therefore, within the range*

$$\frac{c}{\rho} \gamma_{\min}^{-3} < \omega < \frac{c}{\rho} \gamma_{\min}^{+3} \quad (4.18)$$

the expression in square brackets is equal to

$$J_1(\omega) = \sum_{e^+, e^-} \langle \rangle_{\pm} = \begin{cases} c_1 \gamma_{\min} (\omega \rho / c)^{-5/3}, & \omega < \omega_{br}; \\ 3 \text{Ai}'(0) \langle \gamma^{-4} \rangle_+, & \omega > \omega_{br}, \end{cases} \quad (4.19)$$

where

$$\omega_{br} = \frac{c}{\rho} \gamma_{\min}^{-3} \left(\frac{\gamma_{\min}^+}{\gamma_{\min}^-} \right)^{12/5} \quad (4.20)$$

* Remember that we are considering the case where $\gamma_{\min}^- < \gamma_{\min}^+$.

as the main contribution into (4.17) for $\omega < \omega_{br}$ being introduced by the slow and for $\omega > \omega_{br}$ by the fast plasma component. Outside the frequency interval (4.18) the expression (4.19) becomes negative, so that the state established becomes impossible.

Now consider Equation (4.15). We will seek its solution in the form

$$E_{2\omega}(\Omega) = E^A \omega^{\bar{\mu}}.$$

The analysis of the expression (4.15) shows that $\bar{\mu} = -\frac{2}{15}$ for $\omega > \omega_{br}$ and $\bar{\mu} = \frac{23}{15}$ for $\omega < \omega_{br}$. The main contribution into the integral J determined by the relation (4.16) (in which integration over the angle θ' should be carried out up to the angle $\theta_*(\omega)$ (2.18)) is made by the frequencies ω' concentrated near ω_{br} , and in this case $\omega' \ll \omega$. That is why $E_{\omega-\omega'}(\Omega - \Omega')$ in J could be taken out in front of the integral sign*.

On the other hand, for $\omega' \ll \omega$ the integral J coincides in fact with the spectral intensity of the squared amplitude of the electric field because

$$(E^2)_{\omega, \Omega} = \int d\omega' d\Omega' E_{\omega'}(\Omega') E_{\omega-\omega'}(\Omega - \Omega').$$

Therefore, one can estimate the spectral energy density of an ordinary wave, for which in the range of angles $\theta \lesssim \theta_*$

$$U_A^{(2)} = \frac{1}{16\pi} \left\{ \frac{\partial}{\partial \omega} (\omega \varepsilon_{\alpha\beta}) E_\alpha E_\beta^* + |B|^2 \right\} \simeq \frac{1}{8\pi} \omega \left\langle \frac{\omega_p^2}{\gamma^3} \right\rangle^{-1/2} |E_z|^2,$$

as

$$U_\omega^{(2)}(\Omega) = \frac{\omega_{br}}{8\pi} \left\langle \frac{\omega_p^2}{\gamma^3} \right\rangle^{-1/2} J. \quad (4.21)$$

Employing now the relations (4.15) and (4.21), we finally obtain

$$U_\omega^{(2)}(\Omega) \simeq \left(\frac{\tilde{\omega}}{\omega} \right)^{-2} \frac{\langle \gamma^{-3} \rangle^{17/10}}{\langle \gamma^{-4} \rangle} \left(\frac{m_e c}{e} \right)^2 \left(\frac{c}{\rho} \right)^{26/15} \omega_p^{-3/5} \frac{\omega_{br}}{\omega_{\max}} \omega^{-2/15} J_1^{-1}(\omega), \quad (4.22)$$

where $J_1(\omega)$ is given by Equation (4.19). We can see that the spectral energy density has a maximum for $\omega \sim \omega_{br}$: $U_\omega^{(2)}(\Omega) \propto \omega^{23/15}$ for $\omega < \omega_{br}$ and $U_\omega^{(2)}(\Omega) \propto \omega^{-2/15}$ for $\omega > \omega_{br}$. Finally, integrating (4.22) over $d\Omega = \pi d\theta^2$ and over the frequency ω , we obtain for the transformation coefficient

$$\eta^{(2)} \simeq \gamma_c^3 \left(\frac{\tilde{\omega}}{\omega} \right)^{-2} \left(\frac{c}{\rho_{\min} \omega_{p0}} \right)^{21/10} \left(\frac{\gamma_+}{\gamma_-} \right)^{52/25} \left(\frac{l}{R} \right)^{2.1}. \quad (4.23)$$

In our subsequent calculations we put $\tilde{\omega}/\omega \sim \langle \gamma^{-2} \rangle$.

* For simplicity $E_\omega(\Omega)$ is assumed to be independent of Ω within the range of angles $\theta \lesssim \theta_*$.

5. Generation of Radio Emission in Pulsar Magnetosphere

5.1. BASIC PARAMETERS

Now let us discuss the mechanism of electromagnetic wave generation in pulsar magnetosphere. For simplicity we assume a magnetic field \mathbf{B} to be a dipole one – i.e.,

$$\mathbf{B} = \frac{3\mathbf{r}(\mathbf{M}\mathbf{r}) - r^2\mathbf{M}}{r^5}$$

(\mathbf{M} is the magnitude of the magnetic dipole), and consider the wave propagation only near the magnetic axis. In this case the curvature radius of the magnetic field line $\rho(\mathbf{r})$ and its slope angle to the magnetic axis $\alpha(\mathbf{r})$ can be written in the form

$$\rho(\mathbf{r}) = \frac{4}{3} \frac{r^2}{r_{\perp}}, \quad (5.1)$$

$$\alpha(\mathbf{r}) = \frac{3}{2} \frac{r_{\perp}}{r}, \quad (5.2)$$

where r_{\perp} is the distance from the magnetic dipole axis, r is the distance from the star center.

In what follows we use the so-called ‘dipole’ coordinates f and l , where l is the coordinate along the magnetic field line and the dimensionless coordinate

$$f = \frac{c}{2\pi M \Omega} \int \mathbf{B} \, ds, \quad \Omega = 2\pi/P$$

is constant along the field line.

In the normalization of f thus chosen the last open field line for an axisymmetric magnetosphere corresponds to the value $f_* = 1.6$ (Michel, 1973; Mestel and Wang, 1979; Beskin *et al.*, 1983). Near the dipole $f = f_*(r_{\perp}/r_{\perp 0})^2$, where $r_{\perp 0}^2 = (\Omega r/c)r^2$, so on the dipole axis $f = 0$. It is also clear that near the magnetic dipole axis one can put $l = r$.

As a result, the relations (5.1) and (5.2) can be rewritten in the form

$$\rho(\mathbf{r}) = \rho_{\min} f^{-1/2} \left(\frac{l}{R} \right)^{1/2}, \quad (5.3)$$

$$\alpha(\mathbf{r}) = \frac{3}{2} \left(\frac{\Omega R}{c} \right)^{1/2} f^{1/2} \left(\frac{l}{R} \right)^{1/2}, \quad (5.4)$$

where

$$\rho_{\min} \simeq 0.75 \times 10^8 \left(\frac{R}{10^6 \text{ cm}} \right)^{1/2} \left(\frac{P}{1 \text{ s}} \right)^{1/2} \text{ cm};$$

and R is the star radius. The particle density will also vary along the field line. Using Equation (2.2), we obtain

$$\omega_p^2 = 2\lambda\omega_B\Omega \simeq 10^{24} \lambda_4 B_{12} P^{-1} G(f) \left(\frac{l}{R}\right)^{-3} \text{ s}^{-2}, \quad (5.5)$$

where the factor $G(f) \sim 1$ specifies the profile of particle density on the polar cap surface (see Figure 1). In what follows

$$\lambda_4 = \lambda \times 10^{-4}; \quad B_{12} = B_0/10^{12} \text{ G}; \quad R_6 = R/10^6 \text{ cm}.$$

Thus, in a real magnetosphere we have, in fact, only two parameters – the wave frequency $\nu = \omega/2\pi$ and the distance from the star l . All the other parameters are expressed in terms of them by means of the relations (5.3) and (5.4). In particular, the parameter (3.22) introduced in Section 3, takes the form

$$a = 1.5 \times 10^9 \frac{\lambda_4 B_{12} R_6^{2/3}}{\nu_{\text{GHz}}^{2/3} P^{1/3} \gamma_{100}^3} G(f) f^{-1/3} (l/R)^{-7/3}, \quad (5.6)$$

where $\gamma_{100} = \gamma_c/100$, $\nu_{\text{GHz}} = \nu/1 \text{ GHz}$.

Three sectors corresponding to the three distinct regions considered in the previous sections are shown in Figure 12 on the plane $\nu - l$. The coordinates of the ‘particular’ point are equal to

$$\begin{aligned} \nu_* &= \frac{c^{3/4} \Omega^{1/2} \gamma_c^{17/4}}{\lambda^{1/4} \omega_{B_0}^{1/4} R^{3/4}} \simeq 0.6 \frac{\gamma_{100}^{17/4}}{\lambda_4^{1/4} B_{12}^{1/4} R_6^{3/4} P^{1/2}} G^{-1/4}(f) f^{3/4} \text{ MHz}; \\ l_* &= \frac{\lambda^{1/2} \omega_{B_0}^{1/2} R^{3/2}}{\gamma_c^{5/2} c^{1/2}} \simeq 3 \times 10^4 R \frac{\lambda_4^{1/2} B_{12}^{1/2} R_6^{1/2}}{\gamma_{100}^{5/2}} G^{-1/2}(f) f^{-1/2}. \end{aligned}$$

We can see that for the characteristic values $\gamma_c = 100$ the frequency ν_* lies much lower than the observed frequency range and l_* corresponds to distances comparable with the light cylinder radius $R_L = c/\Omega$.

From Equation (5.6) it can be easily obtained that depending on the frequency ν the level $a = 1$ will lie at a height

$$l_a = 6 \times 10^3 R \frac{\lambda_4^{3/7} B_{12}^{3/7} R_6^{3/7}}{\nu_{\text{GHz}}^{2/7} P^{1/7} \gamma_{100}^{9/7}} G^{3/7}(f) f^{-2/7}.$$

As concerns the boundary between regions I and II, according to (3.37) it can be written in the form

$$\nu_{\text{I-II}}(l) = 3.5 \frac{\lambda_4^{1/4} B_{12}^{1/4} \gamma_{100}^{7/4}}{R_6^{1/4} P^{1/2}} G^{1/4}(f) f^{1/4} \left(\frac{l}{R}\right)^{-1} \text{ GHz}. \quad (5.7)$$

Thus we see that the external regions of pulsar magnetosphere correspond to region III due to a strong dependence of particle density on the distance l . As has already

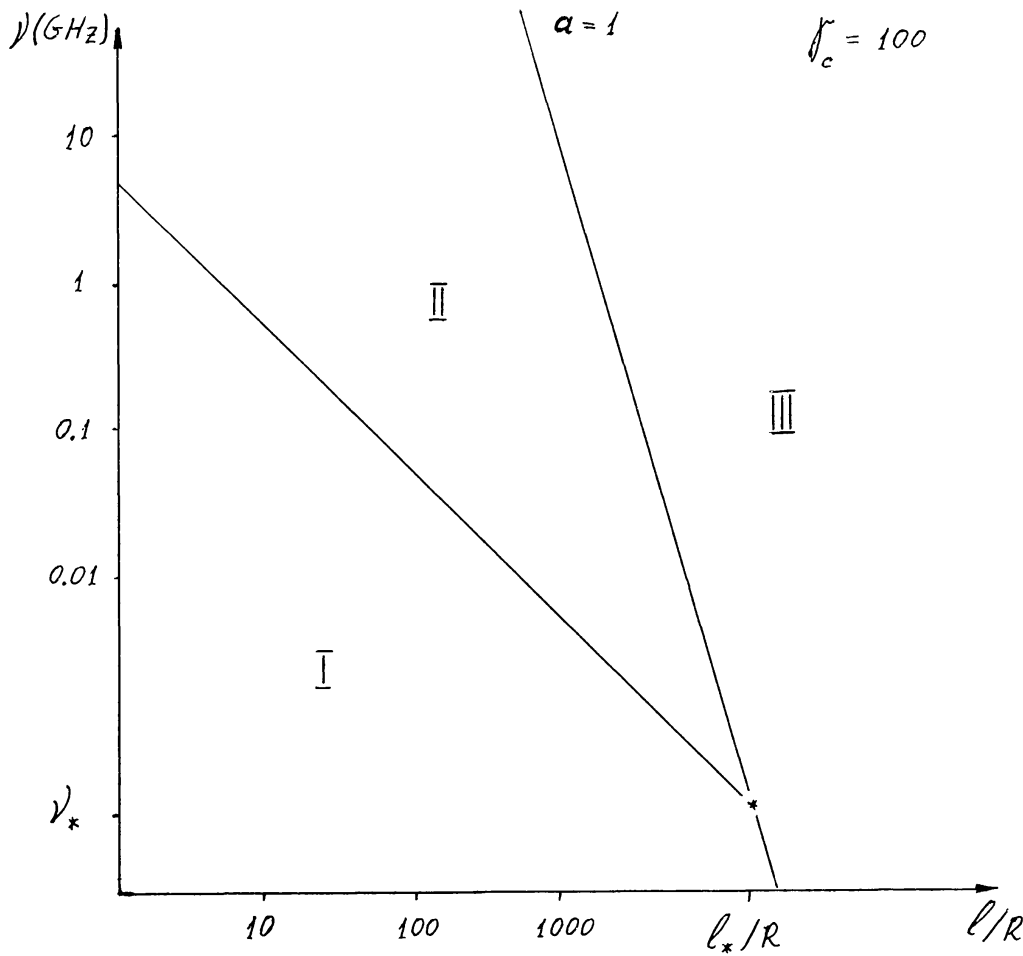


Fig. 12. Three regions of parameters distinguished in pulsar magnetosphere. Maser amplification of curvature-plasma waves is realized in region I. In region III only two transverse waves can propagate.

been mentioned, only two transverse modes can propagate here, and their attenuation can be neglected. Region I in which there exist unstable curvature-plasma waves occupies the internal part of the magnetosphere.

5.2. ELECTROMAGNETIC WAVE PROPAGATION

Now proceed to wave propagation in pulsar magnetosphere. We for simplicity analyze only the case where the wave vector \mathbf{k} lies in the plane of a curved magnetic field. Then in the framework of geometrical optics the equations of motion will be written in the form

$$\frac{dr_{\perp}}{dt} = \frac{\partial}{\partial k_{\perp}} \left(\frac{kc}{n_j} \right), \quad \frac{dk_{\perp}}{dt} = - \frac{\partial}{\partial r_{\perp}} \left(\frac{kc}{n_j} \right), \tag{5.8}$$

where the index \perp again corresponds to the components perpendicular to the dipole axis – e.g., $\theta_{\perp} = k_{\perp}/k$.

The expressions for the refractive indices $n_j(\mathbf{k}, \mathbf{r})$ can, in fact, be borrowed from the theory of a homogeneous magnetic field, which was presented in Section 2. Indeed, as

has already been mentioned, an account of magnetic field inhomogeneity leads only to splitting of an Alfvén wave $j = 4$ into three curvature-plasma modes whose dispersion properties, as shown in Figures 4 and 7 do not change very much. That is why, to determine n_j one can use the relations (2.16), (2.20a), and (2.20b) in which it is, however, necessary to put $\theta = \theta_{\perp} - \alpha(\mathbf{r})$. The last substitution is due merely to the fact that the relations (2.16)–(2.21) involve, in fact, the angle between the vectors \mathbf{k} and \mathbf{B} .

As a result, in region III, where only two transverse waves with $n_j = 1$ exist, we have

$$\frac{dr_{\perp}}{dl} = \theta_{\perp}, \quad \frac{d\theta_{\perp}}{dl} = 0. \quad (5.9)$$

As might be expected, two waves propagate along a straight line in the direction of the wave vector \mathbf{k} . As concerns regions I and II, as shown in Figure 13, it is only the ordinary

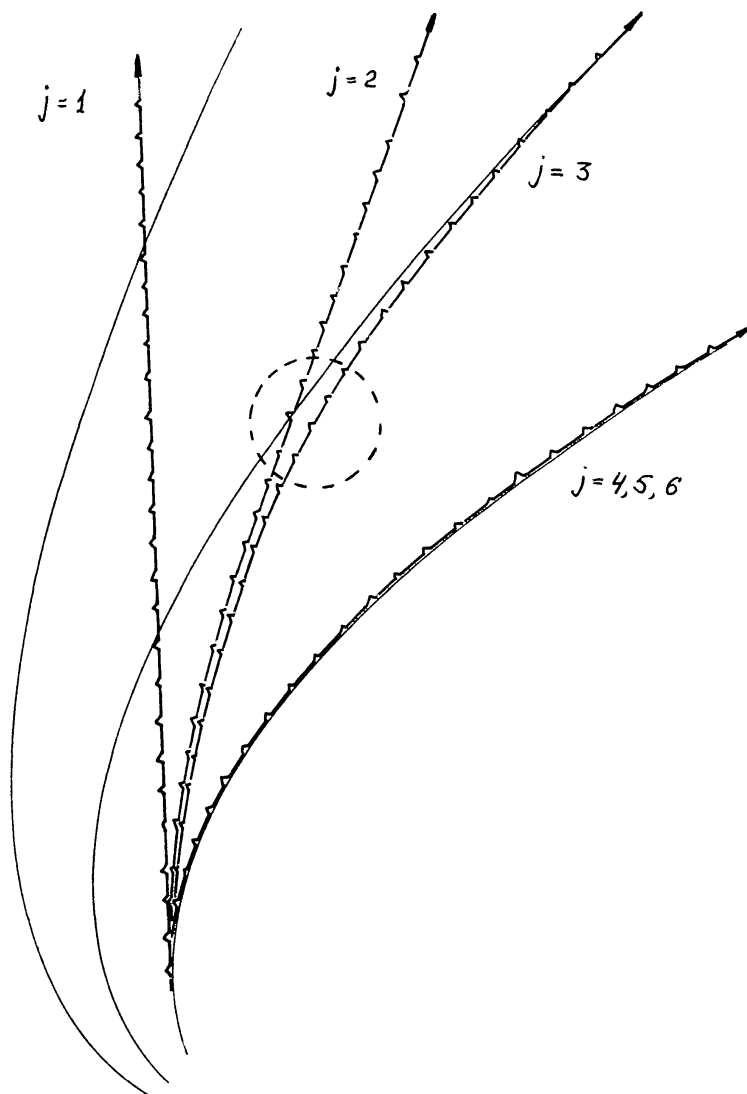


Fig. 13. Normal wave propagation in a curved magnetic field of a neutron star. The circle stands for the 'tearing off region'.

wave $j = 1$ that propagates along a straight line. It is clear that this wave has an angle $\Theta^{(1)} \equiv \theta_{\perp}^{(1)}(\infty)$ which corresponds, in fact, to the opening of the directivity pattern and practically coincides with the value $\theta_{\perp}(l_{\text{rad}})$ taken at the radiation point l_{rad} . Since, as has been shown in Section 4, the energy conversion into an extraordinary wave is possible only for extremely small angles $\theta \ll a^{-3/20} \theta_*$, we obtain that for an extraordinary wave

$$\Theta^{(1)} = \frac{3}{2} \left(\frac{\Omega R}{c} \right)^{1/2} f_{\text{rad}}^{1/2} (l_{\text{rad}}/R)^{1/2}. \quad (5.10)$$

On the other hand, for Alfvén modes with $n_j = 1/\cos \theta$ (and, therefore, for curvature-plasma waves $j = 4, 5, 6$ in region I) Equations (5.7) and (5.8), after passing over to the variables f, l , will be written in the form

$$df/dl = 0, \quad (5.11)$$

$$d\theta_{\perp}/dl = \frac{3}{2} \frac{\alpha(\mathbf{r}) - \theta_{\perp}}{l}. \quad (5.12)$$

Equation (5.11) demonstrates that curvature-plasma waves propagate along magnetic field lines. We have already pointed out this fact (see Figure 7). As regards Equation (5.12), it can be readily integrated. Taking into account the relations (5.3) and (5.4), we come (cf. Barnard and Arons, 1986) to

$$\theta_{\perp}(l) = \alpha(r_0, f) \left[\frac{1}{4} \left(\frac{l}{r_0} \right)^{-3/2} + \frac{3}{4} \left(\frac{l}{r_0} \right)^{1/2} \right];$$

where r_0 is the radius on which the wave vector \mathbf{k} is tangent to the magnetic field vector \mathbf{B} ; so that here we have $\alpha(\mathbf{r}) = \theta_{\perp}(\mathbf{r})$. It is seen that for $l \gg r_0$ the angle θ_{\perp} tends in its magnitude to $\frac{3}{4}\alpha(l)$. Consequently, with an increase of the distance to the star the angle between \mathbf{k} and \mathbf{B} will increase as $\frac{1}{4}\alpha(l)$.

Finally, for normal waves $j = 2, 3$, Equations (5.8) will be rewritten as

$$\frac{dr_{\perp}}{dl} = \theta_{\perp} + \frac{\alpha - \theta_{\perp}}{2} \left[1 \pm \frac{(\alpha - \theta_{\perp})^2}{\left(\frac{16}{\omega^2} \left\langle \frac{\omega_p^2}{\gamma^3} \right\rangle + (\alpha - \theta_{\perp})^4 \right)^{1/2}} \right], \quad (5.13)$$

$$\frac{d\theta_{\perp}}{dl} = \frac{3}{4} \frac{\alpha - \theta_{\perp}}{l} \left[1 \pm \frac{(\alpha - \theta_{\perp})^2}{\left(\frac{16}{\omega^2} \left\langle \frac{\omega_p^2}{\gamma^3} \right\rangle + (\alpha - \theta_{\perp})^4 \right)^{1/2}} \right], \quad (5.14)$$

where the plus sign corresponds to a wave with a negative energy, $j = 3$, while the minus sign to an ordinary wave $j = 2$. In the range of angles $\theta < \theta_*$ both normal waves $j = 2, 3$ propagate in an identical manner because, for $\theta < \theta_*$, Equations (5.13) and (5.14) for

both these modes are as

$$\frac{dr_{\perp}}{dl} = \frac{\alpha + \theta_{\perp}}{2}, \quad (5.15)$$

$$\frac{d\theta_{\perp}}{dl} = \frac{3}{4} \frac{\alpha - \theta_{\perp}}{l}. \quad (5.16)$$

In the range of angles $\theta \gg \theta_*$ an ordinary wave $j = 2$ propagates as a transverse wave along a straight line, whereas a wave with a negative energy (the same as curvature-plasma modes) propagate along magnetic field lines. The region of tearing off, in which for these two modes $\theta \simeq \theta_*$ and, therefore, their trajectories begin diverging, is also shown in Figure 13.

The solutions of Equations (5.15) and (5.16) for the angles $\theta < \theta_*$ can also be written in an explicit form. We have (cf. Barnard and Arons, 1986)

$$f(l) = f_0 \left(\frac{l}{r_0} \right)^{-3} \left[1.12 \left(\frac{l}{r_0} \right)^{1.29} - 0.12 \left(\frac{l}{r_0} \right)^{-0.29} \right]^2,$$

$$\theta_{\perp}(l) = 0.82\alpha_0 \left(\frac{l}{r_0} \right)^{0.29} + 0.18\alpha_0 \left(\frac{l}{r_0} \right)^{-1.29},$$

where $f_0 = f(r_0)$, $\alpha_0 = \alpha(r_0)$. Here again r_0 is the distance on which $\theta_{\perp}(l) = \alpha(l)$. If we use now Equation (5.4) for $\alpha(\mathbf{r})$, we obtain that for $l \gg r_0$

$$\theta = \theta_{\perp} - \alpha = -0.3\alpha_0 \left(\frac{l}{r_0} \right)^{0.29}; \quad (5.17)$$

and, therefore, the angle θ between the vectors \mathbf{k} and \mathbf{B} gradually increases as for curvature-plasma waves. Ultimately, combining the relations (2.18) and (5.17) we obtain for the angle $\Theta^{(2)} \equiv \theta_{\perp}^{(2)}(\infty)$ (cf. Barnard and Arons, 1986) the expression

$$\Theta^{(2)} = f_{\text{rad}}^{0.36} \left(\frac{\Omega R}{c} \right)^{0.36} \left[\frac{\omega_{p0}^2}{\omega^2} \langle \gamma^{-3} \rangle \right]^{0.07} \left(\frac{l_{\text{rad}}}{R} \right)^{0.15}, \quad (5.18)$$

where ω_{p0} is the value of plasma frequency on the star surface. It is seen that the quantity $\Theta^{(2)}$ depends not only on the level of generation l_{rad} , f_{rad} but also on the frequency ω . This is connected with the fact that the 'region of tearing off' r_t which is determined by the condition $\theta(r) = \theta_*(r)$ and is equal according to Equations (2.18) and (5.17), to

$$r_t = R f_{\text{rad}}^{-0.53} \left(\frac{\Omega R}{c} \right)^{0.53} \left[\frac{\omega_{p0}^2}{\omega^2} \langle \gamma^{-3} \rangle \right]^{0.26}$$

depending on the frequency of an ordinary wave.

Thus, the character of normal wave propagation in the internal regions of pulsar magnetosphere is essentially different. In particular, while an extraordinary wave, as shown in Figure 13, propagates practically along a straight line, an ordinary wave for the angles $\theta < \theta_*$ declines from the dipole axis and stops declining only at heights $r \approx r_t$. The opening of the directivity pattern determined by a mode $j = 2$ will be therefore much larger than the opening of pattern determined by an extraordinary wave. We use this fact in the sequel to analyze observations. As regards unstable curvature-plasma modes, they propagate strictly along magnetic field lines.

5.3. AMPLIFICATION OF CURVATURE-PLASMA WAVES

One of the key problems of the paper is estimation of a total optical depth passed by unstable waves in their propagation in internal regions of pulsar magnetosphere. Using the asymptotic expressions (3.31) and (3.32) we obtain

$$\tau_{5,6} = 2 \frac{\omega}{c} \int \text{Im } n_{5,6} dl \simeq -890 s_{5,6} J_{5,6} \frac{\nu_{\text{GHz}}^{1/5} R_6^{1/5} \lambda_4^{1/5} B_{12}^{1/5}}{P^{2/5} \gamma_{100}^{3/5}} f^{1/5}, \quad (5.19)$$

where for two unstable normal modes $s_5 = \sin(2\pi/5) \simeq 0.95$;

$$\left. \begin{aligned} s_6 &= \sin\left(\frac{4\pi}{5}\right) = 0.59, \\ J_{5,6} &= \frac{1}{5} \int dx x^{-4/5} q_{5,6}(x), \end{aligned} \right\} \quad (5.20)$$

in which $x = l/R$ and $q_{5,6} = \text{Im } \xi_{5,6} s_{5,6}^{-1} (2a/\pi)^{-1/5}$. It is clear that $q_{5,6}(x) \simeq 1$ if $\xi_{5,6}$ is given by the asymptotic expression (3.28) and $q_{5,6}(x) < 1$ for all other asymptotics.

The integrals $J_{5,6}$ depend, generally speaking, on the level r_0 on which the wave vector \mathbf{k} is parallel to the magnetic field. But, as shown in Figure 14, for small r_0 – i.e., just where the quantity τ attains its highest value – this dependence can be neglected. On the other hand, for $r_0 \gg R$ the integrals $J_{5,6}$ fall rapidly with increasing r_0 . Consequently, the greatest amplification will apply to those waves for which the angle θ_\perp approaches the asymptotics $\frac{3}{4}\alpha$ already at heights comparable with the star's radius.

Figure 15 demonstrates the magnitude of the optical depth τ_5 determined by Equations (5.19) and (5.20) depending on the frequency ν . For the characteristic pulsar parameters ($\gamma_c \sim 100$; $P \sim 1$ s, $B_0 \sim 10^{12}$ G) the optical depth modulo is seen to be several hundred, which corresponds to an amplification by a factor $e^{-\tau} \sim 10^{100}$.

It is quite clear that such an amplification is unrealistic because the wave energy can by no means exceed the outflowing plasma energy. As we have seen, the amplification will actually stop still earlier due to nonlinear effects. The distance at which much nonlinear interaction becomes essential can be evaluated as

$$\Delta r \sim \Lambda R / \tau,$$

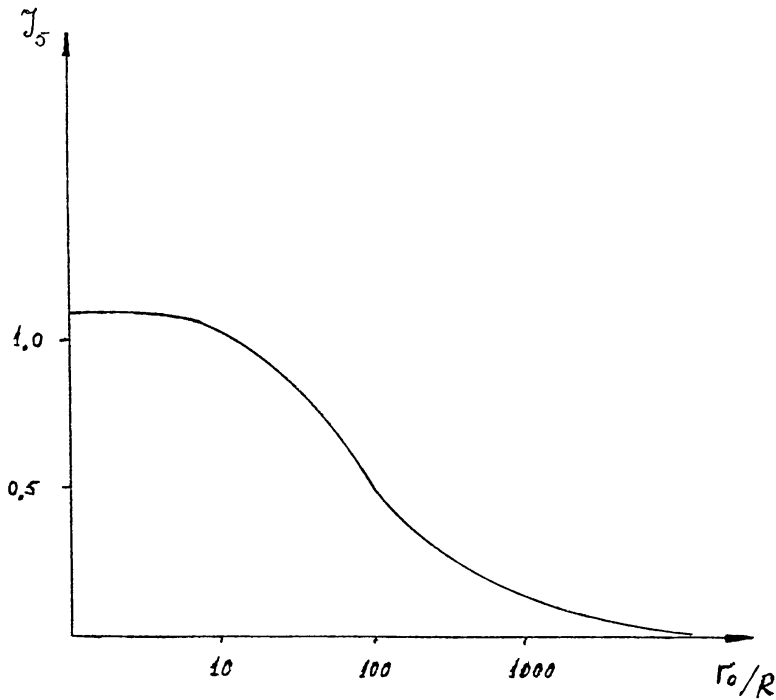


Fig. 14. Dependence of the geometrical factor J_5 on the parameter r_0/R .

where $\Lambda \simeq 10\text{--}30$ is a logarithmic factor. It can be seen that the value Δr does not, in fact, exceed the star radius.

The following fact is, however, important. The point is that in the framework of geometrical optics unstable normal waves cannot leave freely the inner region of a

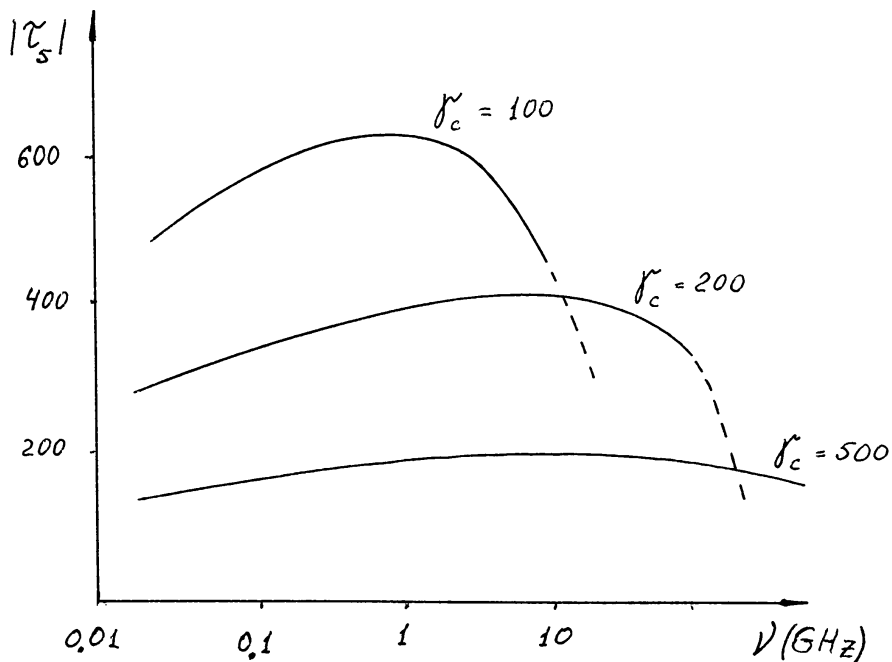


Fig. 15. Module of the optical depth of unstable curvature-plasma wave τ_s subject to the frequency ν .

magnetosphere. To explain this, we recall that unstable modes exist only in the angle interval $|\theta_{\perp} - \alpha| < \theta_{\parallel 5,6}^{\text{out}}$, where $\theta_{\parallel 5,6}^{\text{out}}$ is given by Equation (3.33). Taking into account the equalities (5.4) and (5.6), we obtain

$$\theta_{\parallel 5,6}^{\text{out}} = w_{5,6} \frac{\lambda_4 B_{12} R_6^{1/3}}{v_{\text{GHz}}^{4/3} P^{2/3} \gamma_{100}^3} f^{-1/3} (l/R)^{-8/3},$$

where $w_5 = 1.2 \times 10^3$, $w_6 = 3.2 \times 10^3$. Consequently, the opening of the cone which contains wave vectors of unstable oscillations decreases with increasing distance l from the star surface. Since, as we have seen, the wave vector \mathbf{k} , when propagating along the magnetic field line, declines from the direction of the magnetic field, the unstable normal waves leave the ‘amplification cone’ at a certain distance from the star surface. For instance if the angle between the wave vector \mathbf{k} and the magnetic field \mathbf{B} is close to its asymptotic value $\frac{1}{4}\alpha(\mathbf{r})$, then this happens at a height

$$r_k \simeq 200R \frac{\lambda_4^{1/3} B_{12}^{1/3}}{\gamma_{100} v_{\text{GHz}}^{1/3}} f^{-1/3}.$$

For waves propagating in the ‘amplification cone’ at heights $r > r_k$ (which is possible if $r_0 > r_k$), the transition to the absorption region takes place at still higher altitudes.

Thus, we arrive at the conclusion that already in region I unstable curvature-plasma waves pass over to the attenuation region in which the roots ξ_j of the dispersion equation (3.23) lie in the lower half plane. Such waves cannot propagate freely at altitudes higher than r_k and, therefore, in the framework of geometrical optics they cannot overstep the inner region of a magnetosphere. This fact shows once again that the energy accumulated in unstable curvature-plasma waves can leave pulsar magnetosphere only if there is a sufficiently effective energy repumping from such waves into other modes which are able to propagate freely at large distances from the neutron star. As we have seen, such a conversion actually takes place.

Thus we are led to the following picture of the physical processes leading to generation of intense radio emission of pulsars. The plasma produced in polar regions of a neutron star and flowing along open magnetic field lines turns out to be unstable under excitation of curvature-plasma waves in it. The instability increment appears to be so large that already at a distance of two-three radii from the star surface, where secondary electron-positron plasma is completely formed, the perturbations stop increasing due to nonlinear processes. Nonlinear wave interaction leads not only to saturation of curvature-plasma oscillations but also to an effective energy conversion into other normal waves which are able to leave plasma magnetosphere. As shown below, the above picture makes it possible to explain the basic properties of observed pulsar radio emission.

5.4. THE INTENSITY OF RADIO EMISSION

We shall determine the spectral density $I_{\omega}(\Theta)$ of radioemission into an element of a solid angle $d\Omega = 2\pi\Theta d\Theta$, i.e., in fact, the directivity pattern of pulsar radio emission. For

simplicity we consider here as before only the simplest case of a dipole magnetic field and, besides, assume the directivity pattern to have an axial symmetry.

Let again $U_{\omega}^{(j)}(\theta)$ be the spectral density of established oscillations integrated over 'transverse' angles θ_{\perp} , where the index $j = 1, 2$ corresponds to two orthogonal modes capable of leaving the pulsar magnetosphere. For an extraordinary mode the quantity $U_{\omega}^{(1)}(\theta)$ within the range of angles $\theta < a^{-3/20} \theta_* \equiv \theta_{\perp}$ coincides with the expression (4.12) for unstable curvature-plasma oscillations. For an ordinary mode there holds the relation

$$U_{\omega}^{(2)}(\theta) = \theta_* U_{\omega}^{(2)}(\Omega),$$

where θ_* (Equation (2.18)) corresponds to the characteristic scale of angles θ between \mathbf{k} and \mathbf{B} in which, as has already been said, the nonlinear energy conversion into the mode $j = 2$ is the most effective.

In a curved magnetic field, as we have seen, the wave vector \mathbf{k} of normal waves $j = 1, 2$ will decline from the magnetic field line. As is seen from the relations (5.9) and (5.10), in the region of small angles θ one can put for both modes

$$\frac{d\theta}{dt} \simeq \frac{c}{\rho}. \quad (5.21)$$

The velocity of escape of electromagnetic oscillations (5.21) from the interaction region determines, in fact, the effectiveness of curvature-plasma wave energy transformation into two orthogonal modes that leave pulsar magnetosphere.

We will now use the fact that the transformation is most effective in the region of small angles θ . We may assume in this case that from each volume element dV radiation proceeds only into the angle $\theta = 0$ to which, as shown above, there corresponds quite a definite angle Θ between the dipole axis and the direction of propagation of the wave going out of the magnetosphere limits. The angle Θ , as is seen from the relations (5.10) and (5.18), depends on the coordinate of the radiation point.

As a result, writing the expression for the volume element in the form

$$dV = \pi \frac{\Omega l}{c} l^2 df dl,$$

we obtain for the spectral energy density radiated from the volume element dV within the time dt into the angle element $d\Theta$

$$dI_{\omega}^{(j)}(\Theta) d\Theta dt = U_{\omega}^{(j)}(\theta) \frac{\Omega l}{c} l^2 d\theta df dl. \quad (5.22)$$

When deriving (5.22) we have used the fact that $dU_{\omega}^{(j)} = U_{\omega}^{(j)}(\theta) d\theta$. Integrating now Equation (5.22) over all volume elements from which the emission comes into a given angle Θ and also using the equality (5.21), we have

$$dI_{\omega}^{(j)}(\Theta) = c \int df \frac{\Omega l^3(f)}{c} U_{\omega}^{(j)}(\theta) \frac{1}{\rho} \frac{dl}{d\theta}. \quad (5.23)$$

Next, we again introduce the quantity $\eta^{(j)} = U^{(j)}/U_{\text{part}}$, where $U_{\text{part}} = n_e m_e c^2 \langle \gamma \rangle = U_0 G(f) (l/R)^{-3}$ is the energy density of outflowing particles. The relation (5.23) can be rewritten in the form

$$dI_{\omega}^{(j)}(\Theta) = \pi c \frac{\Omega R}{c} R^2 U_0 \int df \eta^{(j)} \frac{1}{\rho} \frac{dl}{d\Theta} \frac{U_{\omega}^{(j)}(\theta)}{U^{(j)}} G(f).$$

On the other hand, the quantity $\pi c(\Omega R/c)R^2 U_0$ is merely a flux of energy W_{part} (see Section 2.1) transferred by particles within the limits of the light cylinder (Beskin *et al.*, 1983). Finally we have

$$dI_{\omega}^{(j)}(\Theta) = W_{\text{part}} \int df \eta^{(j)} \frac{dl}{\rho d\Theta} \frac{U_{\omega}^{(j)}(\theta)}{U^{(j)}} G(f), \quad (5.24)$$

where the derivatives $dl/d\Theta$ should be determined with the help of the relations (5.10) and (5.18). Equation (5.24) just determines the directivity pattern of pulsar radio emission.

Now we will show how one can obtain the expression for the basic characteristics of observed radio emission using Equation (5.24). Consider, for example, the energy spectrum of pulsars. Recall that in the analysis of the experimental spectra the so-called energy in pulse is used

$$\tilde{E}_{\omega} = \int_0^P I_{\omega} dt, \quad (5.25)$$

i.e., the total energy taken for one pulsar period P at a given frequency ω (Manchester and Taylor, 1977). It is clear that the quantity (5.25) must correspond to the value

$$\tilde{E}_{\omega}^{(j)} = \int d\Theta I_{\omega}^{(j)}(\Theta).$$

Using now the definition (5.24), we obtain

$$\tilde{E}_{\omega}^{(j)} = W_{\text{part}} \int_R^{l_{\max}(\omega)} dl \int_0^{f_*} df \eta^{(j)}(f, l) \rho^{-1} \frac{U_{\omega}^{(j)}(\theta)}{U^{(j)}} G(f), \quad (5.26)$$

where $l_{\max}(\omega)$ corresponds to the maximum frequency $\omega_{\max}(l)$ (Equations (4.10) and (5.7)). Similarly, for the coefficient of plasma energy conservation into radio emission energy $\alpha_T = E_{\text{rad}}/W_{\text{part}}$, where

$$E_{\text{rad}}^{(j)} = \int d\omega \int d\Theta \Theta I_{\omega}^{(j)}(\Theta).$$

we have

$$\alpha_T^{(j)} = \int d\omega \int_R^{l_{\max}} dl \int_0^{f_*} df \eta^{(j)} \rho^{-1} \frac{U_{\omega}^{(j)}(\theta)}{U^{(j)}} G(f) \Theta^{(j)}(f, l), \quad (5.27)$$

where the quantity $\Theta^{(j)}(f, l)$ is determined by Equations (5.10) or (5.18).

Proceed now to calculating the integrals (5.26) and (5.27). For an extraordinary mode, as we have seen, $\eta^{(1)} = \lambda^{-1}$, and

$$\frac{U_{\omega}^{(1)}(\theta)}{U^{(1)}} = \frac{\omega}{\omega_{\max}^2} \frac{1}{\theta_{\parallel}}.$$

Integration over df for both normal modes $j = 1, 2$ is simple because for sufficiently smooth profiles of the densities $G(f)$ the integrals are determined by the upper limit f_* , so that $\int df \dots \simeq 1$. The main contribution into integration over dl will lie near the upper limit $l_{\max}(\omega)$. As a result, we have

$$\tilde{E}_{\omega}^{(1)} \simeq \lambda^{-1} W_{\text{part}} \gamma_c^4 \Omega \omega^{-2};$$

and owing to (5.10) the characteristic opening of the directivity pattern is equal to

$$\Theta_{\max}^{(1)} \simeq \frac{3}{2} f_*^{1/2} \left(\frac{\Omega R}{c} \right)^{1/2} \left(\frac{\omega_{\max}^{(0)}}{\omega} \right)^{1/2}. \quad (5.28)$$

The index '0' implies everywhere that the value is taken on the star surface.

Finally, the transformation coefficient $\alpha_T^{(1)}$ is written in the form

$$\alpha_T^{(1)} \simeq \lambda^{-1} \left(\frac{\Omega R}{c} \right)^{1/2} \Omega \gamma_c^4 \frac{\omega_{\max}^{1/2}}{\omega_{\min}^{3/2}}. \quad (5.29)$$

The numerical estimates of all quantities are given in Section 6.

As concerns the ordinary mode $j = 2$, two cases are possible here. This is connected with the fact that the quantity $\eta^{(2)}$ entering in the expressions (5.26) and (5.27) contains an uncertainty due, in particular, to the dependence of the Lorentz-factor of particles γ_c on the coordinate l . For this reason the integrals over dl in (5.26) and (5.27) can, generally speaking, be determined either by the upper or by the lower integration limit. If the integrals are determined by the lower limit $l \simeq R$ (this case will be called 'internal'), then for frequencies $\omega < \omega_{br}$ we obtain

$$\tilde{E}_{\omega_{\text{in}}}^{(2)} \simeq W_{\text{part}} \frac{R c^{0.6}}{\rho_{\min}^{1.6}} \gamma_c^3 \omega_{p0}^{-2.6} \omega.$$

For frequencies $\omega > \omega_{br}$, as is seen from Equations (4.19) and (4.21), the expression for $\tilde{E}_{\omega_{\text{in}}}^{(2)}$ involves an additional factor $(\omega/\omega_{br})^{-5/3}$. Therefore, near the frequency ω_{br} in the spectrum of the normal mode $j = 2$, a break $\Delta \bar{\alpha}$ must exist whose value is equal to

$$\Delta \bar{\alpha} = 5/3. \quad (5.30)$$

The characteristic dimension of the directivity pattern is equal to

$$\Theta_{\text{in}}^{(2)} \simeq f^{0.36} \left(\frac{\Omega R}{c} \right)^{0.36} \left[\frac{\omega_{p0}^2}{\omega^2} \langle \gamma^{-3} \rangle \right]^{0.07} \left(\frac{l_{\text{rad}}}{R} \right)^{0.15}, \quad (5.31)$$

and the transformation coefficient

$$\alpha_{T_{in}}^{(2)} \simeq \gamma_c^{10} \frac{c^{2.5}}{R^{2.5}} \left(\frac{\Omega R}{c} \right)^{2.1} \omega_{p_0}^{-2.5}. \quad (5.32)$$

If the integrals (5.26) and (5.27) are determined by the upper limit $l_{\max}(\omega)$, then in the region $\omega < \omega_{br}$ we have

$$\tilde{E}_{\omega_{out}}^{(2)} \simeq W_{\text{part}} \gamma_c^{10} \frac{R c^{2.5}}{\rho_{\min}^{3.5}} \omega_{p_0}^{-1} \omega^{-2.5}.$$

It can be easily verified that in this ‘external’ case the spectrum break $\Delta \bar{\alpha}$ is equal to

$$\Delta \bar{\alpha} = \frac{5}{6}. \quad (5.33)$$

The distinction in the values (5.30) and (5.33) is simply due to the fact that the additional factor $(\omega/\omega_{br})^{-5/3} \propto \omega^{-5/3} \rho^{5/3}$, according to Equation (5.3), depends on the coordinate l and the upper limit l_{\max} on the frequency ω . According to (5.18) and (4.10), the directivity pattern is defined as

$$\Theta_{out}^{(2)} \simeq f^{0.36} \left(\frac{\Omega R}{c} \right)^{0.36} \left[\frac{\omega_{p_0}^2}{\omega^2} \langle \gamma^{-3} \rangle \right]^{0.07} \left(\frac{\omega}{\omega_{\max}^{(0)}} \right)^{-0.15}; \quad (5.34)$$

and the transformation coefficient is given by

$$\alpha_{T_{out}}^{(2)} \simeq \gamma_c^{10} \frac{c^{2.5}}{R^{2.5}} \left(\frac{\Omega R}{c} \right)^{2.1} \omega_{p_0}^{-0.85} \omega_{\max}^{(0)0.15} \omega_{\min}^{-1.8}. \quad (5.35)$$

6. Comparison of the Theory with Observational Data

We compare the predictions of our theory with observational data. As has already been said, no consistent theory of pulsar radio emission has not yet been formulated (Manchester and Taylor, 1977; Taylor and Stinebring, 1986). When interpreting observations one usually involved model assumptions which permitted interpretation of individual properties of observed radio emission on the basis of various hypotheses. For example, in the hollow cone model (Ruderman and Sutherland, 1975) the radio emission was assumed to be generated in magnetosphere near the boundary between closed and open field lines. This made it possible to explain the existence of ‘one-hump’ and ‘two-hump’ structures actually observed in integrated profiles of the majority of pulsars (Backer, 1976; Oster and Sieber, 1976). In the model of antenna mechanism of radio emission (Radhakrishnan and Cocke, 1969) connected with curvature radiation of hypothetic bunches of charged particles, the polarization characteristics of radio emission were rather well explained, although the origin of those clusters was not established.

In this paper we develop the theory of radio emission based on no special model assumptions. The starting point is only the reliably-established concept of relativistic

electron-positron plasma flux flowing along open field lines in pulsar magnetosphere. This flux, as shown above (Sections 3 and 5) is unstable – curvature-plasma modes are intensely generated in it. The study of nonlinear processes (Sections 4 and 5) has shown that there proceeds a nonlinear saturation and transformation of such modes into transverse electromagnetic waves capable of leaving the magnetosphere of a neutron star. These outgoing waves are, in fact, pulsar radio emission. Here we are considering the properties of this radio emission and compare the latter with observational data.

6.1. TWO ORTHOGONAL MODES

As has already been shown, the energy of unstable curvature-plasma waves is transformed into two linearly polarized transverse waves that leave the magnetosphere of a pulsar. Their polarization is determined by the magnetic field structure in the region of generation and propagation of such waves. In particular, the electric vector of an extraordinary wave must be orthogonal and that of an ordinary wave parallel to the magnetic field projection onto the plane of the picture.

Since, as is seen in Figure 16, star rotation leads to variation of magnetic field orientation with respect to the line-of-sight, in each of the two orthogonal modes the

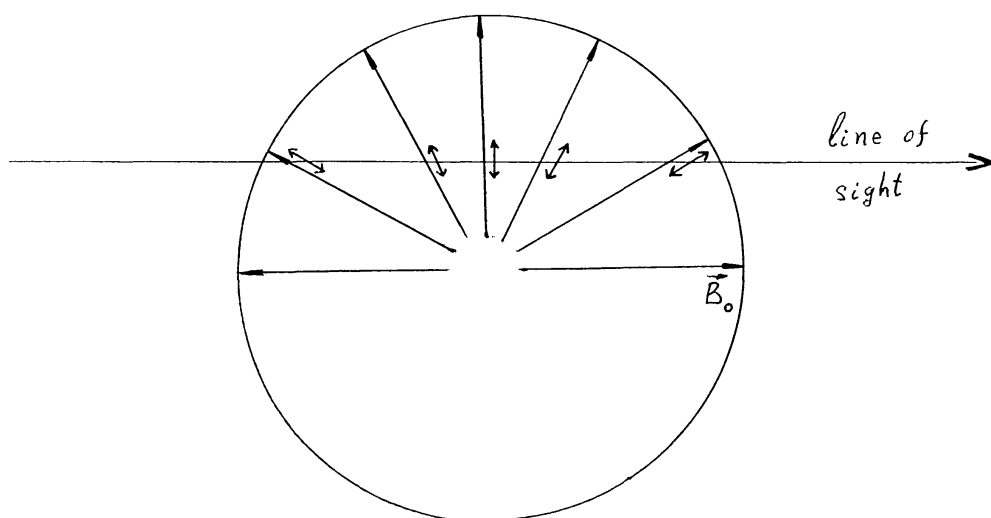


Fig. 16. The character of the position angle variation.

observed polarization angle φ (i.e., the angle between the direction of the electric field of the wave and a given direction lying in the plane of the picture) must vary along the mean profile of the pulsar. Introducing as usual the longitude $\phi = 2\pi t/P$ which characterizes the position of the signal in the mean profile, we obtain

$$\operatorname{tg}(\varphi^{(j)} - \varphi_0^{(j)}) = \frac{\sin \chi \sin \phi}{\sin \xi \cos \chi - \cos \xi \sin \chi \cos \phi}, \quad (6.1)$$

$$\varphi_0^{(1)} - \varphi_0^{(2)} = \pi/2,$$

where ξ and χ are angles between the rotation axis and, respectively, the line-of-sight and the magnetic dipole axis. Equation (6.1) gives the well-known variation of the

position angle discussed usually within the hollow cone model (Radhakrishnan and Cocke, 1969; Ruderman and Sutherland, 1975; Manchester and Taylor, 1977; Hankins and Cordes, 1981; Malov, 1983; Narayan and Vivekanand, 1983).

Thus, the theory predicts the existence of two radiation modes which have an orthogonal linear polarization and vary their position angle along the mean profile according to Equation (6.1). As is well known, such orthogonal modes are actually observed (Manchester and Taylor, 1977; Stinebring *et al.*, 1984a, b; Taylor and Stinebring, 1986). Figure 17 shows the values of the position angle for pulsar 0950 + 08

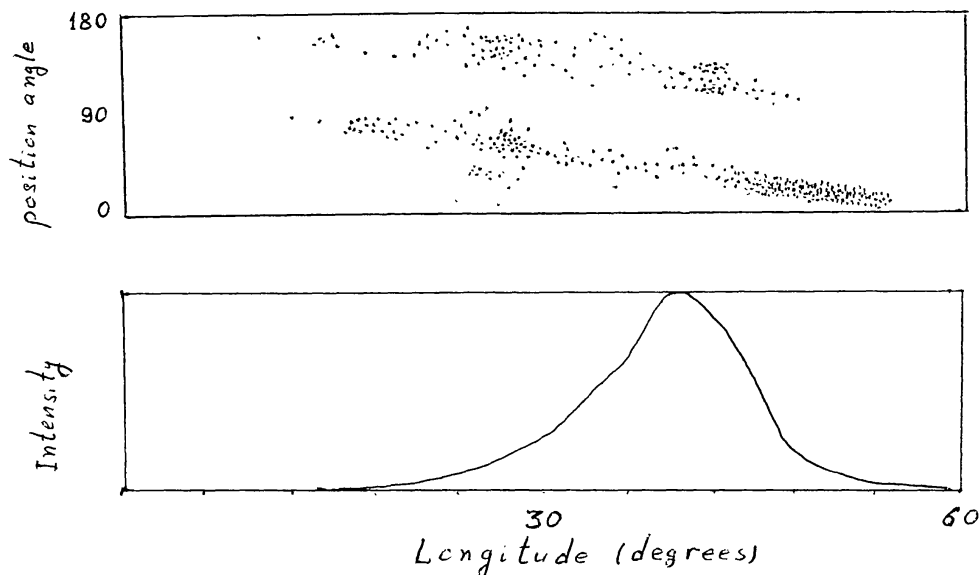


Fig. 17. Two orthogonal modes singled out in radio emission of pulsar 0950 + 08 (Stinebring *et al.*, 1984a, b). The density of points is proportional to the fraction of all pulses that had a given value of the position angle.

(Stinebring *et al.*, 1984a, b). We see that the measurements of the position angle are indeed concentrated near two trajectories that differ from each other by 90° . The variation of the position angle along the profile just corresponds to the relation (6.1). Note that for some pulsars, such as PSR 0525 + 21, 0833 - 45, 2021 + 51, 2045 - 16, Equation (6.1) and the real variation of the position angle correspond to one another so well (Manchester and Taylor, 1977) that the relation (6.1) is used for a direct determination of some geometrical characteristics of neutron stars, for example, for evaluation of the angle χ (Hankins and Cordes, 1981; Malov, 1983). In particular, polarization measurements have shown that for pulsar 0950 + 08 the angle $\chi \approx 2^\circ - 4^\circ$ (Malov, 1986).

The theory also predicts the possibility for circular polarization (see Section 2) observed in some cases with two orthogonal modes (Stinebring *et al.*, 1984a, b). Indeed, according to Barnard (1986), the region where the change of polarization ceased (for pulsars with $P \gtrsim 0.06$ s) lies in the region of cyclotron resonance R_c . In other words, the characteristics of circular polarization of radio emission are determined just by polarization of the normal waves in the region $r \sim R_c$. And as shown in Section 2 (see

Equation (2.26)), polarization of normal waves in the region of cyclotron resonance is already nonlinear. The degree of circular polarization may reach 10–30%, which agrees well with observations. The question of limiting circular polarization (the same as the frequency dependence of the degree of circular polarization) requires a special investigation and is not considered here. Note finally that in some cases observational data testify in favour of the fact that a noticeable interaction of two orthogonal modes takes place in pulsar magnetosphere. Such are, for instance, sharp jumps of position angle in individual pulses which are not, however, accompanied by intensity jumps (Stinebring *et al.*, 1984a, b). Such an interaction may lead to ‘mixing’ two orthogonal modes, as a result of which a continuous run of the position angle determined by the relation (6.1) may be violated. Such irregular run of the position angle is observed, for instance, in pulsars 0329 – 54, 2002 + 31 (Rankin, 1983a). The origin of this interaction also requires a special study.

6.2. THE WIDTH OF THE RADIO WINDOW

The relations (5.28), (5.31), and (5.34) obtained from the theory represent, in fact, the width W of the opening of the directivity pattern of radio emission because $W = 2\Theta$. For the characteristic parameters of radio pulsars they are equal to

$$W^{(1)} = 3.6^\circ P^{-1/2} \nu_{\text{GHz}}^{-1/2}, \quad (6.2)$$

$$W_{\text{in}}^{(2)} = 7.8^\circ f^{0.36} P^{-0.43} \nu_{\text{GHz}}^{-0.14} \lambda_4^{0.07} B_{12}^{0.07} \gamma_{100}^{-0.11} \left(\frac{l}{R}\right)_{3R}^{0.15}, \quad (6.3)$$

$$W_{\text{out}}^{(2)} = 10^\circ f^{0.40} P^{-0.5} \nu_{\text{GHz}}^{-0.29} \lambda_4^{0.1} B_{12}^{0.1} \gamma_{100}^{-0.05}. \quad (6.4)$$

We can see that in most cases the width of the window W must be determined by an ordinary wave $j = 2$. Only in the cases where an ordinary mode is suppressed for some reason, the width of the directivity pattern will be determined by an extraordinary wave $j = 1$.

Consider now in more detail some quantitative relations which follow from our theory. First of all, the quantities W coincide rather well with the characteristic width of the mean profiles of pulsars (Rankin, 1983a). Furthermore, the relations (6.3) and (6.4) make it possible to explain also the observed dependence of the window width W on the frequency ν and on the pulsar period P . Indeed, according to (6.2)–(6.4) for each pulsar the quantity must depend on the frequency ν in a power-law manner: $W \propto \nu^{-\bar{\beta}}$, where

$$\bar{\beta}_{\text{in}}^{(2)} = 0.14, \quad (6.5)$$

$$\bar{\beta}_{\text{out}}^{(2)} = 0.29. \quad (6.6)$$

These values are in a good agreement with observations. Figure 18 demonstrates the distribution of pulsars with respect to the quantity $\bar{\beta}$ borrowed from Rankin (1983b). We can see that pulsars are concentrated near the values of $\bar{\beta}$ determined by Equations (6.5) and (6.6). Besides, according to Kuzmin *et al.* (1986), averaged values of $\bar{\beta}$ are also close to (6.5) and (6.6) (see Table I).

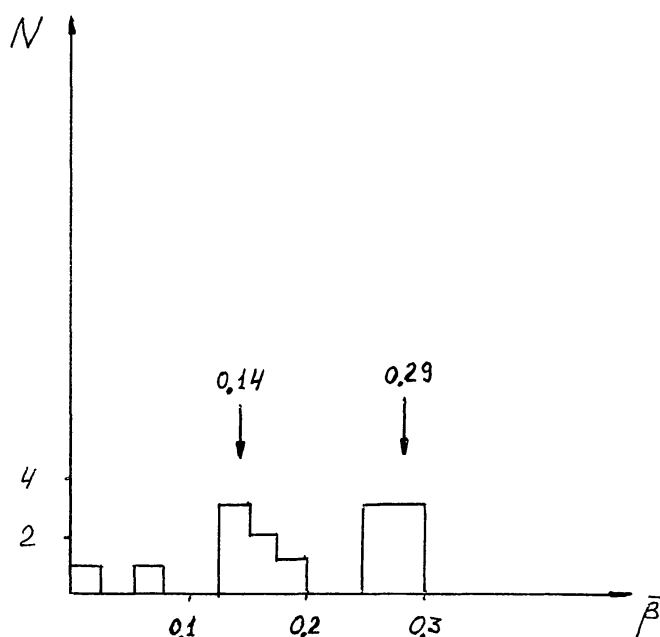


Fig. 18. Distribution of pulsars in the quantity $\bar{\beta}$ (Rankin, 1983b). The arrows indicate the expected values (6.5) and (6.6).

The dependence of the window width W on the period P will be determined not only by the exponential factors $P^{-0.43}$ and $P^{-0.50}$, but also by the dependence on this period of the field line parameter f_g which specifies the opening of the directivity pattern. As shown by Beskin *et al.* (1984), the quantity f_g is in one-to-one correspondence with the parameter Q determined, according to Equation (2.1) directly by observations.

Indeed, as has already been said, in pulsars with $Q < 1$ the generation of secondary plasma proceeds practically on the entire surface of a polar cap. Near the internal boundary of the hollow cone which is determined from the condition (cf. Equation (2.4))

$$f_{\text{in}} = Q^{14/9}, \quad (6.7)$$

there flows an intense jet of surface current (see Fig. 1a). On the other hand, the intensity of radio emission $I \simeq \eta W_{\text{part}}$ increases, naturally, with increasing density of particles. That is why for pulsars with $Q < 1$ we have $f_g \simeq f_{\text{in}}$. For pulsars with $Q > 1$ particles are generated, as shown in Figure 1(b), only within a ring with $f_g \simeq 1$.

In the end, for pulsars with $Q > 1$ one should expect the dependence (6.2)–(6.4) $W \propto P^k$, where $\bar{k}_{\text{in}} = -0.43$ or $\bar{k}_{\text{out}} = 0.50$ and for pulsars with $Q < 1$, due to the change

TABLE I
Frequency dependence of W (Kuzmin *et al.*, 1986)

Frequency interval (GHz)	0.1–0.4	0.4–1.7	1.7–4.6	4.6–10.7
Average of $\bar{\beta}$	0.25 ± 0.04	0.13 ± 0.05	0.16 ± 0.05	0.02 ± 0.08

of $f_{\text{in}}(Q)$ (2.1) and (6.7) it turns out that the value $\bar{k} = -0.07$. The analysis of observations has shown that in pulsars with $Q > 1$, the quantity \bar{k} determined using the method of least squares becomes

$$\bar{k}_{Q > 1} = -0.48 \pm 0.07 \quad (6.8)$$

and in pulsars with $Q < 1$, on the contrary,

$$\bar{k}_{Q < 1} = -0.12 \pm 0.14 \quad (6.9)$$

(see also Malov and Suleimanova, 1982). Thus the theoretical dependence of the radio window width on the period is also in a rather good agreement with the experimental value.

6.3. THE STRUCTURE OF THE MEAN PROFILE

The structure of the mean profile is one of the most important characteristics of pulsar radio emission. According to the theory developed above, the mean profile must contain two components corresponding to two orthogonal modes of radiation. As has already been mentioned, for each of the modes the shape of the directivity pattern must follow the complicated density profile $G(f)$ depicted in Figure 1. This must lead to a good variety of shapes of the mean profiles of radio pulsars.

Discuss the main features of the structure of mean profiles which follow from our theory (see Figure 19). First of all, as we have seen, in pulsars with $Q < 1$ the largest current runs near the internal boundary of the plasma outflow cone. In the integral profile of radiation in such pulsars there must exist, therefore, an intense single central component. As shown in Figure 19(a), it can be connected both with radiation in an ordinary mode of plasma flowing near the internal boundary of the hollow cone and merely with an extraordinary mode $j = 1$. Only in those pulsars with $Q < 1$ in which, as is seen from Figure 19(a), the line-of-sight intersects the inner radius of the directivity pattern, the central profile must be double.

It is clear that for a given inner radius r_{in} of a radiation cone the ratio of the number of pulsars with single and double mean profiles must be equal to

$$\frac{N_1}{N_2} \simeq \frac{R_0 - r_{\text{in}}}{r_{\text{in}}} = \frac{R_0}{r_{\text{in}}} - 1 \quad (6.10)$$

and, according to Equation (2.4), can be directly expressed in terms of the observed quantity Q . As is seen from Figure 20, we deal with a good agreement between theory and experiment.

As concerns pulsars with $Q > 1$, their plasma outflow diagram, as demonstrated in Figure 19(b), has a shape of a sufficiently thin ring. Therefore, depending on mutual orientation of the directivity pattern and the line-of-sight, both single and double mean profiles are possible here. On the other hand, in such pulsars the amplification of current near the internal boundary of plasma outflow is not large (see Section 2). Therefore, in pulsars with $Q > 1$ the central component can be connected only with an extraordinary

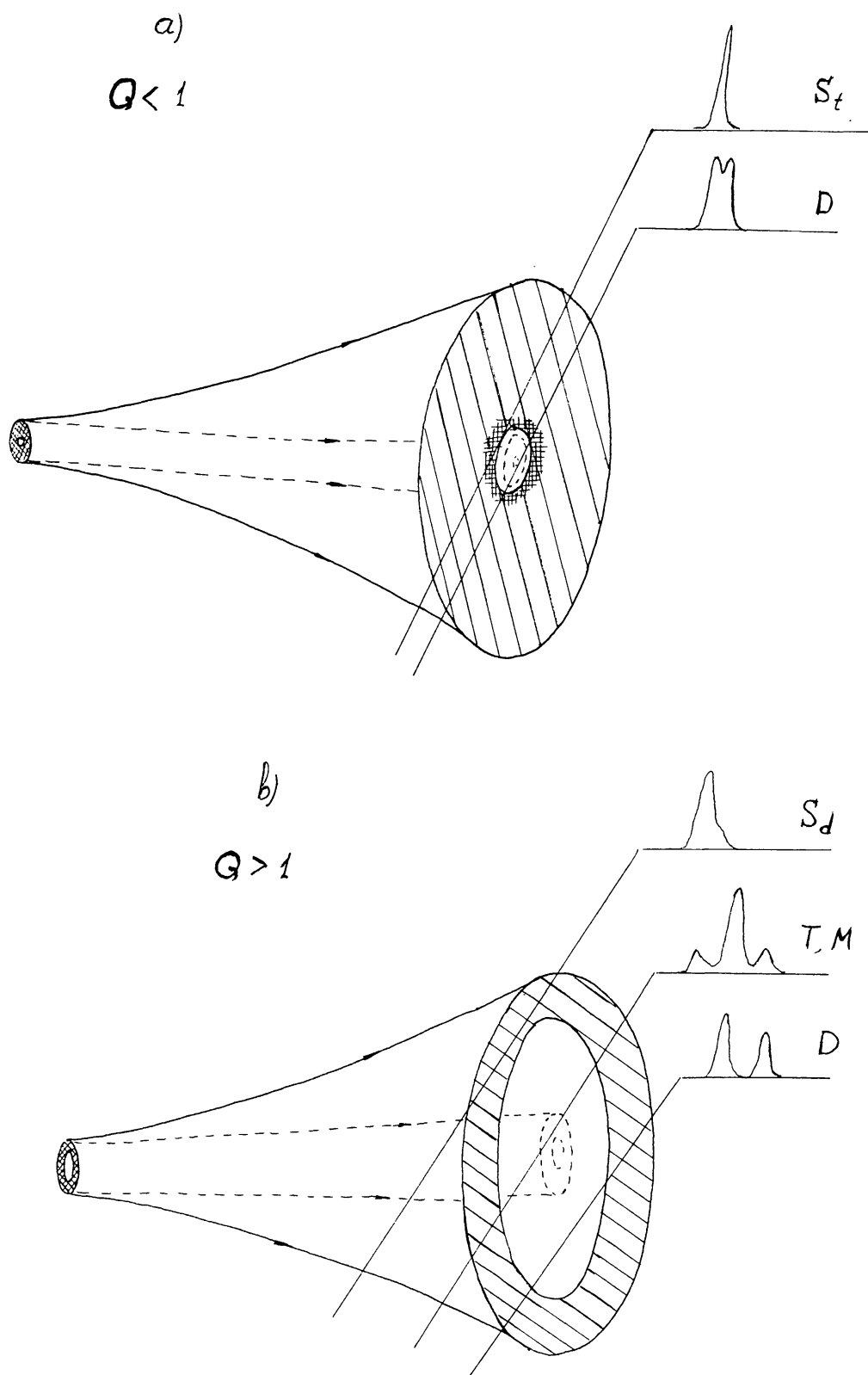


Fig. 19. Various cross-sections of the directivity pattern of radio emission of pulsars with (a) $Q < 1$ and (b) $Q > 1$. The dashed line corresponds to an extraordinary and the solid line to an ordinary modes. Mean profiles appearing for different cross-sections of the directivity pattern are shown. Letters correspond to Rankin's classification.

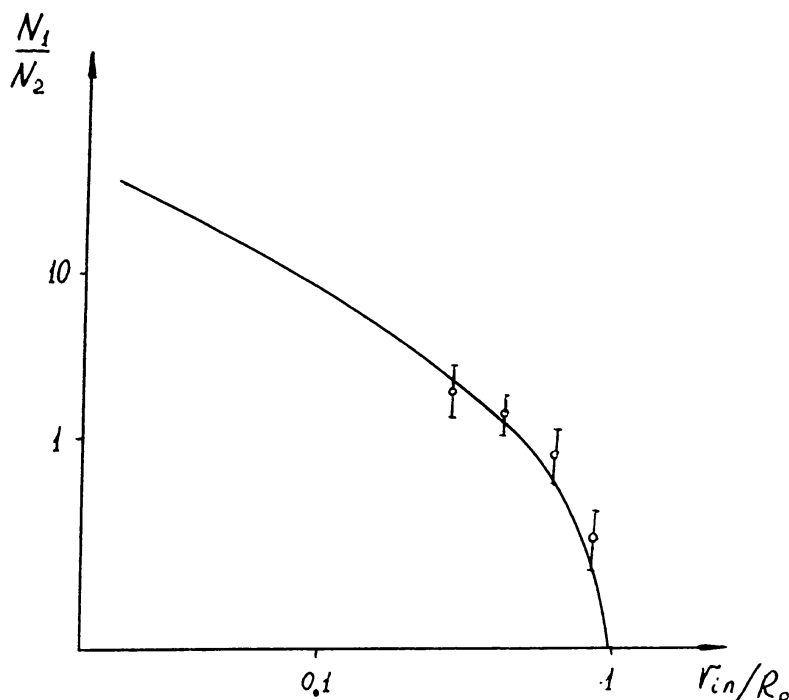


Fig. 20. The relative number of pulsars with single and double mean profiles N_1/N_2 subject to the parameter r_{in}/R_0 . The curve corresponds to the expected dependence (6.10).

mode whose directivity pattern (6.2) has the opening much smaller than the observed radio window width (6.3) and (6.4). The various versions of mean profiles occurring in this case are also shown in Figure 19(b).

The above picture (many elements of which are in agreement with the hollow cone model Ruderman and Sutherland, 1975; Oster and Sieber, 1976; Backer, 1976; Beskin *et al.*, 1984) completely correspond to the most detailed phenomenological classification of mean profiles recently proposed by Rankin (1983a, b, 1986). One can explain, in particular, the existence of two components, Core and Conal, that are now reliably distinguished in pulsar radio emission (Rankin, 1983a; Gil, 1985).

Recall that according to the classification of mean profiles proposed by Rankin, all pulsars can be divided into five classes. Their basic properties are given below.

M – pulsars with complex profiles (multicomponent profiles). One can usually single out one of the components whose properties are essentially distinct from the characteristics of the others (Rankin, 1983a).

T – triple profiles in which the properties of the central pulse are distinct from the properties of lateral components. In particular, sharp jumps of the position angle as well as circular polarization is mostly observed only in the central component (Rankin, 1983a, Weisberg *et al.*, 1986).

D – pulsars with a double profile. In some cases, in bridge region there appear features typical of the central component of the profile *T* (Weisberg *et al.*, 1986, Gil, 1987).

S_c – single profiles whose properties are close to those of the central component of the profile *T*. In particular, at high frequencies two satellites appear on both sides of the

main pulse, so that the profile becomes, in fact, triple (Rankin, 1983a; Hankins and Rickett, 1986).

S_d – single profiles whose properties are close to pulsars of class D . For instance, the drift of subpulses observed also in pulsars of class D was noted only in profiles of class S_d , and not of class S_t (Rankin, 1986).

The central component in pulsars of class T and the main pulse in pulsars of class S_t are interpreted as core components of the directivity pattern, while the lateral pulses of profiles of class T as well as radiation of pulsars S_d and D are interpreted as its conal component.

This classification based, as has already been mentioned, only on the analysis of observations fully agrees with our theory of radio emission. Indeed, as mentioned above, pulsars with $Q < 1$ must have a sharp central peak of radiation and, therefore, it is natural to attribute them to pulsars of class S_t . As is seen from Table II, all S_t pulsars actually have a parameter $Q < 1$.

TABLE II
Comparison of the Rankin's (1983a, 1986) classification with the values of parameter Q (Beskin *et al.*, 1984)

Rankin's classification	M	T	D	S_t	S_d
All	4	16	18	17	14
$Q < 1$	0	5	2	17	1
$Q > 1$	4	11	16	0	13

On the other hand, the directivity pattern of pulsars with $Q > 1$ does not have a noticeable core component. Therefore, pulsars with $Q > 1$ must have a mean profile determined by the conal component, i.e., belong to classes S_d or D . As is seen from Table II, precisely this picture is observed in reality.

Finally, pulsars of class T are intermediate in the sense that the intensity of their core and conal components turns out to be of the same order of magnitude. As might be expected, they have $Q \sim 1$. Besides, in some cases one can single out also a core component connected with an extraordinary mode. Such a component is observed, in particular, in pulsars 1541 + 09, 1737 + 13, 1821 + 05, 1944 + 17, 1952 + 29 (Hankins and Rickett, 1986) (all of them have a parameter $Q > 1$ and belong to classes T and M).

Furthermore, according to Gil (1987), in pulsar 0834 + 06 (class D) one of the orthogonal modes is observed just in the central bridge and the other in the region of the main two-hump profile.

6.4. THE SPECTRUM OF RADIO EMISSION

As shown in Section 5, our theory predicts a power-law spectrum of pulsar radio emission, so we have $\tilde{E}_\omega \propto \omega^{\tilde{\alpha}}$. In the region near the frequency ν_{br} (4.20),

$$\nu_{br} = 3P^{-1/2} \gamma_{100}^3 \left(\frac{\gamma_{300}^+}{\gamma_{100}^-} \right)^{12/5} \text{ GHz} ; \tag{6.11}$$

and in the spectrum of an ordinary wave a break must be observed. The magnitude of this break, as we have seen, is determined by the physical region that makes the main contribution to pulsar radio emission. If radio emission is generated mainly at small distances from the star (internal case), then $\Delta\bar{\alpha} = \frac{5}{3}$ (5.30). It is generated at distances $r \sim l_{\max}(\omega)$ (external case), then $\Delta\bar{\alpha} = \frac{5}{6}$ (5.33).

As to the absolute values $\bar{\alpha}$, according to the results of Section 5, we have:

$$\tilde{E}_{\omega}^{(1)} \propto \omega^{-2}; \quad (6.12)$$

$$\tilde{E}_{\omega_{\text{in}}}^{(2)} \propto \begin{cases} \omega^{0.9}, & \omega < \omega_{br}; \\ \omega^{-0.7}, & \omega > \omega_{br}; \end{cases} \quad (6.13)$$

$$\tilde{E}_{\omega_{\text{out}}}^{(2)} \propto \begin{cases} \omega^{-2.5}, & \omega < \omega_{br}; \\ \omega^{-3.3}, & \omega > \omega_{br}. \end{cases} \quad (6.14)$$

We will show that the theory corresponds to the observations. First of all, the spectrum of pulsar radio emission has indeed a power-law form (Manchester and Taylor, 1977; Izvekova *et al.*, 1981; Slee *et al.*, 1986), in some cases the spectrum exhibits a brak (Manchester and Taylor, 1977; Kuzmin *et al.*, 1986). As shown in Figure 21, the ratio $v_{br}^{\text{obs}}/v_{br}^{\text{th}}$, where v_{br}^{th} is given by Equation (6.11), is close to unity. The

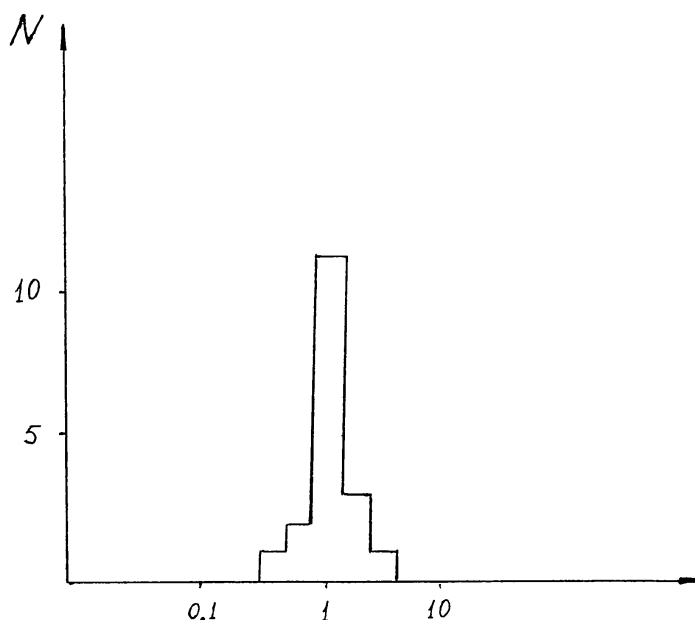


Fig. 21. Distribution of pulsars in the quantity $v_{br}^{\text{obs}}/v_{br}^{\text{th}}$.

difference $\Delta\bar{\alpha}$ as is seen from Figure 22, is also concentrated near the values determined by Equations (5.30) and (5.33).

The absence of a break in the spectrum of some pulsars may be first of all due to an extraordinary mode which must not have a break in the spectrum. On the other hand, as is seen from Equation (6.11), in pulsars with small periods the break frequency may turn out to be sufficiently large and, hence, inaccessible for measurements. It is, there-

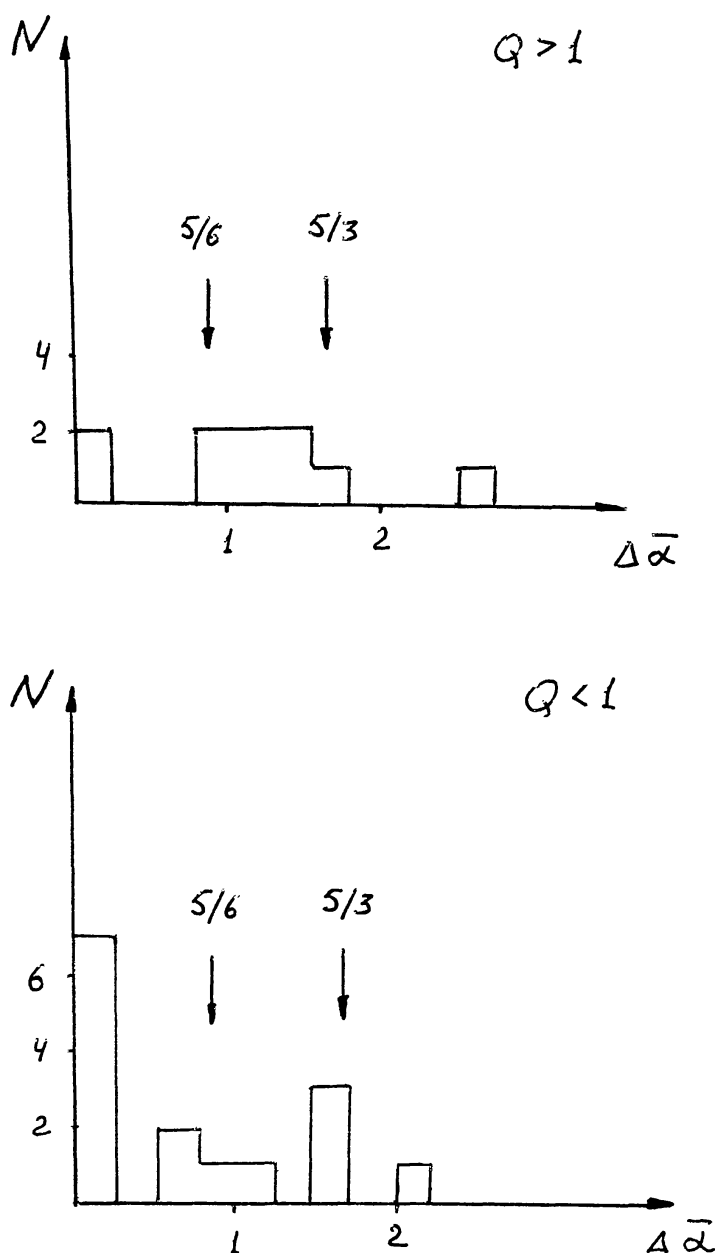


Fig. 22. Distribution of pulsars in the magnitude of the break in the spectrum $\Delta \bar{\alpha}$. Arrows indicate the expected values (5.30) and (5.33).

fore, not surprising that a break is absent for the most part just in pulsars with $Q < 1$, which have small periods P by definition (2.1).

Finally, the absolute values of the spectral index $\bar{\alpha}$ are on the whole in a reasonable agreement with observations. For example, spectral index of the extraordinary wave $\bar{\alpha} = -2$ (6.12) practically coincides with the mean value $\bar{\alpha} = -2.0 \pm 0.1$ obtained by Malov and Malofeev (1981) for 43 pulsars in the high-frequency part of the spectrum. Next, the analysis carried out by Kuzmin *et al.* (1986) for 21 pulsars in whose spectra a break was observed showed that $\bar{\alpha} = -1.7 \pm 0.4$ at frequencies $\omega < \omega_{br}$ and $\bar{\alpha} = -3.1 \pm 1.1$ at frequencies $\omega > \omega_{br}$. Besides, as shown in Figure 23, in 12 pulsars

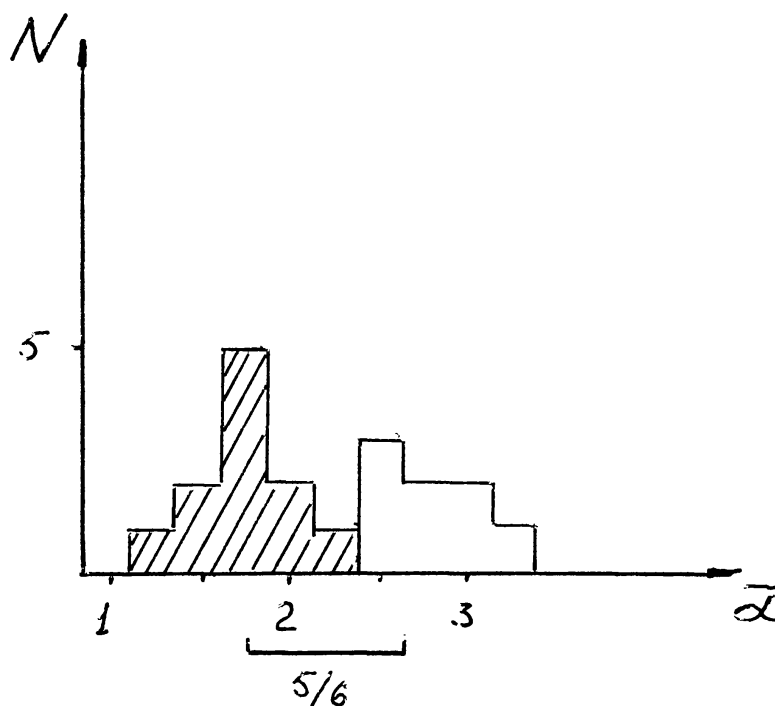


Fig. 23. Distribution of 'old' ($Q > 1$) pulsars in the magnitude of the spectral index $\bar{\alpha}$. Dashed distribution corresponds to frequencies $\nu < \nu_{br}$.

with $Q > 1$ the quantity $\bar{\alpha} = -1.7 \pm 0.3$ for $\omega < \omega_{br}$ and $\bar{\alpha} = -2.8 \pm 0.4$ above the break frequency.

These values are sufficiently close to $\bar{\alpha} = -2.6$ ($\omega < \omega_{br}$) and $\bar{\alpha} = -3.8$ ($\omega > \omega_{br}$) which, according to Equation (6.14) must be observed in the spectrum determined by an ordinary wave in the case when radio emission is formed at large distances from the star ('external' case). Only for the 'internal' version (6.13) the theory leads to the spectrum which has a maximum in the region of the frequency ω_{br} which is not observed in reality.

Unfortunately (as is seen from Figures 22 and 23), the available observational material is not always enough to compare theory with observations. In this connection we would like to mention some correlations which follow from the theory and a discovery of which would be of undoubted interest. First of all, the two versions that exist for the ordinary mode lead to different results both for the dependence of the window width W on the frequency ν (the quantity $\bar{\beta}$) and for the character of radio emission spectrum (the quantities $\bar{\alpha}$ and $\Delta\bar{\alpha}$). For this reason one should expect correlation between the quantities $\bar{\beta}$ and $\bar{\alpha}$. Note that this type of correlation has recently been mentioned by Malofeev *et al.* (1988). Besides, different components of the mean profile (if they are actually connected with different orthogonal modes) must also have different spectral indices $\bar{\alpha}$. Finally, it would be of interest to trace the dependence of all the parameters on the quantity Q .

6.5. FREQUENCY RANGE OF OBSERVED RADIO EMISSION

As has already been shown, an amplification of unstable curvature-plasma waves is possible only for frequencies $\omega < \omega_{\max}$, where ω_{\max} is given by Equation (5.7). Thus, the quantity

$$\nu_{\max} \simeq 3.5 P^{-1/2} \gamma_{100}^{7/4} \text{ GHz} \quad (6.15)$$

is just the upper boundary of the frequencies generated in pulsar magnetosphere. The lowest frequency ν_{\min} can be determined by the conditions of propagation. For example, the refractive index of an ordinary wave n_2 becomes equal to zero for $\nu \lesssim \nu_{\min}$ (2.20a); and, therefore, for frequencies $\nu < \nu_{\min}$ such a wave (for angles $\theta < \theta_*$) can propagate only towards the star. In such a case,

$$\nu_{\min} = 120 P^{-1/2} \gamma_{100}^{-3/2} \lambda_4^{1/2} B_{12}^{1/2} \text{ MHz} . \quad (6.16)$$

Compare these values with the values of a high-frequency and low-frequency limits (where sharp downfall of the spectra take place) observed in the spectra of many pulsars (Malov and Malofeev, 1981)

$$\nu_{\max}^{\text{obs}} = 3 P^{-(0.62 \pm 0.19)} \text{ GHz} , \quad (6.17)$$

$$\nu_{\min}^{\text{obs}} \simeq 100 P^{-(0.38 \pm 0.09)} \text{ MHz} , \quad (6.18)$$

where one can see a good agreement between theory and observations. Comparing the theoretical dependences (6.15) and (6.16) with the observable ones (6.17) and (6.18), we see that the theory also gives a correct dependence of downfall frequencies on the pulsar period P .

Note, however, that the nature of a low-frequency diminution can be connected with other processes as well. For example, as is seen from (4.17), a low-frequency decrease can arise from a cessation of energy conversion into an ordinary wave. In this case

$$\nu_{\min} = 80 P^{-1/2} \gamma_{100}^3 \text{ MHz} . \quad (6.19)$$

This is also close enough to the observed value (6.16).

6.6. CYCLOTRON ABSORPTION

Another reason for a low-frequency decrease may be a cyclotron absorption of electromagnetic waves in the cyclotron resonance region $r = R_c$ (2.11). Indeed, making use of the relations (2.11) and (2.27), we obtain the following estimate for the total optical depth for two orthogonal modes $j = 1, 2$ that propagate at large distances from a neutron star

$$\tau_{1,2} = 2 \frac{\omega}{c} \int \text{Im } n_{1,2} dl \simeq 0.3 P^{-1} \nu_{\text{GHz}}^{-1/3} \gamma_{100}^{1/3} \lambda_4 B_{12} . \quad (6.20)$$

The estimate (6.20) corresponds to the homogeneous magnetic field approximation which, as shown in Section 3, holds for sufficiently wide distribution functions of

particles. One can see that, according to Equation (6.20), the cyclotron absorption can actually turn out to be substantial.

Figure 24 exhibits a typical variation of a total optical depth τ subject to the wave frequency ν . A more exact calculation was carried out in the framework of geometric-

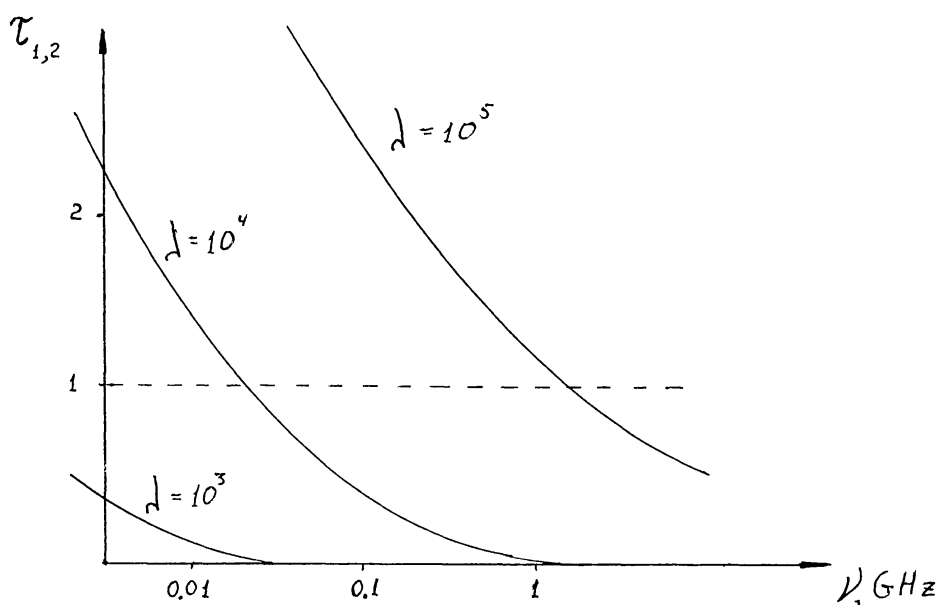


Fig. 24. Total optical depth of cyclotron absorption subject to the frequency ν .

optical wave propagation in the dipole magnetic field of a star. We see that the condition of smallness of absorption $\tau < 1$ is fulfilled if $\nu > \nu_{\min}^c$, where the frequency

$$\nu_{\min}^c \simeq 30 P^{-3} \lambda_4^3 B_{12}^3 \text{ MHz} \quad (6.21)$$

is also close to the observed values of low-frequency diminution.

We should emphasize that as is seen from Figure 24, the frequency ν_{\min}^c depends strongly on the value of the parameter λ (2.2), i.e., on the density of plasma that flows in pulsar magnetosphere (see Equation (2.2)). That is why a detailed comparison of the theory with observational data on cyclotron absorption will make it possible to determine a very important parameter of the theory – the multiplicity of particle production λ . One can now conclude from preliminary analyses that the quantity λ does not exceed the values 10^4 – 10^5 , which is in agreement with theoretical evaluation (Dougherty and Harding, 1982; or Gurevich and Istomin, 1985).

6.7. INTEGRAL INTENSITY OF PULSAR RADIO EMISSION

The theory enables us also to determine the total intensity of radio emission of pulsars (see Section 5). This intensity is convenient to represent as a fraction of energy of a beam of particles accelerated in a double layer which (the fraction) is converted into radio emission, $\alpha_T = E_{\text{rad}}/W_{\text{part}}$. The quantity $W_{\text{part}} \simeq 4 \times 10^{31} P^{-4} B_{12}^2 \text{ erg s}^{-1}$ – the energy transferred by particles – has already been found in Section 2.1.

Using now the relations (5.29), (5.32), and (5.35) for the transformation coefficient α_T as well as the values (6.15) and (6.16) for the quantities v_{\max} and v_{\min} , we obtain

$$\begin{aligned}\alpha_T^{(1)} &\simeq 10^{-4} \lambda_4^{2.2} P^{-1.0} B_{12}^{-0.7}, \\ \alpha_{T_{\text{in}}}^{(2)} &\simeq 10^{-5} \lambda_4^{3.8} P^{-0.9} B_{12}^{-1.2}, \\ \alpha_{T_{\text{out}}}^{(2)} &\simeq 10^3 \lambda_4^{5.0} P^{-1.7} B_{12}^{-1.3}.\end{aligned}\tag{6.22}$$

In the derivation of Equation (6.22) we employed the value $\lambda \sim \gamma_c^2$ (see Equation (2.6)).

Thus, for both modes (and for the characteristic values $P \sim 1$ s, $B \sim 10^{12}$ G) the total intensity of radio emission $E_{\text{rad}} = \alpha_T W_{\text{part}}$ must be of the same order of magnitude, that is, $E_{\text{rad}} \simeq 10^{26}\text{--}10^{28}$ erg s $^{-1}$ (corresponding to $\alpha_T \sim 10^{-3}\text{--}10^{-5}$). As is well known, this is precisely the observed mean intensity of radio emission of pulsars (Manchester and Taylor, 1977; Taylor and Stinebring, 1986).

For a quantitative comparison of the theory and observations we will take the results obtained by Beskin *et al.* (1984), where the quantity α_T was determined from observational data. It has actually proved to be the same for ‘young’ ($Q < 1$, the solid line in Figure 25) and ‘old’ pulsars ($Q > 1$, the dashed line), $\alpha_T \sim 10^{-4}$. This is just the quantity given by our theory of radio emission of pulsars.

Note finally that the theory predicts a weak dependence of transformation coefficient α_T on the pulsar period P . This is due to the fact that the quantity λ involved in the relation (6.22) depends, generally speaking, on the period P . Using, for example, the

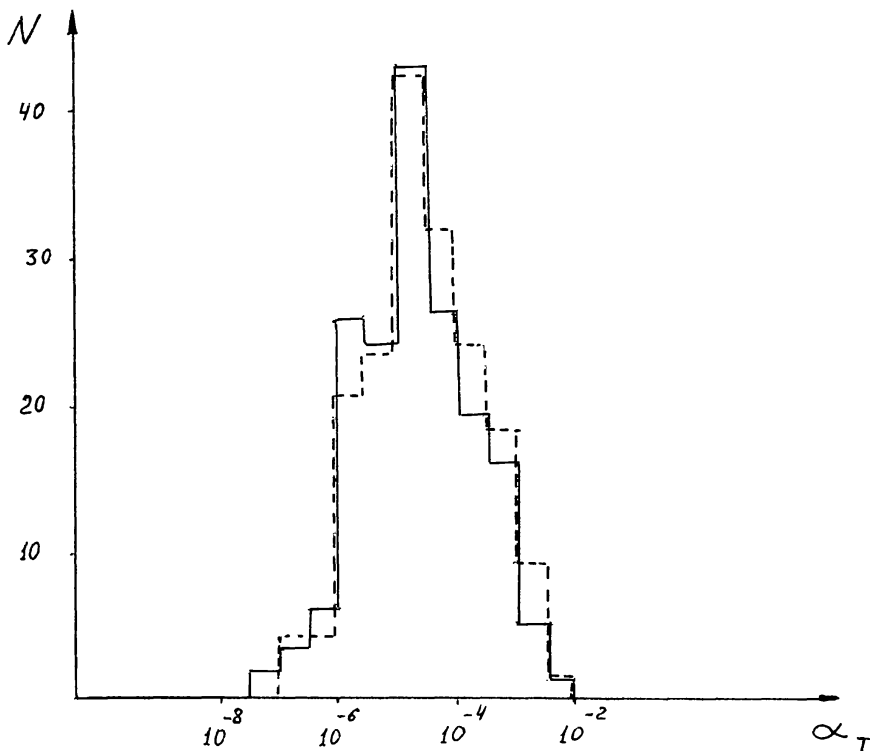


Fig. 25. Distribution in the magnitude of the transformation coefficient α_T for pulsars with $Q < 1$ (solid line) and $Q > 1$ (dashed line) (Beskin *et al.*, 1984).

estimate $\lambda \propto P^{3/7}$ proposed by Gurevich and Istomin (1985) (see Section 2.1), we obtain that $\alpha_T^{(i)} \propto P^{\bar{r}}$, where for all the three versions $|\bar{r}| < 0.3$. Such a weak dependence of α_T on P is, in fact, in agreement with the data shown in Figure 25. Indeed, as is seen from the definition (2.1), the periods of pulsars with $Q < 1$ are on the whole considerably smaller than those of pulsars with $Q > 1$, but nevertheless the transformation coefficient α_T remains practically constant for them.

7. Conclusions

The paper was devoted to presentation of a consistent theory of pulsar radio emission in the construction of which no special model assumptions were made. The only starting point was the now reliably established concept of the flux of a relativistic electron-positron plasma flowing along open field lines in the magnetosphere of a pulsar. As has been shown, the predictions of the theory are in agreement with observational data. We have, in fact, succeeded in explaining all the basic characteristics of pulsar radio emission: their radiation intensity, the range of observed frequencies, the energy spectrum, the shape of the mean profile, and polarization.

We should emphasize that we spoke of averaged characteristics of pulsar radio emission. It was reasonable to compare the predictions of the theory just with these characteristics. We see, however, that averaged characteristics of pulsars vary within a wide range depending on some of the parameters. Our theory has succeeded to explain this variation.

As concerns some other properties, such as radio emission intensity fluctuations (Cordes and Downs, 1985), intensity correlation at different frequencies (Kardashev *et al.*, 1986), a fine time structure of individual pulses, and others (Cordes, 1983; Smirnova *et al.*, 1986), their analysis requires a further development of the theory. In the first place this is formulation of the theory of space-time instability in the region of particle generation and the theory of corresponding fluctuations in a plasma flux. A further analysis could also be aimed at a theory of wave propagation with an account of fluctuations of the parameters of the medium and at clarifying the question of a limiting radio emission polarization and interaction of two orthogonal modes (see Section 6.1).

On the other hand, it would be of great importance to have more observational information on 'averaged' processes proceeding in pulsar magnetosphere. From this point of view it is important, for instance, to clarify and investigate in detail the cyclotron absorption (Section 6.6), the character of formation of circular polarization (Section 6.1), to have more observational data on the break of the radio emission spectrum, etc. This would make it possible to compare more reliably the predictions of the above theory with observations.

Acknowledgement

The authors are grateful to Prof. V. L. Ginzburg for fruitful discussions.

References

- Abramowitz, M. and Stegun, I. A.: 1964, *Handbook of Mathematical Functions*, Dover Publ., New York.
- Arons, J.: 1983, *Astrophys. J.* **266**, 215.
- Arons, J. and Barnard, J. J.: 1986, *Astrophys. J.* **302**, 120.
- Arons, J. and Scharlemann, E. T.: 1979, *Astrophys. J.* **231**, 854.
- Asseo, E., Pellat, R., and Rosado, M.: 1980, *Astrophys. J.* **239**, 661.
- Asseo, E., Pellat, R., and Sol, H.: 1983, *Astrophys. J.* **266**, 201.
- Backer, D. C.: 1976, *Astrophys. J.* **209**, 895.
- Barnard, J. J.: 1986, *Astrophys. J.* **303**, 280.
- Barnard, J. J. and Arons, J.: 1986, *Astrophys. J.* **302**, 138.
- Benford, G. and Buschauer, R.: 1977, *Monthly Notices Roy. Astron. Soc.* **179**, 189.
- Beskin, V. S.: 1982a, *Astrofizika* **18**, 439.
- Beskin, V. S.: 1982b, *Astron. Zh.* **59**, 726.
- Beskin, V. S., Gurevich, A. V., and Istomin, Ya. N.: 1983, *Soviet Phys. JETP* **58**, 235.
- Beskin, V. S., Gurevich, A. V. and Istomin, Ya. N.: 1984, *Astrophys. Space Sci.* **102**, 301.
- Beskin, V. S., Gurevich, A. V., and Istomin, Ya. N.: 1986, *Soviet Phys. Usp.* **29**, 946.
- Beskin, V. S., Gurevich, A. V., and Istomin, Ya. N.: 1987a, *Radiofizika* **30**, 161.
- Beskin, V. S., Gurevich, A. V., and Istomin, Ya. N.: 1987b, *Soviet Phys. JETP* **65**, 715.
- Blandford, R. D.: 1975, *Monthly Notices Roy. Astron. Soc.* **170**, 551.
- Buschauer, R. and Benford, G.: 1978, *Monthly Notices Roy. Astron. Soc.* **185**, 493.
- Canuto, V. and Ventura, J.: 1972, *Astrophys. Space Sci.* **18**, 104.
- Cheng, A. F. and Ruderman, M. A.: 1977, *Astrophys. J.* **212**, 800.
- Chiu, H. Y. and Canuto, V.: 1971, *Astrophys. J.* **163**, 577.
- Chugunov, Yu. V. and Shaposhnikov, V. E.: 1988, *Astrofizika* (in press).
- Cordes, J. M.: 1983, in 'Positron-Electron Pairs in Astrophysics', *AIP Conference Proc.*, No. 101, New York, p. 98.
- Cordes, J. M. and Downs, G. S.: 1985, *Astrophys. J. Suppl.* **59**, 343.
- Daugherty, J. K. and Harding, A. K.: 1982, *Astrophys. J.* **252**, 337.
- Daugherty, J. K. and Harding, A. K.: 1983, *Astrophys. J.* **273**, 761.
- Elitzur, K.: 1974, *Astrophys. J.* **190**, 673.
- Gedalin, M. E. and Machabeli, G. Z.: 1983, *Astrofizika* **19**, 153.
- Gil, J.: 1985, *Astrophys. J.* **299**, 154.
- Gil, J.: 1987, *Astrophys. J.* **314**, 629.
- Ginzburg, V. L.: 1970, *The Propagation of Electromagnetic Waves in Plasmas*, Pergamon Press, Oxford.
- Ginzburg, V. L.: 1971, *Soviet Phys. Usp.* **14**, 83.
- Ginzburg, V. L., Zheleznyakov, V. V., and Zaitsev, V. V.: 1969, *Soviet Phys. Usp.* **12**, 378.
- Godfrey, B. B., Shanahan, W. R., and Thode, L. E.: 1975, *Phys. Fluids* **18**, 346.
- Goldreich, P. and Julian, W. R.: 1969, *Astrophys. J.* **157**, 869.
- Goldreich, P. and Keeley, D. A.: 1971, *Astrophys. J.* **170**, 463.
- Gurevich, A. V. and Istomin, Ya. N.: 1985, *Soviet Phys. JETP* **62**, 1.
- Hankins, T. H. and Cordes, J. M.: 1981, *Astrophys. J.* **249**, 241.
- Hankins, T. H. and Rickett, B. J.: 1986, *Astrophys. J.* **311**, 684.
- Hardee, Ph. E. and Rose, W. K.: 1976, *Astrophys. J.* **210**, 533.
- Hardee, Ph. E. and Morrison, Ph. J.: 1979, *Astrophys. J.* **227**, 252.
- Herold, H., Ruder, H. and Wunner, G.: 1985, *Phys. Rev. Letters* **54**, 1452.
- Hinata, S.: 1976, *Astrophys. J.* **203**, 223.
- Istomin, Ya. N.: 1988, *Soviet Phys. JETP* (in press).
- Izvekova, V. A., Kuzmin, A. D., Malofeev, V. M., and Shitov, Yu. P.: 1981, *Astrophys. Space Sci.* **78**, 45.
- Jones, P. B.: 1981, *Monthly Notices Roy. Astron. Soc.* **197**, 1103.
- Jones, P. B.: 1983, *Monthly Notices Roy. Astron. Soc.* **204**, 9.
- Kardashev, N. S., Nikolaev, N. Ya., Novikov, A. Yu., Popov, M. V., Soglasnov, V. A., Kuzmin, A. D., Smirnova, T. V., Sieber, W., and Wielebinski, R.: 1986, *Astron. Astrophys.* **163**, 114.
- Kaplan, S. A. and Tsytoich, V. N.: 1973, *Nature Phys. Sci.* **241**, 122.
- Kawamura, K. and Suzuki, I.: 1977, *Astrophys. J.* **217**, 832.
- Komesaroff, M. M.: 1970, *Nature* **225**, 612.
- Kuzmin, A. D., Malofeev, V. M., Izvekova, V. A., Sieber, W., and Wielebinski, R.: 1986, *Astron. Astrophys.* **161**, 183.

- Landau, L. D. and Lifshitz, E. M.: 1975, *The Classical Theory of Fields*, Pergamon Press, Oxford.
- Larroche, O. and Pellat, R.: 1987, *Phys. Rev. Letters* **59**, 1104.
- Lominadze, D. G. and Pataraya, A. D.: 1982, *Phys. Scripta* **21**, 215.
- Lominadze, D. G., Machabeli, G. Z., and Usov, V. V.: 1983, *Astrophys. Space Sci.* **90**, 19.
- Lominadze, D. G., Mikhailovskii, A. B., and Sagdeev, R. Z.: 1979, *Soviet Phys. JETP* **50**, 927.
- Malofeev, V. M., Izvekova, V. A., and Shitov, Yu. P.: 1988 (in press).
- Malov, I. F.: 1983, *Astrofizika* **19**, 161.
- Malov, I. F.: 1986, *Astrofizika* **24**, 507.
- Malov, I. F. and Malofeev, V. M.: 1981, *Astrophys. Space Sci.* **78**, 73.
- Malov, I. F. and Suleimanova, S. A.: 1982, *Astrofizika* **18**, 107.
- Manchester, R. and Taylor, J.: 1977, *Pulsars*, Freeman, San Francisco.
- Melrose, D. B.: 1978, *Astrophys. J.* **225**, 557.
- Mestel, L. and Wang, Y. M.: 1979, *Monthly Notices Roy. Astron. Soc.* **188**, 799.
- Michailovski, A. B.: 1980, *Fizika Plasmy* **6**, 613.
- Michailovski, A. B., Onischenko, O. G., and Smolyakov, A. I.: 1985a, *Fizika Plasmy* **11**, 369.
- Michailovski, A. B., Onischenko, O. G., and Smolyakov, A. I.: 1985b, *Pis'ma Astron. Zh.* **11**, 190.
- Michailovski, A. B., Onischenko, O. G., Suramlshvili, G. I., and Sharapov, S. E.: 1982, *Pis'ma Astron. Zh.* **8**, 685.
- Michel, F. C.: 1973, *Astrophys. J.* **180**, 207.
- Narayan, R. and Vivekanand, M.: 1983, *Astron. Astrophys.* **122**, 45.
- Nikishov, A. I. and Ritus, V. I.: 1986, in M. A. Markov (ed.), *Group-theoretical Methods in Physics*, Nauka, Moscow.
- Ochelkov, Yu. P. and Usov, V. V.: 1980, *Astrophys. Space Sci.* **69**, 439.
- Ochelkov, Yu. P. and Usov, V. V.: 1984, *Nature* **309**, 332.
- Onischenko, O. G.: 1981, *Pis'ma Astron. Zh.* **7**, 731.
- Oster, L. and Sieber, W.: 1976, *Astrophys. J.* **203**, 233.
- Radhakrishnan, V. and Cocke, D. J.: 1969, *Astrophys. Letters* **3**, 225.
- Rankin, J.: 1983a, *Astrophys. J.* **274**, 333.
- Rankin, J.: 1983b, *Astrophys. J.* **274**, 359.
- Rankin, J.: 1986, *Astrophys. J.* **301**, 901.
- Ruderman, M. A. and Sutherland, P. G.: 1975, *Astrophys. J.* **196**, 51.
- Shabad, A. E. and Usov, V. V.: 1984, *Astrophys. Space Sci.* **102**, 327.
- Shabad, A. E. and Usov, V. V.: 1986, *Astrophys. Space Sci.* **128**, 377.
- Shafranov, V. D.: 1967, in *Reviews of Plasma Physics*, Vol. 3, Consultants Bureau, New York, p. 1.
- Shaposhnikov, V. E.: 1981, *Astrofizika* **17**, 749.
- Slee, O. B., Alurkar, S. K., and Botra, A. D.: 1986, *Australian J. Phys.* **39**, 103.
- Smirnova, T. V., Soglasnov, V. A., Popov, M. V., and Novikov, A. Yu.: 1986, *Soviet Astron.* **30**, 51.
- Smith, F. G.: 1970, *Monthly Notices Roy Astron. Soc.* **149**, 1.
- Smith, F. G.: 1977, *Pulsars*, Cambridge Univ. Press, Cambridge.
- Stinebring, D. R., Cordes, J. M., Rankin, J. M., Weisberg, J. M., and Boriakoff, V.: 1984a, *Astrophys. J. Suppl.* **55**, 247.
- Stinebring, D. R., Cordes, J. M., Weisberg, J. M., Rankin, J. M., and Boriakoff, V.: 1984b, *Astrophys. J. Suppl.* **55**, 279.
- Sturrock, P. A.: 1971, *Astrophys. J.* **164**, 529.
- Suvorov, E. W. and Chugunov, Yu. V.: 1973, *Astrophys. Space Sci.* **23**, 189.
- Suvorov, E. W. and Chugunov, Yu. V.: 1975, *Astrofizika* **11**, 305.
- Suvorov, E. W. and Chugunov, Yu. V.: 1980, *Fizika Plasmy* **6**, 122.
- Tademaru, E.: 1973, *Astrophys. J.* **183**, 625.
- Taylor, J. H. and Stinebring, D. R.: 1986, *Ann. Rev. Astron. Astrophys.* **24**, 285.
- Ter Haar, D. and Tsytovich, V. N.: 1981, *Phys. Reports* **73**, 177.
- Tsytovich, V. N.: 1971, in S. Hamberger (ed.), *Nonlinear Effects in Plasma*, Plenum Press, New York.
- Usov, V. V.: 1987, *Astrophys. J.* **320**, 333.
- Verga, A. D. and Fontan, C. F.: 1985, *Plasma Phys. Controlled Fusion* **27**, 19.
- Volokitin, A. S., Krasnosel'skikh, V. V., and Machabeli, G. Z.: 1985, *Fizika Plasmy* **11**, 531.
- Weisberg, J. M., Armstrong, B. K., Backus, P. R., Cordes, J. M., Boriakoff, V., and Ferguson, D. C.: 1986, *Astron. J.* **92**, 621.
- Wilhelmson, H., Stenflo, L., and Engelmann, F.: 1970, *J. Math. Phys.* **11**, 1738.
- Zheleznyakov, V. V.: 1973, *Soviet Phys. Usp.* **109**, 777.